AN ABSTRACT OF THE THESIS OF

WILLIAM ERNEST GENETTI for the Ph. D.
(Name) (Degree)

in CHEMICAL ENGINEERING presented on December 6, 1967
(Major) (Date)

Title: HEAT TRANSFER IN A FLUIDIZED BED TUBULAR HEAT EXCHANGER

Redacted for privacy

Abstract approved:
Dr. J. G. Knudsen

Local and average heat transfer coefficients for heat transfer from an internal tube in a bundle of tubes to an air fluidized bed were investigated for both batch fluidization and fluidization with particle recycle. The fluidized bed heat exchanger was compared to a typical baffled heat exchanger in terms of pumping and space requirements.

The fluidized bed tubular heat exchanger consisted of a 44-inch long, 5.75-inch inside diameter shell with 19, 3/4-inch diameter tubes arranged in a 1-1/16-inch triangular pitch. A cyclone separator was used to separate and return particles to the fluidized bed. Two types and three sizes of particles were used in this study. Glass spheres of 0.0052 and 0.0151-inch average diameter were used, and aluminum particles of 0.0306-inch average diameter were used. Tubes at the four possible tube locations were heated electrically. A movable thermocouple probe was fitted inside the heated tube to measure the tube wall temperature at any vertical height. Bulk gas temperatures were determined with protected thermocouples placed

at several locations in the bed.

Variables studied included particle size, shape, and concentration; gas mass velocity; and tube location. Arithmetic average heat transfer coefficients over 11-inch sections of the bed were compared with previous work and correlated with an equation based on a particle mode heat transfer mechanism. Local heat transfer coefficients are estimated to be accurate within ± 10 percent in the most dense sections of the bed and within ± 5 percent in the sparse sections of the bed.

The results of this study are as follows:

1. Tube location had only a slight effect on local heat transfer coefficients. In most cases local heat transfer coefficients for batch fluidization are smallest in magnitude at the central tube location. While a tube location 3/8 of the way out from the center has the largest coefficients, local coefficients for tube locations near the wall are usually of an intermediate value. For fluidization with particle recycle, local coefficients measured at the central tube location were 10 to 20 percent greater than coefficients at the other tube locations.

2. For batch fluidization the average Nusselt number is correlated with an equation based on a particle mode heat transfer mechanism, i. e.

$$Nu_p = \frac{5\,\phi(1-\epsilon)^{0.48}}{\left[1 + \frac{580}{Re_p}\left(\frac{G_{mf}}{G}\right)^{4/3}\left(\frac{k_g}{\rho_s C_s g^{1/2} D_p^{3/2}}\right)\left(\frac{\rho_s}{\rho_g}\right)^{1.1}\right]^2}$$

where ϕ is the ratio of the average surface area of a particle to the surface area of a sphere of the same average diameter. This equation relates the variables studied to the average Nusselt number.

3. For fluidization with particle recycle average Nusselt numbers are correlated with the following equation:

$$j_H = \frac{Nu_p}{Re_p\,Pr^{1/3}} = 0.14\left(\frac{Re_p}{\phi}\right)^{-0.68}$$

4. It is concluded that the fluidized bed tubular heat exchanger is advantageous in terms of pumping and space requirements over the conventional baffled exchanger when batch fluidization with of fine glass particles is employed.

Heat Transfer in a Fluidized Bed Tubular Heat Exchanger

by

William Ernest Genetti

A THESIS

submitted to

Oregon State University

in partial fulfillment of
the requirements for the
degree of

Doctor of Philosophy

June 1968

TO MY LOVING WIFE

APPROVED:

Redacted for privacy

Professor of Chemical Engineering
in charge of major

Redacted for privacy

Head of Department of Chemical Engineering

Redacted for privacy

Dean of Graduate School

Date thesis is presented December 6, 1967

Typed by Marion F. Palmateer for William Ernest Genetti

ACKNOWLEDGMENTS

I wish to extend my grateful appreciation to the following:

To Dr. James G. Knudsen for his professional assistance and encouragement throughout the duration of this investigation.

To Dow Chemical Company and Oregon State University Engineering Experiment Station for their financial support during this study.

To William B. Johnson for his contributions to the construction of experimental equipment.

To William Cosart for reading and criticizing this dissertation.

To my brother, Guy, for his continuous encouragement during my college career.

TABLE OF CONTENTS

Page

INTRODUCTION 1

THEORETICAL ASPECTS AND LITERATURE SURVEY 4

- Proposed Fluidized Bed Heat Transfer Mechanisms 5
- Experimental Study of Fluidized Bed Heat Transfer 9
  - Particle-to-Fluid Heat Transfer 9
  - Surface-to-Fluidized-Bed Heat Transfer 13
- Presently Proposed Heat Transfer Model 27

EXPERIMENTAL EQUIPMENT 37

- The Model Heat Exchanger 37
- The Air Blower 42
- The Direct Current Power Supply 43
- The Cyclone Separator 43
- Measuring Devices 45

EXPERIMENTAL PROGRAM 49

- Particle Size and Thermal Conductivity 50
- Particle Concentration and Distribution 53
- Gas Mass Velocity 54
- Heating Tube Location 54

EXPERIMENTAL PROCEDURE 56

CALCULATIONS 59

- Calculations Using Original Data 59
- Calculations from Calculated Data 64

ANALYSIS OF DATA 66

- Average Nusselt Numbers without Fluidization 66
- Radial and Vertical Bulk Gas Temperature Profiles 68
  - Radial Bulk Gas Temperature Profiles 68
  - Vertical Bulk Gas Temperature Profiles 70
- Local Heat Transfer Coefficients for Batch Fluidization 70

Page

Average Sectional Coefficients for Batch Fluidization 82
Local Heat Transfer Coefficients for Fluidization with Particulate Reflux 91
Average Heat Transfer Coefficients for Fluidization with Particulate Reflux 99
Power and Space Considerations 101
Estimation of Experimental Errors 106

RESULTS AND CONCLUSIONS 110

Average Nusselt Numbers without Fluidization 110
Bed Thermal Gradients 110
Heat Transfer with Batch Fluidization 111
Heat Transfer with Particle Recycle Fluidization 113
Comparisons of the Fluidized Bed Exchanger to a Typical Baffled Exchanger 114

RECOMMENDATIONS FOR FURTHER STUDY 115

BIBLIOGRAPHY 117

APPENDICES 121

APPENDIX A NOMENCLATURE 121

APPENDIX B CALIBRATION OF THE ORIFICE METER 128

APPENDIX C CALIBRATION OF THERMOCOUPLES AND THE TUBE WALL PROBE ANALYSIS 131

APPENDIX D SAMPLE RAW DATA SHEET 138

APPENDIX E RADIAL BULK BED TEMPERATURE DATA 141

APPENDIX F EXPERIMENTAL AND CALCULATED DATA 145

APPENDIX G CALCULATED AVERAGE PARTICLE FRACTIONS AND NUSSELT NUMBERS FOR BATCH FLUIDIZATION 177

LIST OF FIGURES

Figure		Page
1	Particle-to-Fluid Nusselt Numbers in a Fluidized Bed vs. Particle Reynolds Number	12
2	Typical Heat Transfer Coefficients vs. Mass Velocity Curves	14
3	Types of Local Heat Transfer Coefficient Profiles	18
4	Ratio of Internal Surface to External Surface Heat Transfer Coefficients vs. Mass Velocity	23
5	Correction for Nonaxial Tube Location	25
6	Schematic of Proposed Heat Transfer Mechanism	29
7	Photograph of Experimental Equipment	38
8	Tube Layout: Showing Locations of Heating Element and Transverse Thermocouple	41
9	Diagram of Electrical System	44
10	Drawing of Cyclone Separator	46
11	Exploded View of the Tube Wall Temperature Probe	47
12	Particle Size Distributions	51
13	Photographs of Particles	52
14	Average Nusselt Numbers in an Unbaffled Heat Exchanger	67
15	Radial Bulk Gas Temperature Profiles	69
16	Vertical Bulk Gas Temperature Profiles	71
17	Local Heat Transfer Coefficients for Batch Fluidization	73
18	Local Heat Transfer Coefficients for Batch Fluidization	74

Figure		Page
19	Local Heat Transfer Coefficients for Batch Fluidization	76
20	Local Heat Transfer Coefficients for Batch Fluidization	77
21	Local Heat Transfer Coefficients for Batch Fluidization	79
22	Local Heat Transfer Coefficients for Batch Fluidization	80
23	Correlation for Average Contact Time	83
24	Correlation for Average Sectional Nusselt Numbers	85
25	Comparison of the Correlation for Average Sectional Nusselt Numbers with Noë's Data	87
26	Comparison of Average Sectional Nusselt Numbers with Gamson's Correlation for a Single Vertical Tube	89
27	Comparison of Average Sectional Nusselt Numbers with Kruglikov and Ainshtein's Correlation for a Single Vertical Tube	90
28	Local Heat Transfer Coefficients for Particulate Reflux Fluidization	92
29	Local Heat Transfer Coefficients for Particulate Reflux Fluidization	93
30	Local Heat Transfer Coefficients for Particulate Reflux Fluidization	94
31	Local Heat Transfer Coefficients for Particulate Reflux Fluidization	95
32	Local Heat Transfer Coefficients for Particulate Reflux Fluidization	96
33	Local Heat Transfer Coefficients for Particulate Reflux Fluidization	97

Figure Page

34 j_H vs. Re_p/ϕ for Particulate Reflux Fluidization 100

35 Comparison of Pressure Drops in Baffled and Fluidized Bed Exchangers for Batch Fluidization 103

36 Comparison of Pressure Drops in Baffled and Fluidized Bed Exchangers for Particulate Reflux Fluidization 104

37 Orifice Meter Calibration Data 130

38 Thermocouple Calibration Data 133

LIST OF TABLES

Table Page

I Percent Occurrence of Type I Profiles 81

II Percent Error in Local Heat Transfer Coefficients 108

III Radial Bulk Bed Temperature Data 141

IV Experimental and Calculated Data 145

V Calculated Average Particle Fractions and Nusselt Numbers for Batch Fluidization 177

HEAT TRANSFER IN A FLUIDIZED BED TUBULAR HEAT EXCHANGER

INTRODUCTION

Industrial process heat transfer usually involves transferring energy from a hot flowing fluid to a cold flowing fluid, or as is the case in nuclear reactors, transferring energy from an energy generating source to a flowing fluid. To solve this problem engineers have devised many types of heat exchangers. The type most used in industrial processes is the baffled tubular heat exchanger. The tubular heat exchanger consists of a tube bundle located inside a cylindrical shell. One fluid usually flows inside the tubes and another fluid on the shell-side of the tubular heat exchanger.

Many devices have been used to decrease the resistance to heat transfer. Some of these devices include rough surfaces, extended surfaces, scraped surfaces, and baffled tubular heat exchangers. When trying to decrease heat transfer resistance, one or more of the following methods are usually used:

1. The laminar film thickness is decreased by promoting turbulence.
2. The effective resistance to heat transfer is decreased by an extended surface area. (This is used often in compact heat exchangers.)

Both of these methods, unfortunately, increase operating expense, usually in the way of pumping power cost.

The term fluidization was first used to describe a certain mode of contacting granular solids with fluids. When a fluid is passed up through a bed of granular solids, there is a certain flow rate at which the solids are suspended. This state is known as minimum fluidization. At this flow rate and at higher rates, the solids act as a fluid; however, due to rapid irregular motion of the solids, the fluidized bed appears as a well mixed tank.

Although recorded application of fluidization dates back to the Sixteenth Century when it was used in ore processing, important industrial applications did not come into existence until the Twentieth Century. In 1921 the Winkler Gas Generator for manufacturing producer gas was developed in Germany (18, p. 5). In this process a fluidized bed of coal was used to contact coal with air and steam. The first large scale application in the United States was the catalytic cracking of oil vapors developed in 1940. This unit consisted of two vessels, a reactor and a regenerating vessel. Solid catalyst was transferred in a loop from the reactor to the regenerator and back to the reactor. With the application of fluidization to catalytic reactors, the need for transferring energy to and from the reactor arose. Since that time considerable effort has been applied to investigating heat transfer in fluidized beds.

Heat transfer coefficients for heat transfer from a surface to the fluid in a gas-fluidized bed are many times larger than the corresponding gas film coefficients in one phase flow (18, p. 183). This increase in heat transfer is attributed to the increased turbulence the fluidized bed offers, as well as the energy transferred by solids in contact with the surface.

This investigation is a study of local and average heat transfer rates on the shell-side of a fluidized bed tubular heat exchanger. Local heat transfer coefficients were measured with a moving thermocouple probe inside an electrically heated tube. This probe made it possible to measure local heat transfer coefficients at any point along the tube and for any tube location for various gas rates and particle concentration.

THEORETICAL ASPECTS AND LITERATURE SURVEY

The transfer of energy in the form of heat is an operation occurring in most fields of engineering whether of a mechanical, electrical, chemical, or nuclear nature. Heat is transferred by one or more of three possible modes: conduction, convection, and radiation. Pure conduction occurs in solids, but it seldom occurs in fluids because fluids are free to move. The transfer of heat by radiation is significant only at high temperatures. Convective heat transfer is the transfer of heat by fluid motion. If the fluid motion is due to density gradients, the energy is transferred by free convection. If the fluid motion is forced by pumping, the energy is transferred by forced convection.

It has been observed that convective heat transfer resistance can be decreased by increasing the turbulence in the fluid flow. The increase is attributed to a reduction in the thickness of the laminar sublayer which usually provides most of the resistance to heat transfer. Such devices as spiral wire, twisted strips, and sand granules affixed to heat transfer surfaces have been used to increase the scale and intensity of turbulence (16, p. 396). Pulsations and vibrations have also been used to increase turbulence (16, p. 396). Baffles are used in most tubular heat exchangers to increase heat transfer coefficients. A large increase in heat transfer coefficient can also be obtained by providing a fluidized bed of solid granules adjacent to the heat transfer surface (18, p. 183).

Proposed Fluidized Bed Heat Transfer Mechanisms

There have been several theoretical mechanisms of fluidized bed heat transfer proposed in the literature (4;5;18, p. 183-185; 39). A brief description of some of these will be given in order to provide a basis for understanding correlations to be presented.

The film theory proposed by Leva, Weintraub, and Grummer (19) postulated that a thin laminar film exists near the wall of the heat transfer surface. The major resistance to heat flow was considered to be in this thin film. The scrubbing action of the fluidized particles against this film decreases its thickness, thereby decreasing the resistance to heat flow. The film thickness is believed to be affected by the particle velocity adjacent to the surface and the particle concentration. Since these two factors have opposite effects on heat transfer, a maximum heat transfer coefficient would be observed when the heat transfer coefficient is plotted versus the mass velocity, G.

Walton and Levenspiel (20) proposed a film model in a different perspective. They considered the major resistance to be in a laminar layer which forms on the heat transfer surface. This laminar layer is destroyed when particles pass through it. Therefore, in fluidized beds the average laminar layer is thinner than in the corresponding one phase flow.

Wicke and Fetting, as reviewed by Leva (18, p. 185) proposed a fluid-film-fluidized-core model. This model postulates the existence of a film adjacent to the surface, a boundary layer, and a fluidized core. Particle motion in the boundary layer is parallel to the surface except for some lateral particle exchange between the fluidized core and the boundary layer. Particles are visualized as stirring agents, and since heat capacities of solids are much greater than heat capacities of gases, particles are chiefly responsible for energy transfer in the bed. This model assumes that the film is the major resistance to heat transfer.

Mickley and Fairbanks (23) proposed a mechanism in which "packets" of particles contact the surface wall for a short duration. Unsteady state conduction of energy into the packet is the controlling resistance to heat transfer. "Packets" are visualized as leaving the surface, breaking up, and dissipating heat to the bulk of the bed. The "packet" properties were assumed to be those of a quiescent bed. They presented a mathematical model of this mechanism which predicted the heat transfer coefficient to be proportional to the quiescent bed thermal conductivity, heat capacity, and density, i. e.

$$h = \sqrt{k_{qb} C_{qb} \rho_{qb} s} \qquad (1)$$

where

s = stirring factor (dependent upon the bed dynamics)

By using several gases of different thermal conductivities, they were able to show that h is proportional to $k_{qb}^{1/2}$.

There have been several extensions, modifications, and additions (4; 5; 40) to the theory presented by Mickley and Fairbanks. One of the most recent is the theory presented by Ziegler, Koppel, and Brazelton (40). The theory postulates that a particle moves from the bulk of the bed at a temperature, T_b, to the heat transfer surface. Conduction at the point of contact is assumed to be small, and radiation from the surface to the particle is assumed to be negligible. The particle gains energy from the fluid flowing around it while it is at the surface. After some time the particle returns to the bulk of the bed and dissipates its energy, the average time that the particle remains at the wall is a function of the state of fluidization. The surface is assumed to be covered in a hexagonal packing with spherical particles. With these assumptions these workers were able to derive the following theoretical equation:

$$Nu_p = \frac{hD_p}{k_g} = \frac{4\pi/\sqrt{3}}{\left[1 + \frac{6k_g\overline{\theta}}{\rho_s C_s D_p^2}\right]^2} \qquad (2)$$

where

$\overline{\theta}$ = average contact time

This relationship predicts a well established fact (22, p. 303), that the Nusselt number is independent of the solid thermal conductivity. The dependency of the heat capacity of the solids, C_s, was experimentally confirmed by these authors.

An experiment performed by Ziegler and Brazelton (39) confirms a particle mode heat transfer mechanism. These experimenters measured simultaneous heat and mass transfer from a 1-1/2-inch diameter celite sphere. The celite sphere was saturated with water. The rates of mass and heat transfer were simultaneously measured when the sphere was placed in an air stream and when the sphere was placed in a fluidized bed. The particles used had negligible absorptivity for the diffusing water and consequently had no capacity for mass transfer.

As a result the only mechanism of importance for transfer of mass is diffusion through the film. Without fluidized particles the transfer of mass and heat are analogous, that is, both types of transfer can be considered as diffusion through the film. If heat is not transferred by a particle mode, mass and heat transfer coefficients would increase by the same factor. If heat is transferred by a particle mode the analogy breaks down and mass and heat transfer would increase by different factors.

These experimenters observed increases in heat transfer coefficients from 10 to 20 fold, but mass transfer coefficients only increased from 1-1/2 to 2 times. They concluded that 80 to 95 percent of the heat must be transferred by a particle mode.

A complete discussion of a modification of the model presented by Ziegler, Koppel, and Brazelton will be proposed by the present author in the last part of this section.

Experimental Study of Fluidized Bed Heat Transfer

The experimental study of fluidized bed heat transfer has been broken down into two categories: Particle-to-Fluid Heat Transfer and Surface-to-Fluidized-Bed Heat Transfer.

Particle-to-Fluid Heat Transfer

In a fluidized bed the particles serve as energy carriers. The particles gain energy at the heat transfer surface and then release it to the fluid phase. In particle-to-fluid heat transfer, one is interested in the rate of heat transfer from the particle to the fluid. As a starting point, experimental work done with a single spherical particle will be considered.

Froessling, as cited by Knudsen and Katz (16, p. 511) correlated rates of evaporation of water drops and obtained the following relationship for mass transfer:

$$\frac{K_m D_p}{D_{AB}} = 2.0 + 0.60\, Sc^{1/3} Re_p^{1/2} \qquad (3)$$

By substituting Nu and Pr for $K_m D_p / D_{AB}$ and Sc respectively, a relationship for the analogous heat transfer correlation is obtained, i. e.

$$Nu_p = 2.0 + 0.60\, Pr^{1/3} Re_p^{1/2} \tag{4}$$

Other workers (16, p. 511; 39) have confirmed this correlation.

In a fluidized bed there are many particles, and particle interactions would be expected. Two possible interactions that would be expected in a fluidized bed are particle agglomeration and disturbed velocity and temperature profiles. Particle agglomeration will increase the effective particle diameter which will result in poor gas-solid contacting. This effect will decrease the Nusselt number from the single particle case (11). The flow of fluid around each particle will affect the velocity and temperature profiles around neighboring particles as will particle collisions. This will in turn affect the heat transfer coefficient.

Particle-to-fluid heat transfer in fluidized beds has been experimentally investigated by several workers (9; 13; 14; 15; 30; 35; 36). Walton, Olson, and Levenspiel (35) investigated particle-to-fluid heat transfer using sized Utah coal for the solid phase. They obtained the following relationship for the Nusselt number:

$$Nu_p = 0.0028\, Re_p^{1.7} \left(\frac{D_p}{D_t}\right)^{-0.2} \tag{5}$$

where

D_t = bed diameter

Juveland, Deinken, and Dougherty (14) recently measured particle-to-fluid-heat transfer coefficients in beds of ZrC particles fluidized by helium or argon. The particles were heated by induction to temperatures as high as 1150° C. These workers were able to get large temperature differences between the gas and the particle which should increase the accuracy of measurement greatly. Their results are shown in Figure 1. For comparison the results of Zenz and Othmer (38), which are representative of much of the published data, are shown. The broken line represents the work of Walton, Olson, and Levenspiel (35). Froessling's correlation for a single sphere is also included for comparison.

More recently Holman, Moore, and Wong (13) measured heat transfer from stainless steel and lead spheres fluidized in water. The spheres were heated by an induction heating field. These authors correlated particle Nusselt numbers with the following equation:

$$Nu_p = 1.28 \times 10^{-5} (Re_p F_\epsilon)^{2.0} Pr^{2/3} \left(\frac{D_t}{D_p}\right)^{1/2} \left(\frac{\rho_f}{\rho_s}\right)^{2} \left(\frac{\mu}{\mu_o}\right)^{0.83} \qquad (6)$$

The velocity correction factor, F_ϵ, was used to account for variations in porosity.

As can be noted from Figure 1, particle-to-gas Nusselt numbers

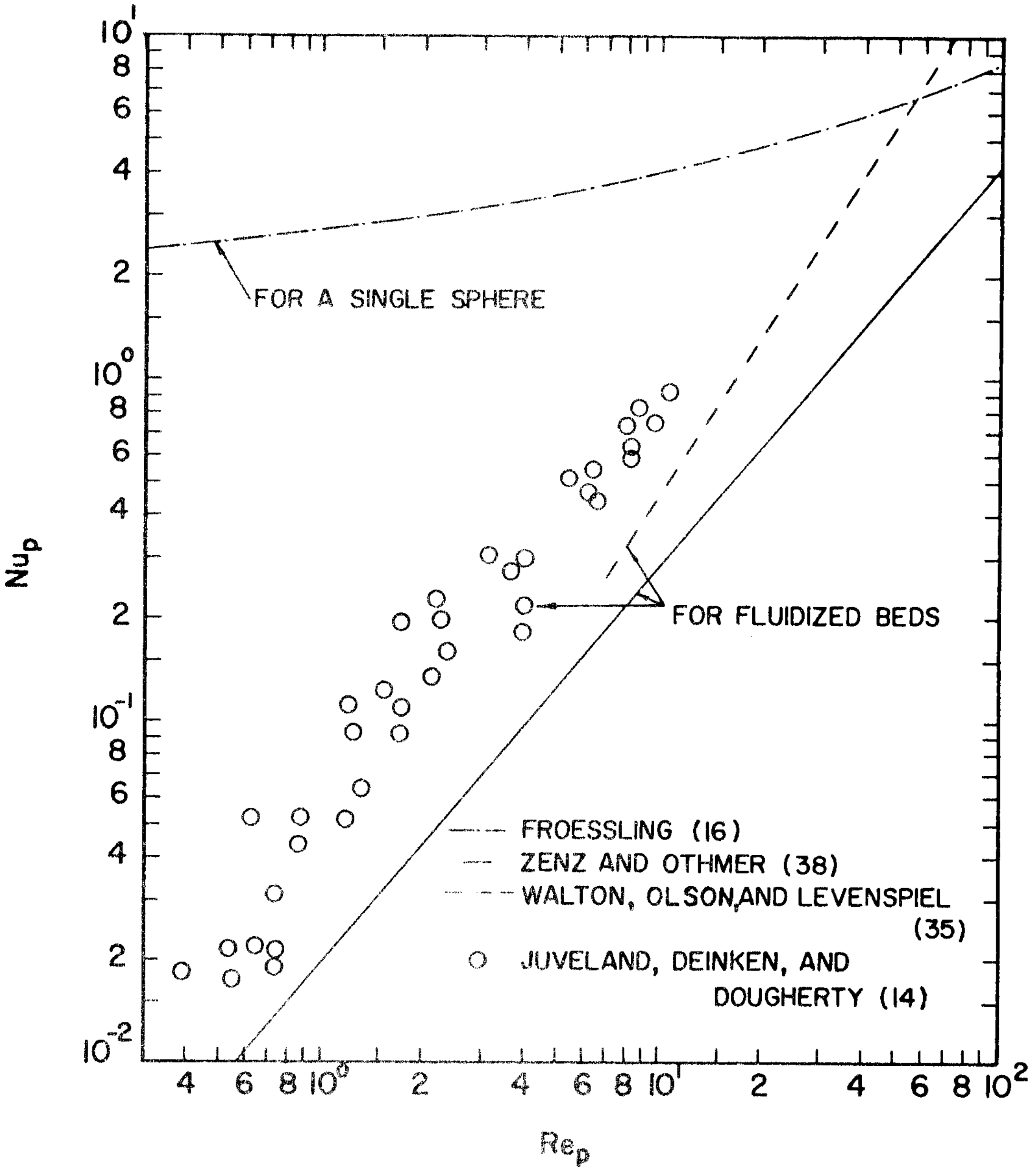

Figure 1. Particle-to-Fluid Nusselt Numbers in a Fluidized Bed vs. Particle Reynolds Number

for fluidized beds are one to two orders of magnitude lower than for a single sphere. Juveland, Deinken, and Dougherty explained these low values in terms of poor gas-solid contacting resulting from gas by-passing around aggregates of particles.

Surface-to-Fluidized-Bed Heat Transfer

Heat transfer from a surface to the fluidized bed has been investigated for both external wall and internal heating surfaces (1). It has been observed that a plot of the heat transfer coefficient, h, versus the mass velocity, G, has a maximum. The data of Lemlich and Caldas (17) shown in Figure 2 illustrate this fact.

Several workers have developed correlations to predict the maximum Nusselt number. Most of these correlations are power functions of the Archimedes number, Ar. Martyushin and Varygin; Zabrodskii; and Gel'perin, Ainshtein, and Romanova, as reviewed by Ainshtein and Gel'perin (1) report the exponent on Ar to be in the range, 2/10 to 1/4. Agreement among workers is poor, probably because gas properties, void fractions, measurement location, and bed geometry were different among the various investigations.

Gel'perin, Ainshtein, and Romanova, as reviewed by Ainshtein and Gel'perin (1) measured heat transfer from a vertical bundle in a fluidized bed and obtained the following correlation for the maximum Nusselt number:

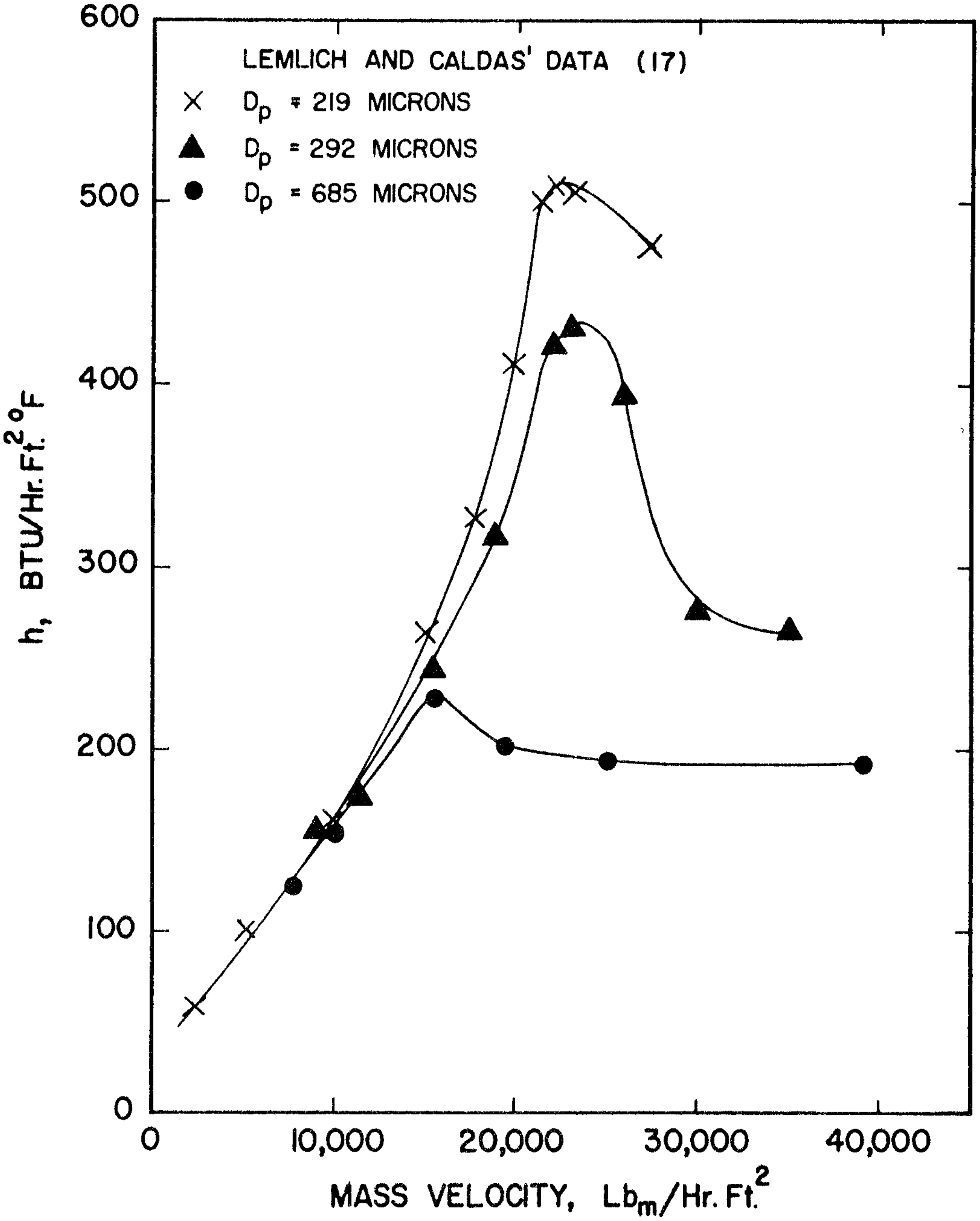

Figure 2. Typical Heat Transfer Coefficients vs. Mass Velocity Curves

$$Nu_{max} = 0.64\ Ar^{0.22}\left(\frac{S}{d_t}\right)^{0.09} \tag{7}$$

where

$$Ar = \frac{g\,D_p^3}{\nu^2}\ \frac{\rho_s - \rho_f}{\rho_f}$$

S = distance between the axes of tubes

d_t = tube diameter

There have been numerous correlations for the particle Reynolds number when the Nusselt number is a maximum (1). Most workers present their data as a power function of Ar, and they agree that the exponent is approximately 1/2. Calculated Reynolds numbers differ by an order of magnitude (1). The correlation presented by Sarits, as reviewed by Ainstein and Gel'perin (1) gives the largest values. His correlation is

$$Re_{opt} = 0.66\ Ar^{1/2} \tag{8}$$

where Re_{opt} is the particle Reynolds number when the Nusselt number is a maximum. The correlation presented by Martyushin and Varygin, as cited by Ainshtein and Gel'perin (1) gives the smallest values, i. e.

$$Re_{opt} = 0.118\ Ar^{1/2} \tag{9}$$

Surface-to-fluidized-bed heat transfer has been correlated in two branches, the ascending and descending branches of the h-G curve. Most of the available data represent the ascending branch.

Mickley and Trilling (24) measured heat transfer coefficients in a fluidized bed with a heated outer wall. They used air as the fluidizing medium and glass spheres of diameters: $D_p = 14.8 \times 10^{-4}$ ft, $D_p = 8.83 \times 10^{-4}$ ft, $D_p = 5.08 \times 10^{-4}$ ft, $D_p = 3.33 \times 10^{-4}$ ft, and $D_p = 2.29 \times 10^{-4}$ ft. These workers presented the following tentative dimensional correlation:

$$h = 0.0118 \left(\frac{\rho_m G}{D_p^3}\right)^{0.263} \qquad (10)$$

where h, ρ_m, G, and D_p are expressed in $\frac{\text{Btu}}{\text{hr ft}^2\,{}^\circ\text{F}}$, $\frac{\text{lb}_m}{\text{ft}^3}$, $\frac{\text{lb}_m}{\text{hr ft}^2}$ and ft respectively.

Gamson (10) correlated the data of Mickley and Trilling using dimensional analysis and obtained the following equation:

$$j_H = \frac{Nu}{Re_p Pr^{1/3}} = 2.0 \left(\frac{6G}{a\mu}\right)^{-0.69} (1 - \epsilon)^{-0.30} \qquad (11)$$

where

a = the particle surface area per unit volume of the bed

Walton and Levenspiel (20) studied heat transfer from an external wall to a dense-phase fluidized bed. They used glass, coal, and an industrial catalyst of several diameters as the solid phase. They correlated their data in terms of their proposed film theory, i. e.

$$\frac{h}{C_f G} = 0.6\, Re_p^{-0.7} \qquad (12)$$

Toomey and Johnstone (31) measured simultaneously heat transfer from a vertically inserted tube in the center of a fluidized bed and from the bed to a water cooled outer wall. Air was used as the fluidizing medium and several sizes of glass beads were used as the solid phase. These authors claimed that the quantity, $D_p G_{mf}/\mu$, is proportional to the Reynolds number in the void spaces adjacent to the wall, and that Log G/G_{mf} reflects the effect of the particle velocity. These workers obtained the following correlation for heat transfer to the outer wall:

$$Nu_p = 3.75 \left[\left(\frac{D_p G_{mf}}{\mu} \right) \text{Log} \left(\frac{G}{G_{mf}} \right) \right]^{0.47} \qquad (13)$$

where G_{mf} is the mass velocity when the bed begins to expand.

The data of Mickley and Trilling agree well with data of Toomey and Johnstone for particle concentrations over 20 lb_m/ft^3. Agreement between these two workers shows that heat transfer coefficients in fluidized beds are independent of heat flow direction.

These workers (31) also measured local heat transfer coefficients for transfer to the outer wall at various vertical positions in the bed. Two types of curves were observed, as is shown in Figure 3. In Type I the coefficients are higher at low strata and decrease as higher strata of the bed are examined. In Type II coefficients pass through a maximum. Which type exists depends on the particle size,

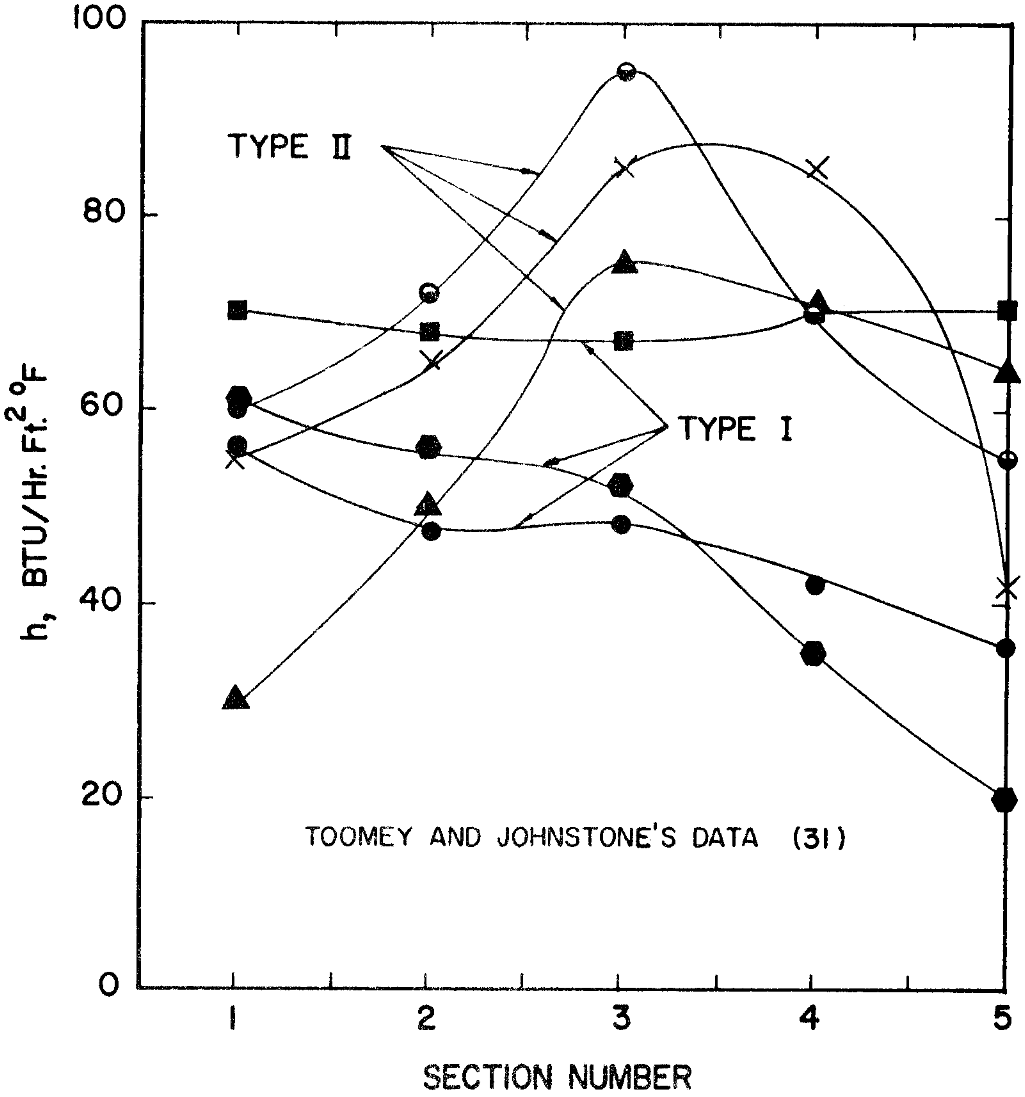

Figure 3. Types of Local Heat Transfer Coefficient Profiles

bed cross-sectional area and the fluidization height. They suggested the dimensionless group, $D_p L_f/A$, as a possible criterion, i. e.

$$\frac{D_p L_f}{A} > 0.008 \qquad \text{Type I} \tag{14a}$$

$$\frac{D_p L_f}{A} < 0.008 \qquad \text{Type II} \tag{14b}$$

Dow and Jakob (8) investigated heat transfer from an outer wall to a fluidized bed of two and three inches in diameter. Aerocat, pitch coke, and iron were used as solid phases and air was used in all cases as the fluidizing agent. They considered all possible variables that might affect heat transfer and with the aid of dimensional analysis their data gave the following experimental correlation:

$$\frac{hD_t}{k_g} = 0.55 \left(\frac{D_t}{L_f}\right)^{0.65} \left(\frac{D_t}{D_p}\right)^{0.17} \left[\frac{(1-\epsilon)\rho_s C_s}{\epsilon \rho_g C_g}\right]^{1/4} \left(\frac{D_t G}{\mu}\right)^{0.8} \tag{15}$$

The data of Dow and Jakob extend over a mass velocity range of about 50 to 300 $lb_m/hr\ ft^2$. This correlation fits the data well over this range but the exponent on the mass velocity, G, seems to decrease as G approaches and increases beyond 300 (18, p. 197). The mass velocities investigated by both Mickley _et al._ and Walton _et al._ were greater than 300. Gamson reports an exponent of 0. 31 on G for the data of Mickley and Trilling; Walton and Levenspiel report an exponent of 0. 30 on G. Van Heerden _et al._ (32) report an exponent on 0.45 on G.

Lemlich and Caldas (17) investigated the descending branch of the h-G curve for external wall heat transfer to a fluidized bed. Water was used as the fluidizing agent and glass spheres were the solid phase. They correlated the heat transfer j factor within ± 19 percent as follows:

$$j_H = \frac{Nu_p}{Re_p Pr^{1/3}} = 1.4 \left(\frac{D_t}{D_p}\right)^{0.79} \left(\frac{D_t G}{\mu}\right)^{-1} \epsilon^{-1} \qquad (16)$$

Rukenshtein, as cited by Ainshtein and Gel'perin (1) also investigated the descending branch of the curve for external wall heat transfer to a fluidized bed. This experimenter correlated his data in terms of the Reynolds, Prandtl, Archimedes, and Nusselt numbers, i. e.

$$Nu_p = 0.067\, Re_p^{0.237} Pr^{1/3} Ar^{0.522} \qquad (17)$$

Sarkits, as cited by Ainshtein and Gel'perin (1) investigated both the ascending and descending branch of the h-G curve for a fluidized bed with an internal coil heater. For the ascending branch the author proposed the following correlation:

$$Nu_p = 0.0133\, Re_p^{0.4} Ar_b^{0.27} Pr^{1/3} \left(\frac{C_s}{C_g}\right)^{0.45} \left(\frac{D_t}{D_p}\right)^{0.16} \left(\frac{H_0}{D_p}\right)^{0.45} \qquad (18)$$

For the descending branch the following correlation was proposed:

$$Nu_p = 0.00705\, Re_p^{-0.14} Ar_b^{0.49} Pr^{1/3} \left(\frac{C_s}{C_g}\right)^{0.45} \left(\frac{D_t}{D_p}\right)^{0.16} \left(\frac{H_0}{D_p}\right)^{0.45} \qquad (19)$$

where

H_0 = height of the surface

Traber, Pomerantsev, Mukhlenov, and Sarkin, as cited by Ainshtein and Gel'perin (1) studied heat transfer from an internal coil heater to a fluidized bed for both the ascending and descending branches of the h-G curve. They excluded the heat capacity ratio, i. e., for the ascending branch

$$Nu_p = 0.024\, Re_p^{0.65} Ar_b^{0.1} Pr^{1/3} \left(\frac{D_t}{D_p}\right)^{0.13} \left(\frac{H_0}{D_p}\right)^{0.16} \tag{20}$$

for the descending branch

$$Nu_p = 0.0165\, Re_p^{-0.34} Ar_b^{0.57} Pr^{1/3} \left(\frac{D_t}{D_p}\right)^{0.13} \left(\frac{H_0}{D_p}\right)^{0.16} \tag{21}$$

Kagan, Fastovskii, and Rovinskii, as cited by Ainshtein and Gel'perin (1) studied the ascending branch of the h-G curve for heat transfer from a coil in a fluidized bed. They proposed a correlation in terms of the particle Reynolds number, void fraction, particle and equipment dimensions, and fluid and solid properties, i. e.

$$\frac{Nu_p\, \epsilon}{6(1-\epsilon)} = 0.019 \left[\frac{Re_p}{6(1-\epsilon)}\right]^{0.6} Pr^{1/3} \left(\frac{C_s \rho_s}{C_g \rho_g}\right)^{0.4} \left(\frac{S - d_t}{D_p}\right)^{0.27} \tag{22}$$

where

d_t = coil tube diameter

S = coil tube spacing

Vreedenberg (33) investigated heat transfer from a horizontal heating tube in a fluidized bed. This worker correlated the Nusselt number in terms of the Reynolds number, void fraction, and fluid and solid properties, i. e.

$$Nu_t = \frac{hd_t}{k_g} = 0.66\left(\frac{C_s\mu}{k_g}\right)^{0.3} \left[Re_t \frac{(1-\epsilon)\rho_s}{\epsilon \quad \rho_g} \right]^{0.44} \tag{23}$$

Gel'perin, Kruglikov, and Ainshtein, as cited by Ainshtein and Gel'perin (1) also studied heat transfer from a horizontal tube to a fluidized bed. These experimenters reported the following correlation for the ascending branch:

$$\frac{Nu_p \; \epsilon}{6(1-\epsilon)} = 1.18 \left[\frac{Re_p}{6(1-\epsilon)}\right]^{0.32} \tag{24}$$

As previously mentioned, Toomey and Johnstone (31) simultaneously measured heat transfer with respect to the outer wall and a tube inserted vertically in the center of the bed. This study enabled a comparison of external surface and internal surface heat transfer coefficients. Figure 4 is a plot of the ratio of internal to external heat transfer coefficients versus the mass velocity, G.

Even though particle size was varied about 15 fold, the correlation is quite satisfactory. This correlation indicates that at low mass velocities internal coefficients are three to four times greater than the corresponding external coefficients. As the mass velocity is increased, this ratio decreases and becomes less than one when G is greater than 1000. These workers presented no correlation for the internal heat transfer coefficients.

Mickley and Trilling (24) investigated heat transfer in a fluidized bed with an internal vertical heater at the center of the bed.

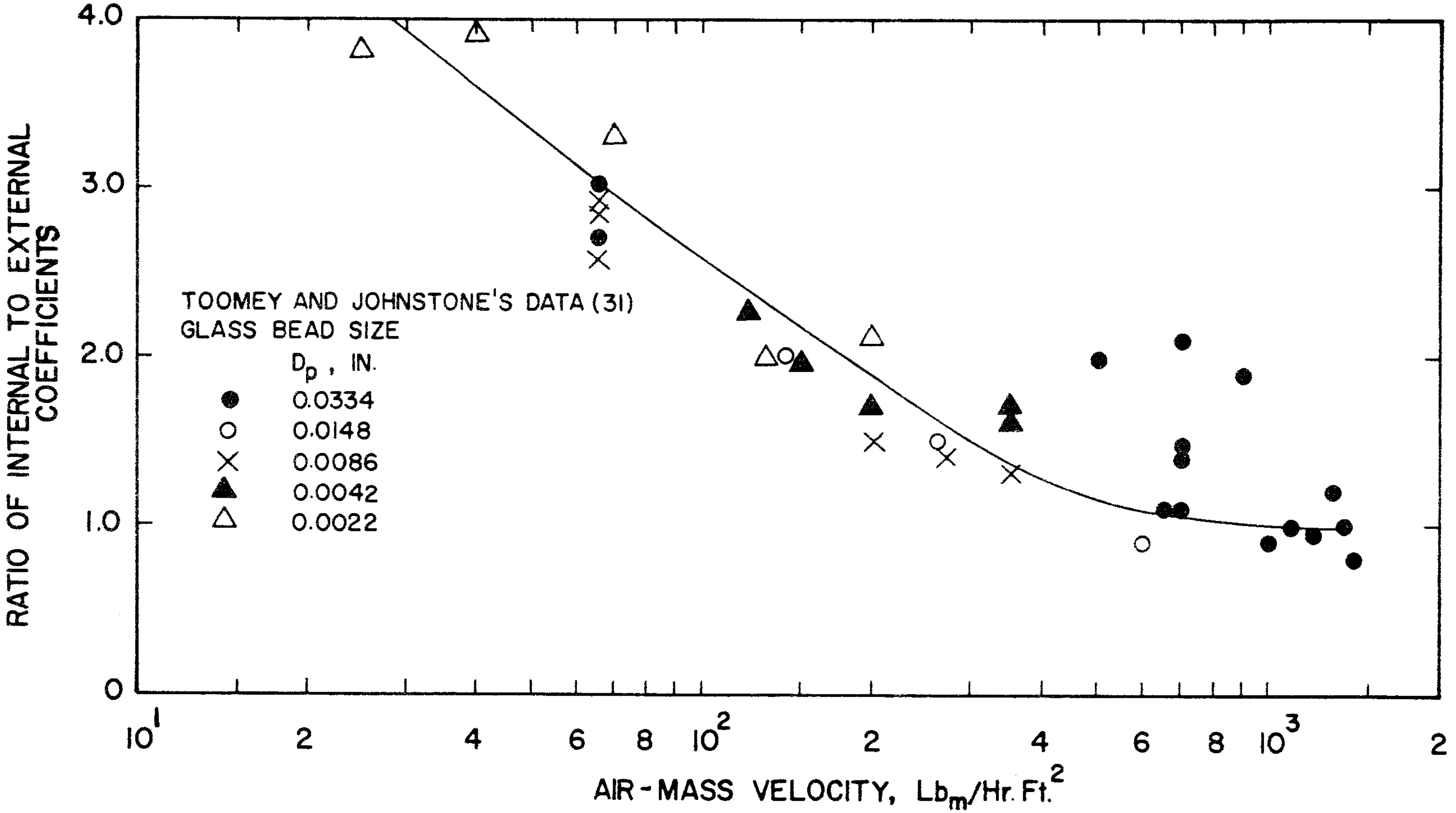

Figure 4. Ratio of Internal Surface to External Surface Heat Transfer Coefficients vs. Mass Velocity

These authors used several sizes of glass beads as the solid phase and air as the fluidizing agent. Gamson (10) correlated their data in terms of j factors for heat transfer, i. e.

$$j_H = \frac{Nu_p}{Re_p Pr^{1/3}} = 2.53 \left(\frac{6\,G}{a\,\mu}\right)^{-0.8} (1 - \epsilon)^{-0.3} \tag{25}$$

Gel'perin, Kruglikov, and Ainshtein, as cited by Ainshtein and Gel'perin (1) experimentally investigated heat transfer from a vertical tube in a fluidized bed. These authors considered several radial locations of the vertical tube. The following correlation was proposed:

$$\frac{Nu_p\,\epsilon}{6(1-\epsilon)} = 1.18 \left(\frac{G_{mf}}{G}\right)^{0.2} \left[\frac{Re_p}{6(1-\epsilon)}\right]^{0.285} \left(1 - \frac{r}{R}\right)^{0.36} \tag{26}$$

where

r = the radial position in the bed

R = the radius of the bed

Vreedenberg (34) studied the effect of tube location on heat transfer coefficients by using a vertical tube at three locations. The ratio of the heat transfer coefficient at a radial location, r, to that at the axis varied as is shown in Figure 5. This investigation indicates that the largest heat transfer coefficients occur at $r/R = 0.4$.

Using the results of Vreedenberg, and assuming the heat transfer coefficient to be proportional to $(1 - \epsilon)$, Wender and Cooper (37) reviewed the literature and proposed the following correlation:

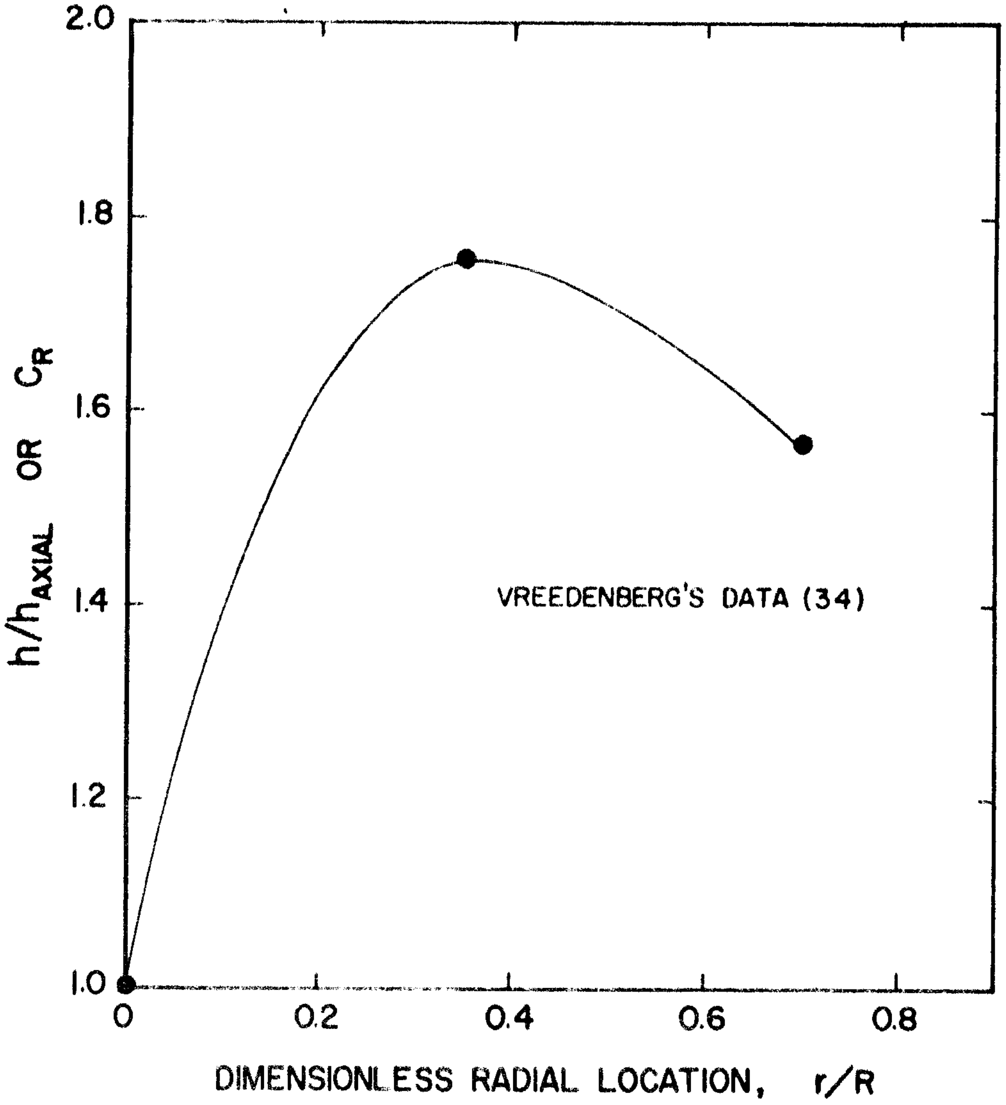

Figure 5. Correction for Nonaxial Tube Location

$$\frac{Nu_p}{1-\epsilon} = 0.033\, C_R Re_p^{0.23} \left(\frac{C_s}{C_g}\right)^{0.80} \left(\frac{\rho_s}{\rho_g}\right)\left(\frac{C_g \rho_g}{k_g}\right)^{0.43} \qquad (27)$$

where C_R is read from Figure 5 and $C_g \rho_g / k_g$ has the units of hour per square foot.

Both Gel'perin *et al.* and Vreedenberg discuss the effects of tube location on the heat transfer coefficient as a function of only the tube location. The results of Toomey and Johnstone (31), as they are shown in Figure 4, indicate that the effect is also a function of the mass velocity. This leaves some question as to the validity over a large mass velocity range of the correlations presented by Gel'perin *et al.* and Wender and Cooper. The correlation presented by Gel'perin *et al.* indicates that the Nusselt number approaches zero as the vertical tube location approaches the outer wall. This is not feasible. Cooper and Wender propose an exponent of one for $(1 - \epsilon)$ which is in disagreement with several authors (1; 10; 23; 24; 27, p. 47).

Gel'perin, Ainshtein, and Romanova, as cited by Ainshtein and Gel'perin (41) studied heat transfer from a vertical tube in a bundle of vertical tubes located in a fluidized bed. They proposed a correlation of the Nusselt number as follows:

$$Nu_p = 0.64\, Ar^{0.22} \left(\frac{S}{d_t}\right)^{0.09} \left[1 - K\left[\mathrm{Tanh}\left(\frac{bG}{G_{mf}} - b\right)\right]\right] \qquad (28)$$

where

$$b = 2.24 - 1.29\left(\frac{G_{mf}D_p}{\mu} + 0.4\right)^{-1}$$

$$K = 0.73\left(1 - \frac{r}{R}\right)$$

This correlation does not indicate a dependence on the void fraction.

Noë (27) made a preliminary study of heat transfer from a vertical tube located in a bundle of vertical tubes in a fluidized bed. Air was used as the fluidizing agent and two sizes of glass spheres were used as the particulate phase. Mass velocities from 700 to 2800 $lb_m/hr\ ft^2$ were investigated. The heat transfer coefficients were observed to be proportional to the particle fraction, $(1 - \epsilon)$, raised to about the 1/2 power. It was also noted that local heat transfer coefficients in the dense phase varied with tube location. Lowest local coefficients in the dense phase were observed at the center tube location and the highest values were observed at tube locations near the wall. For the mass velocities investigated, this observation is in agreement with the results of Toomey and Johnstone (see Figure 4).

Presently Proposed Heat Transfer Model

The model that is proposed here is an extension of the model proposed by Ziegler, Koppel, and Brazelton (40). In formulating this model the following assumptions are made:

1. Fluidized particles are spheres of uniform diameter.

2. The physical properties of the solids and the fluids are constant.

3. Particles from the bulk of the fluidized bed, having the bulk medium temperature, T_b, move adjacent to the transfer surface. While adjacent to the surface, the particle receives energy by convection from the fluid around the particle. This fluid is assumed to be at the arithmetic mean of the wall and the bulk medium temperature, i. e.

$$T_f = \frac{T_w + T_b}{2} \tag{29}$$

   After some time the particle leaves the surface and returns to the bulk of the bed. This mechanism is sketched for a typical particle in Figure 6.

4. The major portion of the heat transfer occurs by the mechanism described above.

5. Radiant heat transfer from the surface to the particle is neglected. Baddour and Yoon (3) have shown this effect to be negligible for packed beds at temperatures below 600° C.

6. Conduction at the point of contact is negligible. Botterill _et_ _al._, as cited by Ziegler, Koppel, and Brazelton (40), have shown that this effect is very small.

The boundary value problem describing the temperature in the particle while it is near the wall, given the above assumptions, may

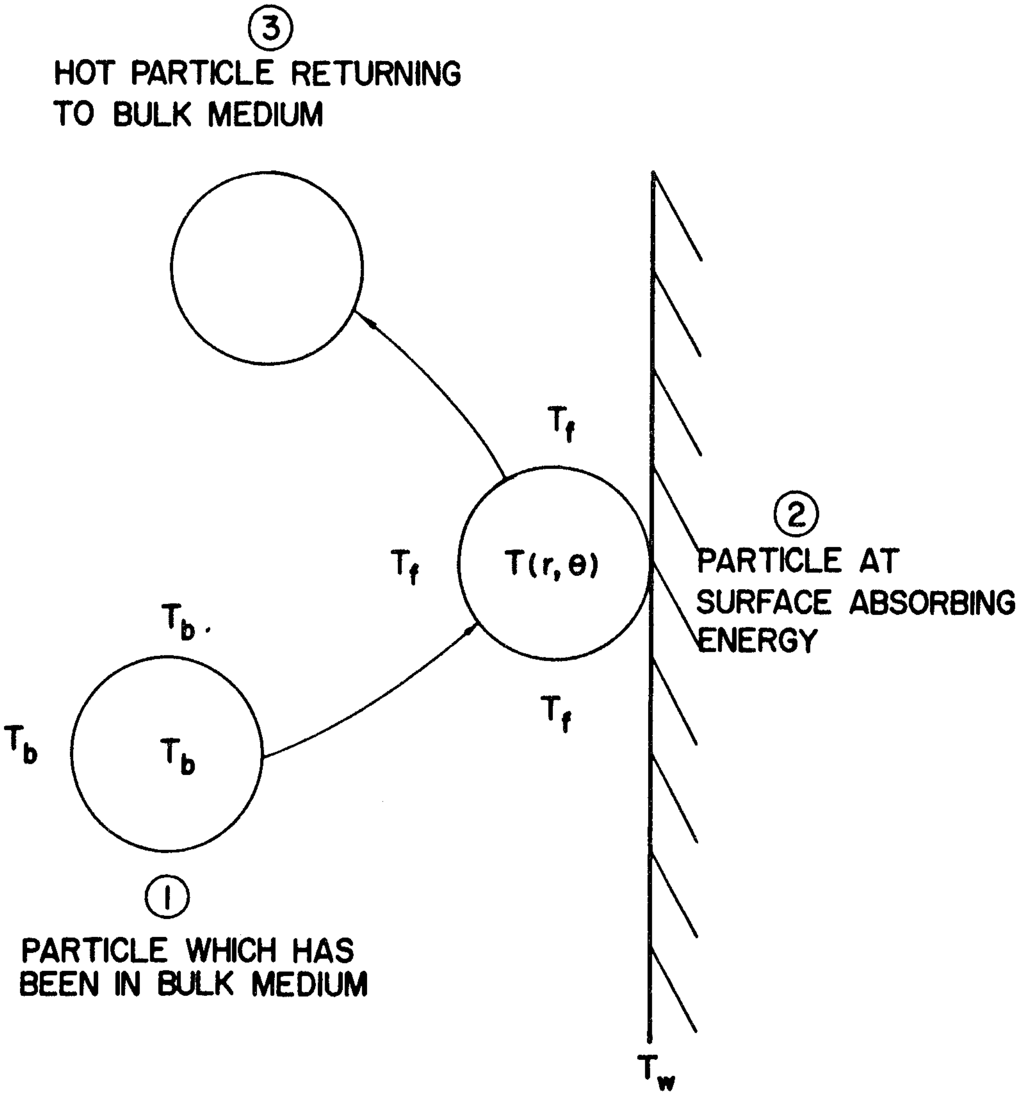
③
HOT PARTICLE RETURNING TO BULK MEDIUM
T_f
T_f
$T(r,\theta)$
②
PARTICLE AT SURFACE ABSORBING ENERGY
T_b
T_b
T_b
T_f
①
PARTICLE WHICH HAS BEEN IN BULK MEDIUM
T_w

Figure 6. Schematic of Proposed Heat Transfer Mechanism

be written as follows:

$$\frac{\partial \Phi(\eta, \tau)}{\partial \tau} = \frac{1}{\eta^2} \frac{\partial}{\partial \eta}\left(\frac{\eta^2 \partial \Phi(\eta, \tau)}{\partial \eta}\right)$$

$$\Phi(\eta, 0) = 1 \tag{30}$$

$$\frac{\partial \Phi(0, \tau)}{\partial \eta} = 0$$

$$\frac{\partial \Phi(1, \tau)}{\partial \eta} + N\,\Phi(1, \tau) = 0$$

where

$$N = \frac{h_c D_p}{2 k_s}$$

$$\Phi = \frac{T_f - T}{T_f - T_b}$$

$$\tau = \frac{4 k_s \theta}{\rho_s C_s D_p^2}$$

$$\eta = \frac{2r}{D_p}$$

The solution to this boundary value problem (40) is well known and is given by the following equation:

$$\Phi = \frac{2N}{\eta} \sum_{1}^{\infty} e^{-\lambda_n^2 \tau} \left[\frac{[\lambda_n^2 + (N-1)^2] \sin \lambda_n}{\lambda_n^2 [\lambda_n^2 + N(N-1)]}\right] \sin \lambda_n \eta \tag{31}$$

where the eigenvalues, λ_n, are the roots of

$$\lambda_n \cot \lambda_n = 1 - N \tag{32}$$

Since the fluid velocity near the wall is small, the Nusselt number for fluid-to-particle heat transfer near the wall can be approximated by the limiting value of Froessling's single spherical particle correlation. This value will be high since Nusselt numbers in a fluidized bed are lower than those predicted by Froessling's correlation; however, this will compensate for omitting transfer by other mechanisms. The following approximation can now be made for N:

$$N = \frac{h_c D_p}{2\ k_s} \cong \frac{2\ k_g D_p}{D_p 2 k_s} = \frac{k_g}{k_s} \tag{33}$$

For most gases and solids used in fluidization,

$$\frac{k_g}{k_s} < 0.1 \tag{34}$$

The first eigenvalue, λ_1, is small (40) and can be approximated by expanding the eigenvalue equation in a power series, i. e.

$$\lambda_1 - \frac{\lambda_1^{\ 3}}{6} + \ldots = \frac{\lambda_1}{1 - N} - \frac{\lambda_1^{\ 3}}{2(1 - N)} + \ldots$$

$$\lambda_1^{\ 2} = \frac{6\ N}{2 + N} \cong 3\ N \tag{35}$$

$$\lambda_1 \cong \sqrt{3N}$$

From eigenvalue tables (6, p. 492), it can be shown that for all N, $\lambda_n > 4$ if $n \geq 2$; therefore, only the first term in the series solution is of any significance. By using the approximation for λ_1 and series approximations for the trigonometric functions, Equation 31, evaluated at $\eta = 1$ can be reduced for small N to

$$\Phi = e^{-3N\tau} = e^{-M\theta} \tag{36}$$

where

$$M = \frac{12\ k_g}{\rho_s C_s D_p^{\ 2}}$$

Calculations show that Equation 36 is within ten percent of Equation 31 for all $N < 0.2$.

The quantity, M, is independent of the solid thermal conductivity; therefore, this model predicts that the solid thermal conductivity has no effect on heat transfer, an experimentally observed fact (22, p. 303).

Equation 36 can now be used to evaluate the instantaneous rate of heat transfer at the surface of the particle as a function of the time it has been at the wall. Using the limiting Nusselt number of two,

$$q_p(\theta) = h_c \Pi D_p^{\ 2} [T_f - T(1)] \tag{37a}$$

$$q_p(\theta) = 2k_g \Pi D_p (T_f - T_b) e^{-M\theta} \tag{37b}$$

$$q_p(\theta) = \Pi D_p k_g (T_w - T_b) e^{-M\theta} \tag{37c}$$

The length of time that a particle remains at the surface will vary, conceivably from zero to infinity. Let $f(\theta)\ d\theta$ be defined as the fraction of particles at the surface at any time which has been at the surface for a time between θ and $\theta + d\theta$. It seems reasonable that $f(\theta)$ will have a maximum, that is, a contact time which occurs most often. A function which is convenient to use and does have such a maximum is the gamma distribution function, i. e.

$$f(\theta) = \frac{1}{a!\,\beta^{a+1}}\,\theta^{a} e^{-\theta/\beta} \tag{38}$$

The time average heat flux is then given by

$$q_p = \int_0^\infty f(\theta) q(\theta) d\theta = \frac{\Pi D_p k_g (T_w - T_b)}{(1 + \frac{M\bar{\theta}}{a+1})^{a+1}} \tag{39}$$

where

$\bar{\theta}$ = the average contact time

Ziegler, Koppel, and Brazelton observed that the distribution shape factor, a, equal to one gave a dependency on the solid heat capacity which was consistent with their experimental results. With this in mind, a value of one will be used for a, i. e.

$$q_p = \frac{\Pi D_p k_g (T_w - T_b)}{(1 + \frac{M\bar{\theta}}{2})^2} \tag{40}$$

In order to obtain an expression for the heat transfer flux based on the wall surface, the number of particles at the surface per unit area will have to be derived. The number of particles per unit area,

γ_p, will be related to the particle fraction, $(1 - \epsilon)$, and the particle diameter. The heat transfer coefficient has been reported (10; 23; 24; 27, p. 47) to be proportional to $(1 - \epsilon)^{0.48}$; therefore, a relation of the following form can be proposed:

$$\gamma_p = K_1 (1 - \epsilon)^{0.48} f(D_p) \tag{41}$$

For a completely covered surface with hexagonal packing, γ_p and $(1 - \epsilon)$ are

$$\gamma_p = \frac{2/\sqrt{3}}{D_p^{\,2}} \tag{42}$$

$$(1 - \epsilon) = 14/27 \tag{43}$$

Therefore

$$K_1 = 1.59 \tag{44}$$

and

$$f(D_p) = \frac{1}{D_p^{\,2}} \tag{45}$$

By substituting Equations 44 and 45 into Equation 41, we can get the following equation for γ_p:

$$\gamma_p = \frac{1.59(1 - \epsilon)^{0.48}}{D_p^{\,2}} \tag{46}$$

By multiplying q_p by γ_p, we can write an equation for the heat flux from the wall surface, i. e.

$$q = \gamma_p q_p = \frac{5.0(1-\epsilon)^{0.48} k_g (T_w - T_b)}{D_p \left(1 + \frac{6k_g \bar{\theta}}{\rho_s C_s D_p^2}\right)^2} \tag{47}$$

The particle Nusselt number is

$$Nu_p = \frac{5(1-\epsilon)^{0.48}}{\left(1 + \frac{6k_g \bar{\theta}}{\rho_s C_s D_p^2}\right)^2} \tag{48}$$

The average contact time, $\bar{\theta}$, would be affected by the following variables:

1. mass velocity, G
2. particle diameter, D_p
3. particle density, ρ_s
4. gas density, ρ_g
5. gas viscosity, μ
6. mass velocity at minimum fluidization, G_{mf}
7. acceleration due to gravity, g

The variable, G_{mf}, is not an independent variable. It can be related to the other variables by the dimensionless correlation presented by Miller and Logwinuk (25), i. e.

$$G_{mf} = \frac{0.00125\, D_p^2 (\rho_s - \rho_g)^{0.9} \rho_g^{1.1} g}{\mu} \tag{49}$$

With the aid of dimensional analysis the following dimensionless groups can be obtained:

$$\left(\frac{G}{G_{mf}}\right), \qquad \left(\frac{\rho_s}{\rho_g}\right), \qquad \left(\frac{\bar{\theta}\, g^{1/2}}{D_p^{1/2}}\right), \qquad \left(\frac{D_p G}{\mu}\right)$$

With these groups an equation of the following form for $\bar{\theta}$ is obtained in the form:[1]

$$\bar{\theta} = C_1 \left(\frac{D_p}{g}\right)^{1/2} Re_p^{\,e} \left(\frac{G}{G_{mf}}\right)^f \left(\frac{\rho_s}{\rho_g}\right)^{\ell} \qquad (50)$$

The exponents in this equation have to be determined experimentally. Substituting Equation 50 into Equation 48, the following is obtained:

$$Nu_p = \frac{5.0(1-\epsilon)^{0.48}}{\left[1 + \frac{6k_g C_1}{\rho_s C_s D_p^2} \left(\frac{D_p}{g}\right)^{1/2} Re_p^{\,e} \left(\frac{G}{G_{mf}}\right)^f \left(\frac{\rho_s}{\rho_g}\right)^{\ell}\right]^2} \qquad (51)$$

---

[1] It would be expected that the average contact time, $\bar{\theta}$, would also depend on the particle fraction, $(1-\epsilon)$; however, no such dependency was observed experimentally in the correlation obtained. The assumed temperature of the gas surrounding the particle of the wall and the average contact time are not independent in the model and the effect of particle fraction appears to be not too significant in the range of the present experiment. In the final equation (51) the interdependency of assumed temperature and contact time cancel.

EXPERIMENTAL EQUIPMENT

The experimental equipment was designed and assembled in order that a study could be made of local shell-side heat transfer coefficients in a fluidized bed tubular heat exchanger. Some of the equipment components used in this study were used in a preliminary study undertaken by Noë (27, p. 10). Since a complete description of these components is given by Noë, only modifications and additions to these components will be discussed in detail. The major components of the equipment include the model fluidized bed tubular heat exchanger, the air blower, the direct current power source, the cyclone separator, and measuring devices. A general set-up of the equipment, with the exception of the air source, is shown in the photograph in Figure 7.

The Model Heat Exchanger

The model heat exchanger consisted of a tube bundle containing a heating element and a shell. The shell consisted of a conical air distributing section, a test section, and a disengaging section.

The conical air distributing section was used to expand the flow cross section from 2 inches to 5.75 inches. Two thermocouples were inserted through the walls of this section to measure the air inlet temperature. This section is described by Noë (27, p. 10).

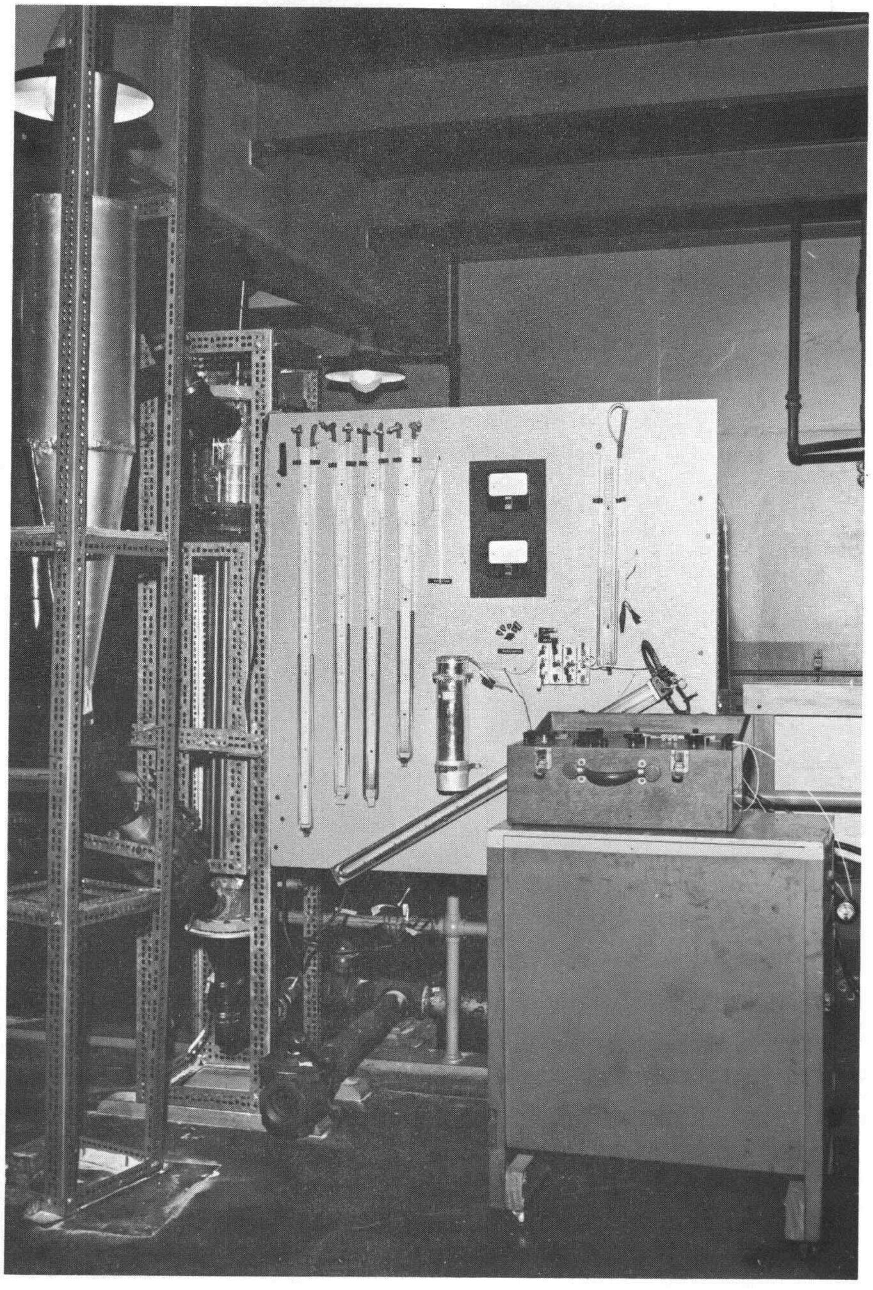

Figure 7. Photograph of Experimental Equipment

The disengaging section was a nine-inch OD by 1/8-inch wall by 12 inches long, cast acrylic tube. Four, three-inch diameter acrylic nipple exhaust ports were mounted on the tube one inch from the top. Flexible rubber tubes were connected to the nipples for exhaust to the cyclone separator. The disengaging and test sections were connected as described by Noë (27, p. 13). A thermocouple was inserted through the wall of the disengaging section 3/4 inch from the bottom. This thermocouple was used to measure the temperature of the particle-air mixture in the disengaging section.

The test section was constructed from a six-inch OD 44-inch long cast acrylic tube with a 1/8-inch wall. A three-inch OD acrylic nipple inlet was mounted two inches from the bottom for returning particles from the cyclone separator. A three-inch neoprene seated quick-opening valve was placed between the separator and the particle inlet to control the particle flow rate. Four thermocouples and thermocouple shields were mounted at 9. 25, 17. 25, 27. 25, and 38. 25 inches from the bottom. The shields consisted of cylinders made of fine wire mesh and were inserted through the test section shell. The thermocouples were placed inside the wire mesh shields to give contact with the gas only. Four pressure taps located 5. 5 inches from the bottom of the tube and every 11 inches thereafter were affixed to the test section. A description of the taps is given by Noë (27, p. 13). A transversing thermocouple was placed at a height of 8.5 inches from the bottom of the tube. This probe consisted of a 1/16-inch stainless steel tube and a thermocouple protruding out of the tube wall. The stainless steel tube goes across the tube bundle between rows of tubes as shown in Figure 8. A screw type moving device was used to move the thermocouple to various radial positions. This probe was designed to determine any radial variation in the bulk shell-side temperature. The test section was connected to the air intake section with a 1/2-inch thick, seven-inch diameter, plastic flange and secured by 12, two-inch by 1/4-inch bolts.

The tube bundle consisted of 19, 3/4-inch OD, 60 inches long, 321 stainless steel tubes arranged in a 1-1/16-inch triangular pitch. The tube layout is shown in Figure 8. One end of each tube was fitted with a 3/4-inch plastic plug to facilitate fitting into the lower tube sheet.

The top tube sheet, fabricated from two, one-inch thick 11-inch diameter, plywood disks was connected to the disengaging section by six, two-inch by 1/4-inch bolts.

The bottom tube sheet, placed between the air intake and test sections, consisted of 100 mesh wire cloth placed on 14 mesh wire screen.

The heating element, type 321 stainless steel tube, had a 3/4-inch OD by .012-inch wall and 60-inch length. The heating element

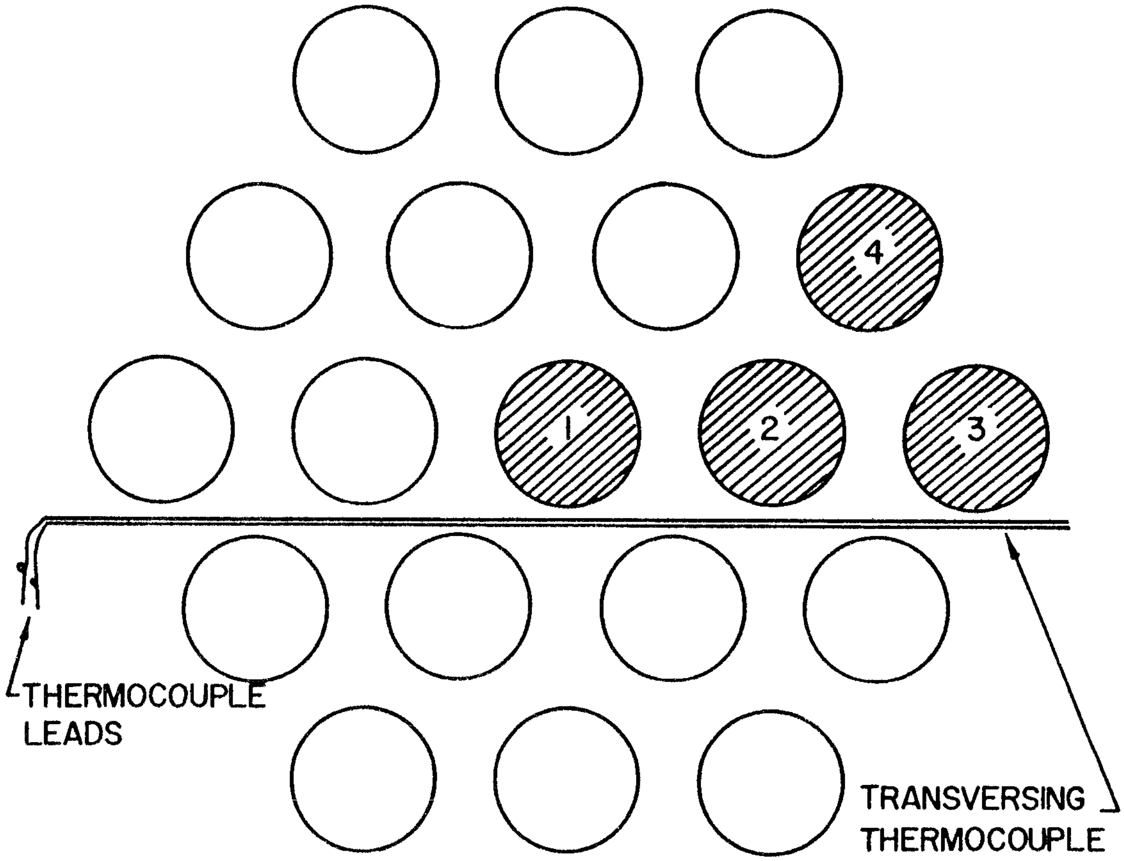
4
1
2
3
THERMOCOUPLE LEADS
TRANSVERSING THERMOCOUPLE

Figure 8. Tube Layout: Showing Locations of Heating Element and Transverse Thermocouple

was equipped with electrical connectors as described by Noë (27, p.17).

The entire model heat exchanger, excluding the air intake, was mounted in a three-foot long "cradle" made of slotted angle iron. This was mounted inside a 7.5-foot high vertical frame.

The Air Blower

Air was supplied from a Sutorbilt 8HB blower driven by a 30 hp, 1760 RPM General Electric AC induction motor. The blower was rated at 550 cfm (one atm. and 68° F) at 9 psi outlet pressure.

Three-inch standard steel pipe was used to carry the air to the model heat exchanger. To eliminate vibration from the blower, flexible hose was installed between the blower and the pipe entrance. The three-inch pipe was reduced to two inches and connected to the air intake section by a rubber hose.

The air flow rate was controlled by two gate valves. One, a two-inch-by-pass valve controlled the air flowing through a by-pass to the atmosphere. The other control valve was in the three-inch air supply line. A three-inch-quick-opening neoprene seated valve was used in another by-pass from the air supply line. This valve was physically placed near the quick-opening valve in the line which returns particles from the cyclone separator in order that both valves could be closed or opened simultaneously.

The air was metered by a two-inch diameter, 16 gauge, square edged orifice located in the three-inch air supply line. The orifice was machined accurately from a smooth brass plate to desired specifications, and pressure taps were located at the proper distances from the orifice plate. The orifice meter was calibrated with a pitot tube which was placed in the three-inch air supply line. Details of this calibration are given in Appendix B.

The Direct Current Power Supply

A battery charger and a constant voltage transformer were used to supply energy to the stainless steel tube. A diagram of the electrical circuit is shown in Figure 9, and a description of the components of the circuit is given by Noë (27, p. 17). The resistance in the circuit was adjusted so that the current was about 39 amperes.

The emf and current were measured by a DC voltmeter with a range of zero to three volts and a DC ammeter with a range from zero to 50 amps. Both instruments were manufactured by Simpson Electric Company and are accurate to ±2 percent at full scale.

The Cyclone Separator

In order to obtain measurements at gas velocities greater than the terminal velocity of the particles in the heat exchanger, a cyclone separator was designed and fabricated to separate the particles from the air leaving the model heat exchanger.

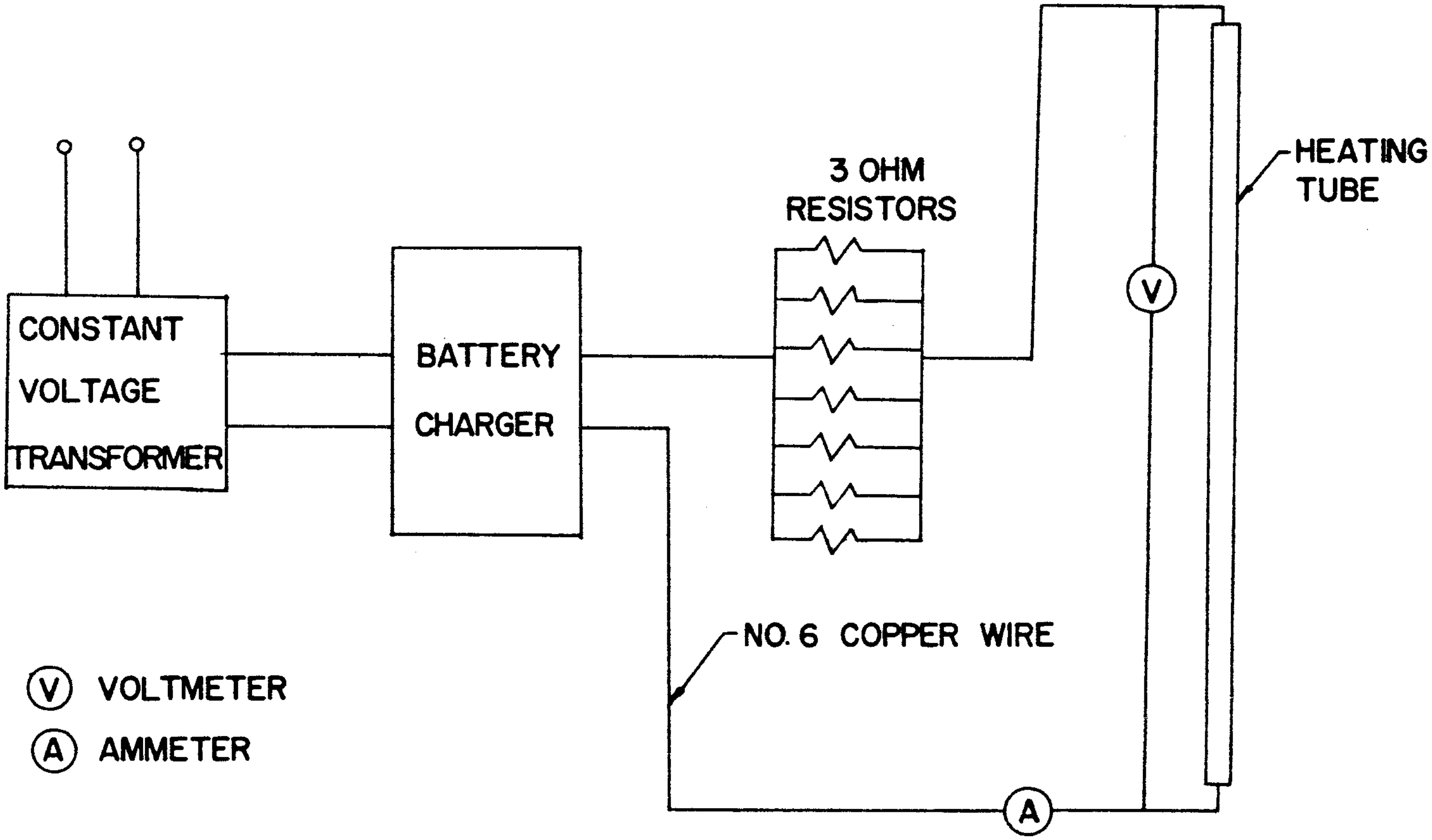
CONSTANT
VOLTAGE
TRANSFORMER
BATTERY
CHARGER
3 OHM
RESISTORS
HEATING
TUBE
V
NO. 6 COPPER WIRE
A
V VOLTMETER
A AMMETER

Figure 9. Diagram of Electrical System

The separator was made out of 1/32-inch steel sheet metal. It was 60 inches long and 12 inches in diameter. The various sections of the cyclone were proportioned as recommended by Perry (29, sec. 20 p. 69). A drawing of the separator is given in Figure 10.

Measuring Devices

The pressure drop across the bed and orifice was measured by a manometer system using Meriam manometer fluid with a specific gravity of 0.827. The supply line pressure was measured by a manometer using mercury as the fluid.

The wall temperature was measured at various positions by a thermocouple probe which moved up and down inside the tube wall. The probe consisted of two copper contacts rounded to the shape of the tube wall. A thermocouple was embedded in each contact but electrically insulated from the copper. Each copper contact was held in contact with the wall by a spring. An enlarged view of the probe is shown in Figure 11. A detailed description of the probe is given by Noë (27, p. 19).

All temperatures were measured with copper-constantan thermocouples. Number 30 B. and S. gauge, Leeds and Northrup thermocouple wire, was used. Thermocouple emf was read using a Leeds and Northrup potentiometer model 8662.

The probe thermocouples and the air inlet thermocouples were

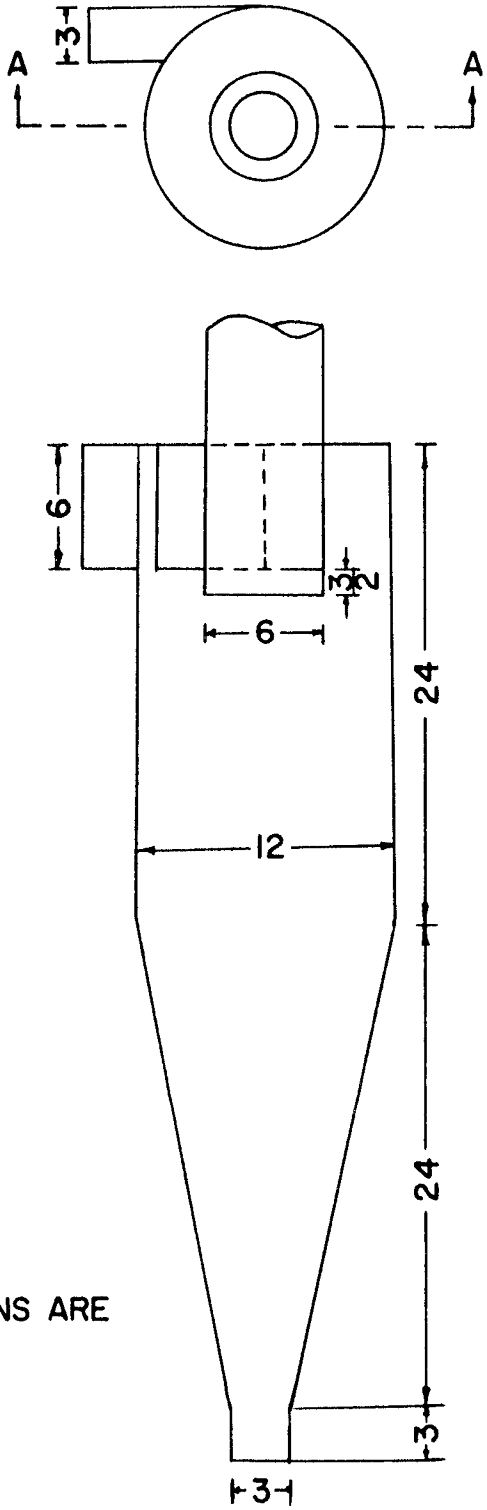
3
A
A
6
3/2
6
24
12
24
3
3

SECTION A-A

ALL DIMENSIONS ARE IN INCHES

Figure 10. Drawing of Cyclone Separator

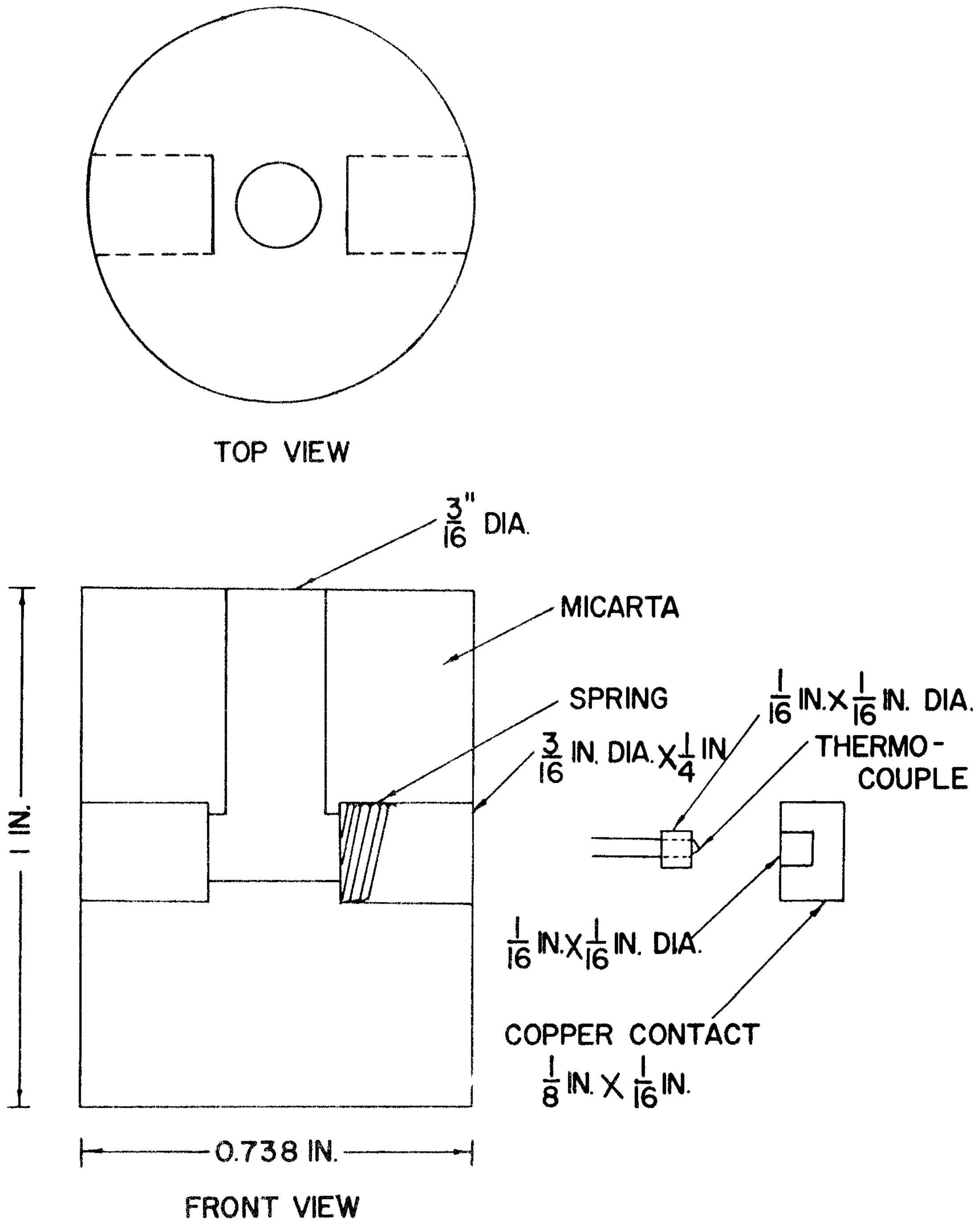
TOP VIEW
3/16" DIA.
MICARTA
SPRING
1/16 IN. X 1/16 IN. DIA.
3/16 IN. DIA. X 1/4 IN.
THERMO-COUPLE
1 IN.
1/16 IN. X 1/16 IN. DIA.
COPPER CONTACT 1/8 IN. X 1/16 IN.
0.738 IN.
FRONT VIEW

Figure 11. Exploded View of the Tube Wall Temperature Probe

each connected in series to read twice the average probe emf and twice the average air inlet emf respectively. Thermocouples placed in the shell-side of the model heat exchanger were used to determine the bulk temperature of the air flowing through. As previously mentioned, the transversing thermocouple was used to detect radial variation in the bulk air temperature. All reference junctions were kept in an ice bath at 32° F. A description of the thermocouple calibration and the tube wall probe temperature correction is given in Appendix C.

A switching system was used to complete the thermocouple circuits. A Leeds and Northrup type G speedomax recorder was used to record the probe readings and therefore indicate when the probe was at steady state.

EXPERIMENTAL PROGRAM

The objective of this investigation was to determine local and average heat transfer coefficients for transfer of energy from a heated tube in a tube bundle to air flowing through a fluidized bed at various operating conditions. The experimental program was designed to fulfill this objective.

The variables that are most likely to affect the transfer of energy from an internal surface to a fluidized bed can be broken into three general groups; (1) properties of the fluidizing medium and fluidized particles, (2) operating conditions and (3) equipment geometry and design.

Fluidizing medium's properties would include such quantities as thermal conductivity, density, heat capacity, and viscosity. Fluidizing particles' properties would include thermal conductivity, density, heat capacity, size, and shape. Operating conditions would include particle concentration and distribution, superficial gas velocity, heat flux, and the temperature driving force. The size, location, and arrangement of the heat transfer surface as well as the boundary geometry of the fluidized bed are also variables to consider.

Variables under consideration in this investigation are particle concentration or static bed height, particle distribution, superficial gas velocity and heating tube location. Heat flux, tube wall temperature profile, and vertical bulk gas temperature profile were measured in order to calculate the desired coefficients. Bed section pressure drops were also measured in order to calculate power requirements and particle distributions.

Air was used as the fluidizing medium. The air used was approximately at the same temperature for all runs which enabled keeping the thermal conductivity, heat capacity, viscosity and density of the air constant. Only one tube bundle configuration was considered.

Particle Size and Thermal Conductivity

Two types and three sizes of particles were used in this investigation. Glass spheres, manufactured by the Minnesota Mining and Manufacturing Company, of 0.0052 and 0.0151-inch average diameter were used. Aluminum particles, manufactured by Aluminum Metallurgical Granules, of 0.0306-inch average diameter were used. The average diameters were determined by arithmetic averages of measurements taken from photographs of microscope enlargements of the particles. The size distributions of the particles were also determined by such photographs; the distributions are shown in Figure 12. Representative photographs of the particles are shown in Figure 13. The fine and coarse glass spheres were screened to give 65/100 mesh and 20/35 mesh ranges respectively in order to have a more

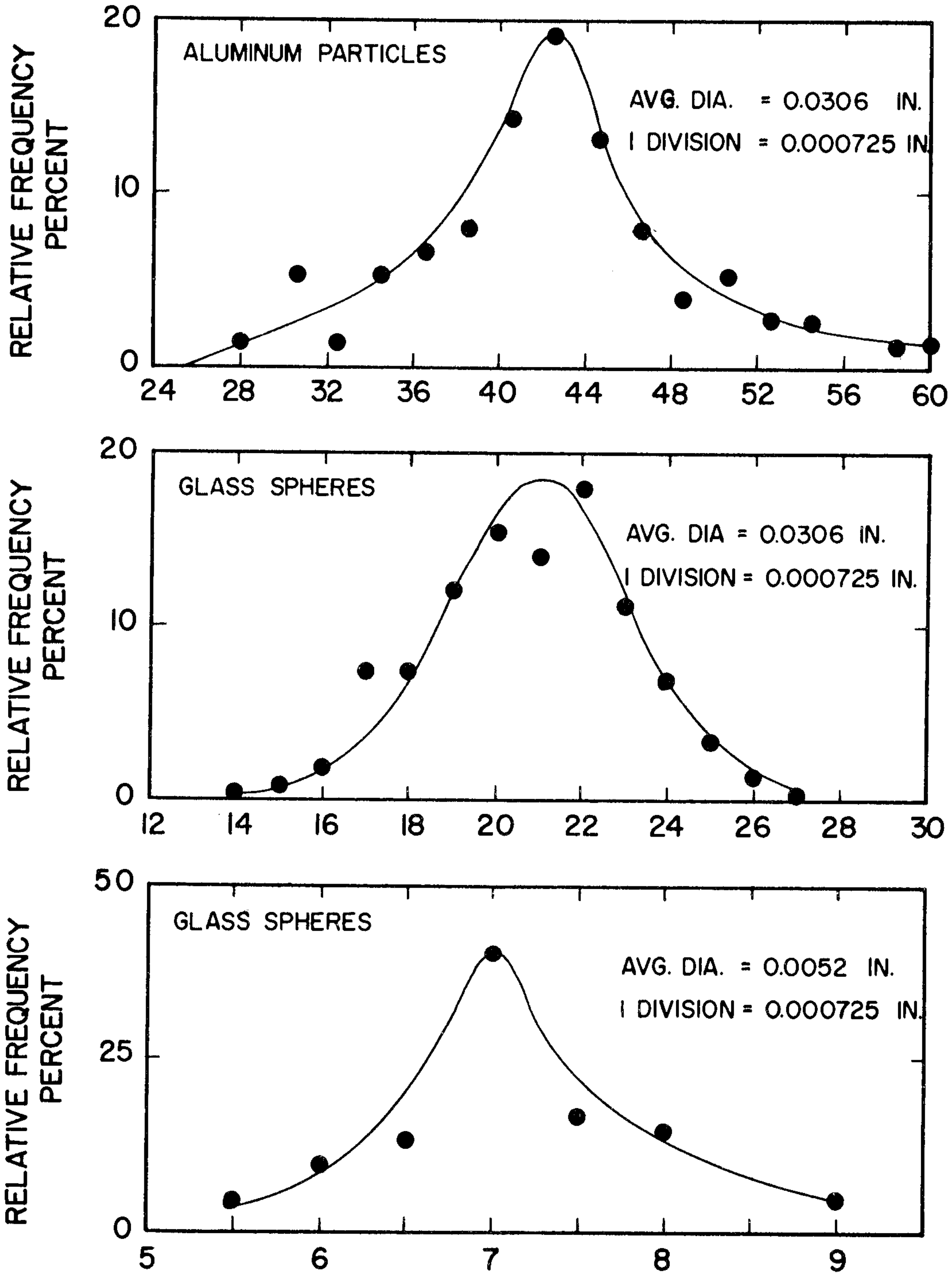

Figure 12. Particle Size Distributions

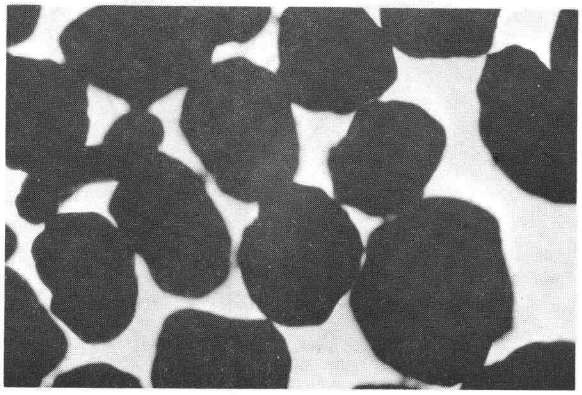

Aluminum Particles

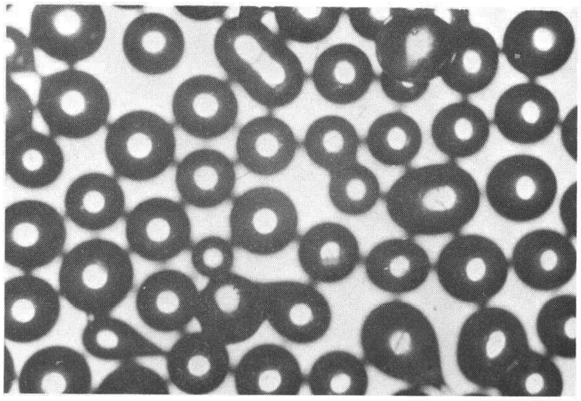

Coarse Glass Particles

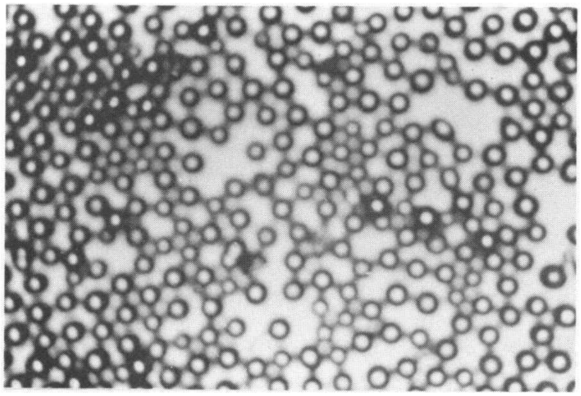

Fine Glass Particles

Figure 13. Photographs of Particles

narrow range. It can be seen from Figure 13 that the fine and coarse glass particles are spherical whereas the coarse aluminum particles are somewhat irregular in shape, but still generally spherical. The densities of the glass and aluminum particles are 156 lbs/ft^3 and 169 lbs/ft^3 respectively.

Aluminum and glass have densities and heat capacities which are similar in magnitude, but the thermal conductivity of aluminum is 200 times greater than the conductivity of glass. This allows an investigation of the effect of particle thermal conductivity on heat transfer.

Particle Concentration and Distribution

Static bed heights of four and nine inches were investigated at all heater tube locations, which gave average particle concentrations of 9 and 20 lbs/ft^3 respectively. At some tube locations, data were taken at static heights of two and six inches. Data were also taken without particles in the system in order to compare with data reported in the literature (2, p. 93; 7). The static bed heights were measured with a scale which was on the test section shell.

At high gas velocities (well above the terminal velocities of the particles) an even distribution of particles existed in the test section; thus, particle concentration is a constant in the test section. At low velocities (where particles are not circulated through the cyclone separator), the particle distribution in the test section was determined by measured values of the vertical pressure gradient (21).

Gas Mass Velocity

A wide range of gas velocities was used in this investigation to determine the most effective velocity in terms of heat transfer and power requirements. The mass velocity ranged from 680 to 8580 lbs/hr ft^2. Four flow rates were investigated at each static bed height. The first rate was chosen so that the fluidized bed height was about half way up the test section. The second rate was adjusted to give a fluidized bed height equal to the height of the test section. The remaining rates were above the minimum rate necessary for recycling of solids. These four rates averaged 1530, 1860, 3100, and 3900 lbs/hr ft^2 for the fine glass spheres; 2740, 3210, 5380, and 6860 lbs/hr ft^2 for the coarse glass spheres; and 2800, 4300, 5400, and 6500 lbs/hr ft^2 for the aluminum particles. Deviation from these averages was ± 25 percent; therefore, approximately the same flow rates for the different static bed heights were used.

Heating Tube Location

Figure 8 shows the tube layout. Since the tube bundle layout is symmetrical, only four heating tube locations were needed to investigate all possible heating tube locations. The tube locations are numbered in Figure 8 and will be referred to by number. The center location is numbered one; the location half the distance from the center is numbered two; and the two outer locations are numbered three and four. Heat transfer was studied at all four locations for various static bed heights and gas velocities.

The heating tube wall temperature was measured at 11 positions along the tube. For most runs the locations 1.0, 3.0, 5.0, 11.0, 17.0, 23.0, 29.0, 35.0, 41.0, 43.0, and 45.0 inches from the bottom were used to get the necessary data to obtain the temperature profile along the tube.

EXPERIMENTAL PROCEDURE

The following preliminary procedure was performed before each experimental run:

1. The stainless steel heating tube was placed in its desired location.
2. A thermos flask was filled with crushed ice and water. The thermocouple reference junctions were placed in the flask to give a reference temperature of 32° F.
3. The potentiometer was balanced against an internal standard cell.
4. The tube wall probe thermocouple was set to its initial position.
5. The power supply was turned on.
6. For low flow rates (no solid circulation), the desired amount of particles was placed in the test section. The air blower was turned on, and the control gate valves adjusted to give the desired flow rate. For high flow rates (with solid circulation), the blower was turned on and the flow rate adjusted. Solids were then allowed to flow from the cyclone separator through the quick-opening neoprene particle control valve. The desired static bed height was obtained by finding the correct opening for this control

valve. The quick-opening neoprene by-pass valve was used to reroute the air while the static bed height was being measured.

7. The speedomax recorder was turned on and set to record the tube wall thermocouples' emf. When steady state was observed, the recording of data commenced.

The following procedure was followed in recording the necessary data:

1. The tube wall probe emf was measured with the potentiometer. The probe was then placed in the second position and the recorder was turned on in order to observe when the probe reached steady state. At steady state the procedure was continued until all 11 probe positions were measured.
2. While the probe was coming to steady state between probe emf measurements, the remaining data were taken. The current, voltage, gas inlet temperature, gas outlet temperature, four bulk gas temperatures, transversing thermocouple temperature (three positions), gas line pressure, orifice pressure drop, and bed pressure drops were recorded at four equal time intervals during the course of the run.

After all the data were recorded for one run, the flow rate was increased to transfer particles to the cyclone separator. At this point, the equipment was turned off, or the procedure was repeated for another run.

In this manner, data were taken for the various static bed heights, gas flow rates, and particles. A typical data sheet can be found in Appendix D.

CALCULATIONS

Calculations have been divided into two categories: Calculations of temperatures, local temperature differences, heat flux, local heat transfer coefficients, average heat transfer coefficient, gas rate, and bed section pressure drops were calculated from the original data; and calculations of bed section void fractions and bed section average heat transfer coefficients were calculated from the above calculated data. The calculations of the former category were performed on a digital computer, and the latter calculations were performed with a desk calculator.

Calculations Using Original Data

In order to calculate temperatures from thermocouple emf values, equations were developed from data obtained in calibrating the thermocouples (see Appendix C). Milne type fifth order interpolating formulas were used (26, p. 64). The equation used for the local tube wall temperature (see Appendix C for tube wall temperature correction) and gas inlet temperature is as follows:

$$\begin{aligned} T = {} & 32 + 22.728\,\text{emf} - 0.296\,\text{emf}\,(\text{emf} - 2) + 0.00956\,\text{emf} \\ & (\text{emf} - 2)(\text{emf} - 4) - 0.000437\,\text{emf}\,(\text{emf} - 2)(\text{emf} - 4) \\ & (\text{emf} - 6) - 0.0000354\,\text{emf}\,(\text{emf} - 2)(\text{emf} - 4)(\text{emf} - 6) \qquad (52) \\ & (\text{emf} - 8) - 0.00000281\,\text{emf}\,(\text{emf} - 2)(\text{emf} - 4)(\text{emf} - 6) \\ & (\text{emf} - 8)(\text{emf} - 10) \end{aligned}$$

The equation used for the gas outlet temperature, local bulk gas temperatures, and transversing probe temperature is the following:

$$T = 32 + 45.455\,\text{emf} - 1.184\,\text{emf}(\text{emf}-1) + 0.0765\,\text{emf}(\text{emf}-1)(\text{emf}-2) - 0.007\,\text{emf}(\text{emf}-1)(\text{emf}-2)(\text{emf}-3) + 0.00113\,\text{emf}(\text{emf}-1)(\text{emf}-2)(\text{emf}-3)(\text{emf}-4) - 0.00018\,\text{emf}(\text{emf}-1)(\text{emf}-2)(\text{emf}-3)(\text{emf}-4)(\text{emf}-5) \qquad (53)$$

A fifth order equation was used to insure a good fit over a large temperature range.

A relationship between the gas bulk temperature and the distance from the entrance of the heat exchanger was developed from the gas inlet temperature and the local gas bulk temperatures. The following Milne type fourth order interpolating formula was used, i. e.

$$T_b = T_{b_2} + A_1(Z - Z_2) + A_2(Z - Z_1)(Z - Z_2) + A_3(Z - Z_1)(Z - Z_2)(Z - Z_3) + A_4(Z)(Z - Z_1)(Z - Z_2)(Z - Z_3) \qquad (54)$$

The coefficients A_1, A_2, A_3, and A_4 are determined by divided differences of the local gas bulk temperatures T_{in}, T_{b_1}, T_{b_2}, and T_{b_3} and the distances from the entrance of the heat exchanger Z_1, Z_2, and Z_3. From this equation values of the bulk gas temperature are calculated for the 11 tube wall probe positions. The local temperature difference is then calculated from the following equation:

$$\Delta T_{loc} = T_w - T_b \qquad (55)$$

The heat flux was calculated by determining the power dissipated in the heating element. The product of the measured current and voltage drop gives the power dissipated in the heating element and the connecting leads. The electrical resistance of the leads is estimated to be 0.00395 ohms; therefore, the expression used for the heat flux is:

$$q = 3.475\,(I\,V - 0.00395\,I^2) \qquad (56a)$$

The local heat transfer coefficient is calculated as follows:

$$h_{loc} = q/\Delta T_{loc} \qquad (56b)$$

To calculate an average heat transfer coefficient, it is first necessary to calculate an average temperature difference. An integral average of the temperature difference is used as is recommended by Leva (18, p. 187), i.e.

$$\Delta T_{av} = \frac{1}{L}\int_0^L \Delta T_{loc}\,dZ \qquad (57)$$

This integral was numerically evaluated. The average heat transfer coefficient was then calculated as follows:

$$h_{av} = q/\Delta T_{av} \qquad (58)$$

The equation for calculating the gas flow rate from the pressure drop across a square edged circular orifice is (28, p. 405)

$$G = \frac{3600\ C\ Y_0 S_2}{A} \sqrt{\frac{2 g_c \Delta P_0 \rho_1}{1 - \beta^4}} \qquad (59)$$

where

G = mass flow rate, $lb_m/hr\ ft^2$

g_c = 32.174 $lb_f\ ft/lb_m\ sec^2$

ρ_1 = gas density upstream, lb_m/ft^3

A = cross sectional area of heat exchanger, ft^2

S_2 = cross sectional area of orifice opening, ft^2

ΔP_0 = pressure upstream - pressure downstream, lb_f/ft^2

C = coefficient of discharge, dimensionless

Y_0 = expansion factor, dimensionless

β = ratio of the orifice diameter to the pipe diameter, dimensionless

The expansion factor for a square edged circular orifice is given by the following:

$$Y_0 = 1 - \frac{(\rho_1 - \rho_2)}{P_1 K}(0.41 + 0.35\ \beta^4) \qquad (60)$$

where

$K = \hat{C}_p / \hat{C}_v$

β = ratio of the orifice diameter to the pipe diameter

From the calibration of the orifice meter (see Appendix B), the coefficient of discharge, C, was determined to be 0.6024 over the range of interest.

The pressure drop across the orifice was measured with a manometer inclined at 30°. The manometer fluid used had a specific gravity of 0.824; thus, the following equation gives the pressure drop:

$$\Delta P_0 = \frac{g}{g_c} \frac{\Delta h\,(51.39 - 0.08)\sin(30°)}{30.5} \tag{61}$$

where

Δh = the manometer reading in centimeters

The line pressure downstream, P_2, was measured with a mercury manometer. Gas densities were calculated by using the ideal gas law, P_2, P_1, and inlet temperature.

The pressure drop over the three 11-inch sections of the fluidized bed were measured with manometers using a manometer fluid having a specific gravity of 0.824. The following equation gives this pressure drop:

$$\Delta P_b = \frac{\Delta h\,(51.39 - 0.08)}{30.5} \frac{g}{g_c} \tag{62}$$

where

Δh = the manometer reading in centimeters

It is necessary to know the total pressure drop across the heat exchanger in order to calculate power requirements. The total pressure drop is the sum of the three section pressure drops, taking into account the first five inches and the last six inches of the heat exchanger. The following equation was used for the total pressure drop:

$$\Delta P_T = \frac{16}{11}\Delta P_{b_1} + \Delta P_{b_2} + \frac{17}{11}\Delta P_{b_3} \tag{63}$$

Calculations from Calculated Data

For batch fluidization, where particles are not circulated, the void fractions, ϵ, is calculated for each of the three 11-inch sections of the heat exchanger from the measured values of bed section pressure drops. The following equation is a good approximation for batch fluidization (21):

$$(1 - \epsilon) = \frac{\Delta P_b g (\rho_s - \rho_g)}{L g_c} \tag{64}$$

where

L = section length, ft

ϵ = void fraction

ρ_s = solid density, lb_m/ft^3

ρ_g = gas density, lb_m/ft^3

ΔP_b = bed section pressure drop, lb_f/ft^2

When particles are circulated, the void fraction is assumed to be constant throughout the test section. The void fraction is then calculated from the length of the shell-side of the test section, static bed height, and solid densities, i. e.

$$\epsilon = 1 - \frac{12}{45} S_b \frac{\rho_b}{\rho_s} \tag{65}$$

where

S_b = static bed height

ρ_b = bulk density of solids

ρ_s = density of solids

Under the conditions of batch fluidization, arithmetic average heat transfer coefficients are calculated in each of the three 11-inch sections of the heat exchanger. When particles are circulated, the average coefficient for the entire heat exchanger is used.

ANALYSIS OF DATA

Average Nusselt Numbers without Fluidization

Data were taken without fluidization to compare the resulting average Nusselt numbers with those reported in the literature. Average Nusselt numbers in unbaffled heat exchangers have been correlated by an equation of the following form (2, p. 93; 7):

$$Nu_{av} = \frac{h_{av}\, d_t}{k_g} = C_1\, D_e^{0.6} \left(\frac{d_t G}{\mu}\right)^{0.6} Pr^{1/3} \tag{66}$$

where D_e is the equivalent diameter in inches based on four times the hydraulic radius.

The term $Nu_{av} Pr^{-1/3}$ was calculated from the data with $Pr = 0.7$ in all cases. In Figure 14 this dimensionless term is plotted versus the dimensional term $D_e \frac{d_t G}{\mu}$ in order to make a comparison with Equation 66. The correlations of Ambrose (2, p. 93) and Donohue (7) are also represented in Figure 14. Donohue's correlation of available data in the literature for tube diameters of less than 5/8 inch has a scatter of ± 25 percent. Ambrose's correlation is for one-inch diameter tubes arranged in a 2 - 3/16-inch triangular pitch. Calculated Nusselt numbers using Ambrose's correlation are somewhat higher than those calculated from Donohue's correlation. Ambrose (2, p. 93) attributes this difference to the larger tubes used in his investigation.

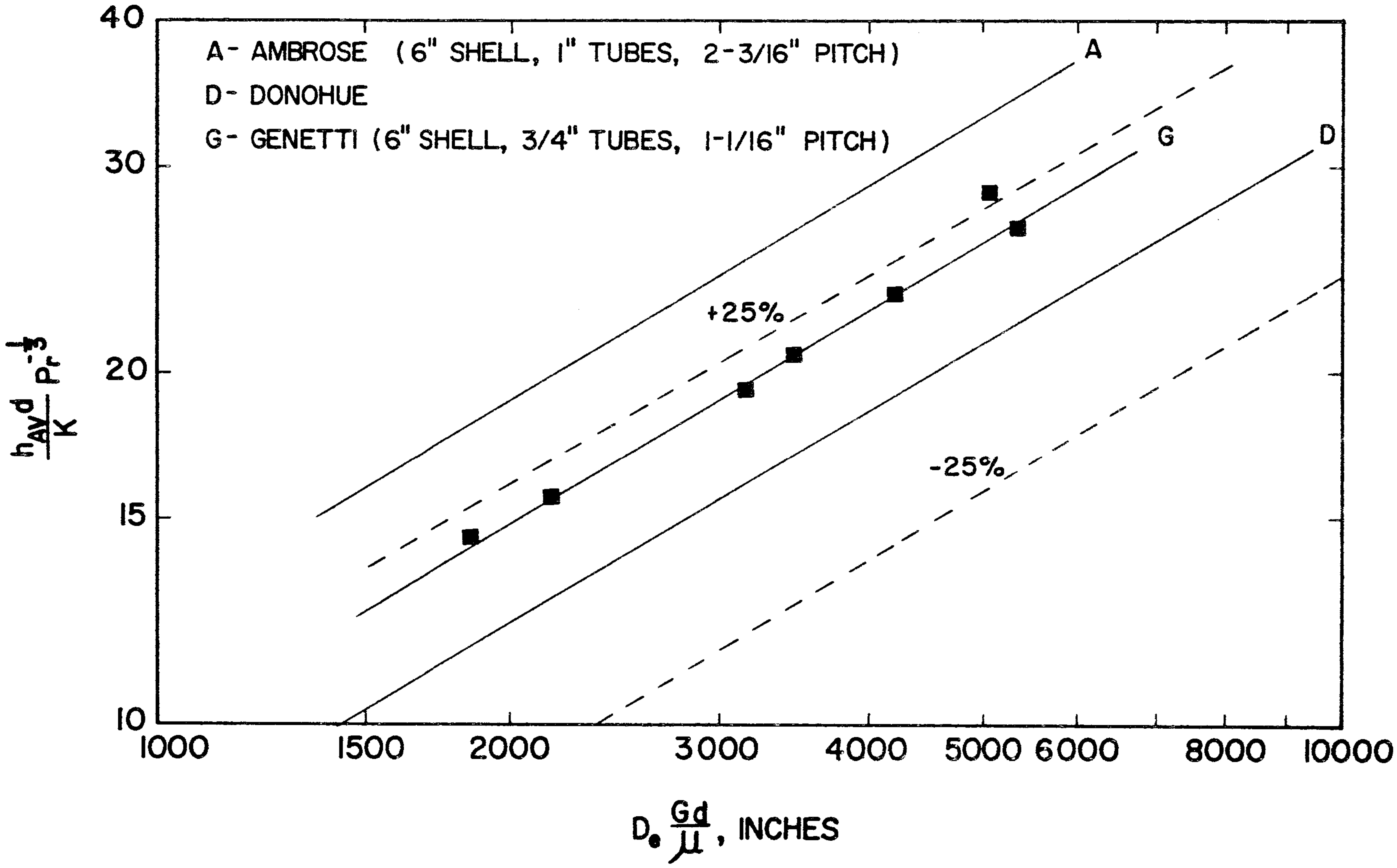

Figure 14. Average Nusselt Numbers in an Unbaffled Heat Exchanger

The data of the present investigation are within the ± 25 percent scatter of Donohue's correlation, and the data are between Ambrose's and Donohue's correlations as would be expected, since 3/4-inch diameter tubes were used in the present investigation. The results of this investigation, as shown in Figure 14, has the characteristic 0.6 slope. The results indicate agreement with published correlations and also indicate that the measured heat transfer coefficients have reasonable values.

Radial and Vertical Bulk Gas Temperature Profiles

Radial Bulk Gas Temperature Profiles

At a vertical height of 8.5 inches, a transversing thermocouple was used to determine the radial bulk gas temperature profile.

Measured temperature differences for radial locations near the heating tube and the outer wall are as large as 2.0° F, but differences in the range 0.1 to 0.6° F are more common. Figure 15 shows radial temperature profiles which are representative of most runs. The profiles shown represent all four tube locations of the tube bundle. As would be expected, highest values of the bulk gas temperature are located near the heater tube location.

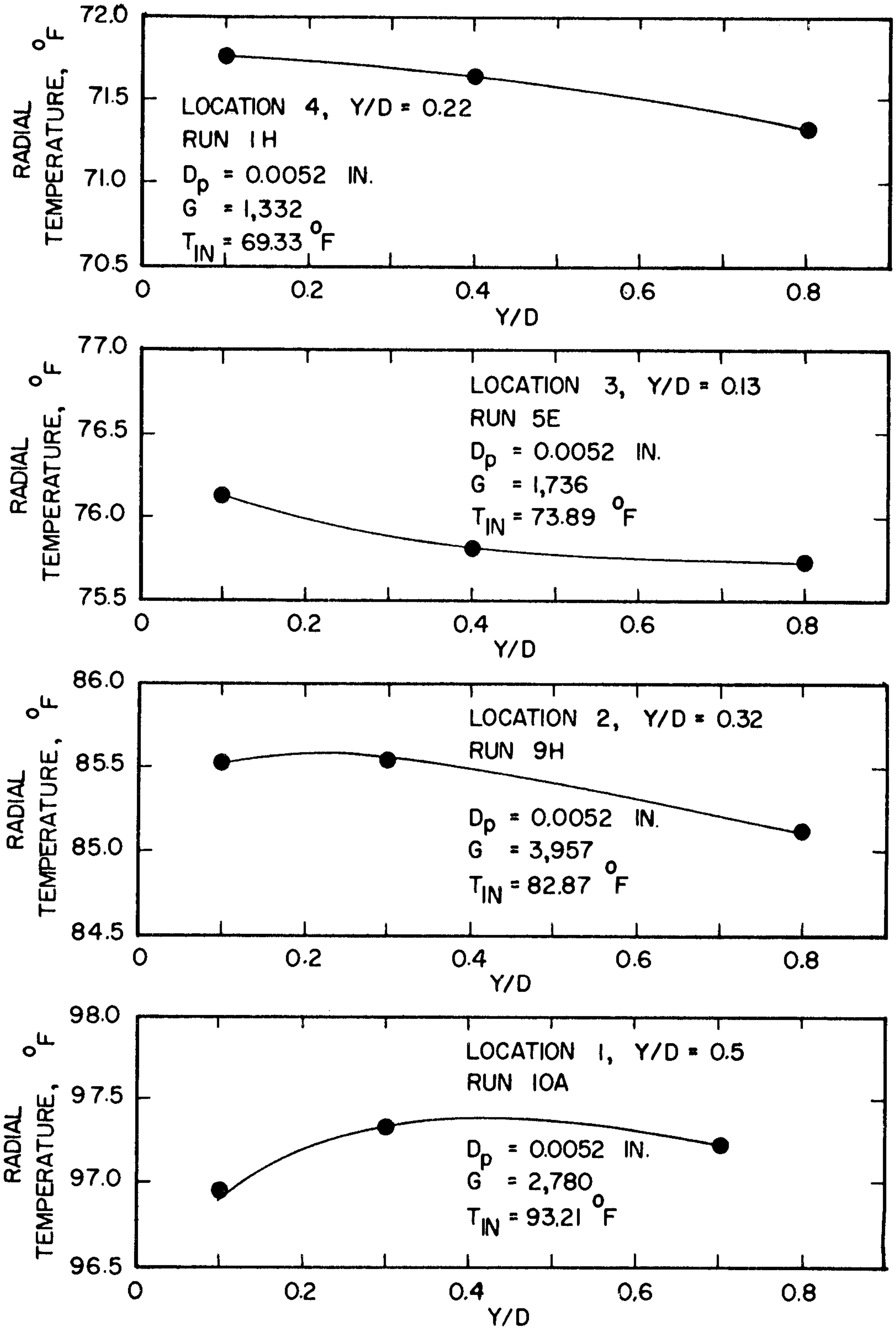

Figure 15. Radial Bulk Gas Temperature Profiles

Vertical Bulk Gas Temperature Profiles

A vertical bulk gas temperature profile was determined with the aid of several thermocouples protruding from the test section outer wall.

Typical vertical bulk gas temperature profiles are shown in Figure 16. The four mass velocities studied for aluminum particles are shown. The top two profiles are for batch fluidization, and the lower profiles are for higher mass velocities where the particulate was refluxed.

At all mass velocities the bulk gas temperature increases several degrees in the first few inches of the fluidized bed. Above five inches a constant bulk temperature is observed in the bed, i. e., backmixing exists. This observation has also been reported in the literature (11;13). For G = 2500 the fluidization height was approximately 30 inches. As would be expected, an increase in the gas bulk temperature is observed above 30 inches.

Local Heat Transfer Coefficients for Batch Fluidization

Local heat transfer coefficients are plotted versus the distance from the test section entrance at a constant gas mass velocity, G. Weighted average local heat transfer coefficients for the entire heat exchanger (that is, weighted proportional to the number of tubes at

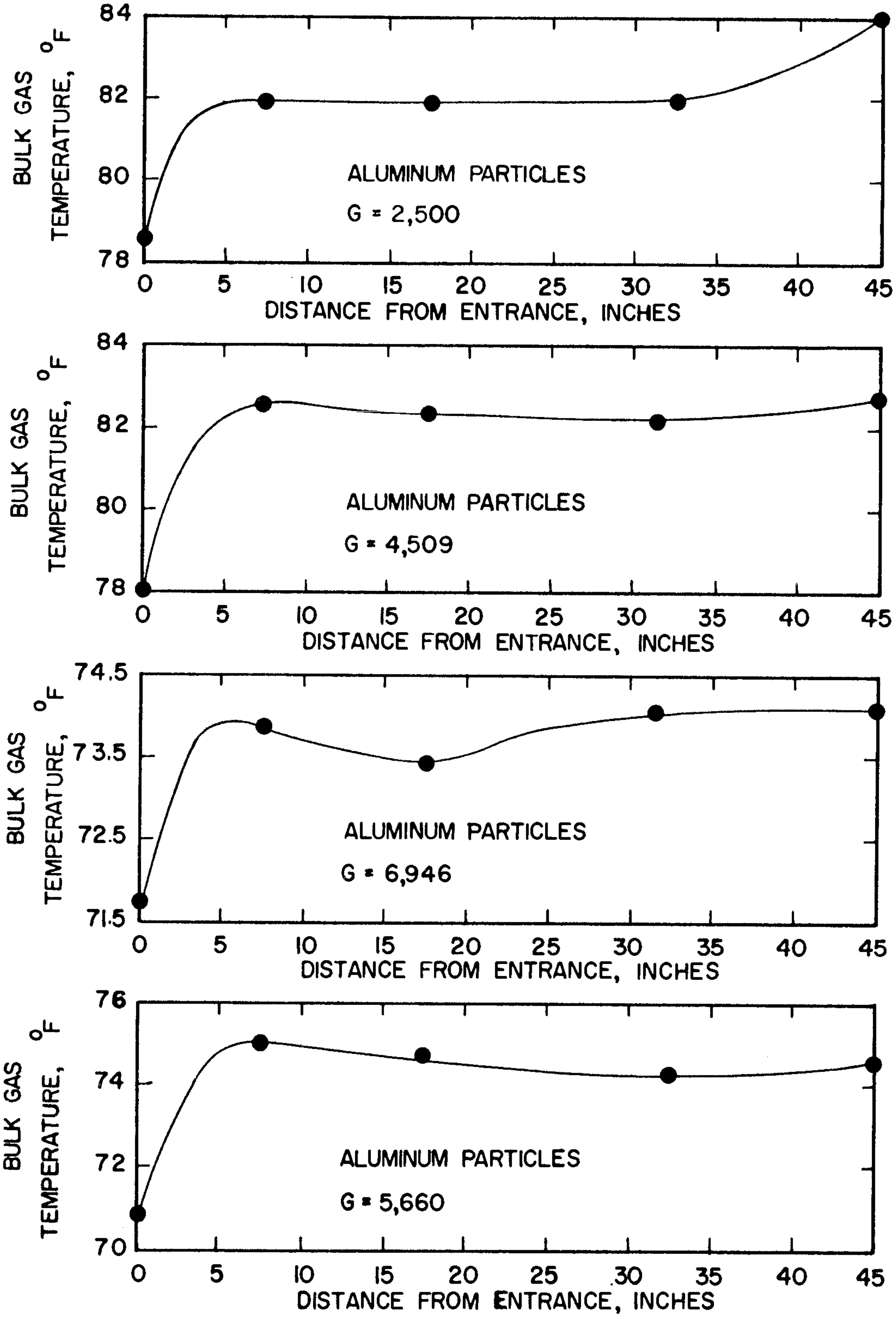

Figure 16. Vertical Bulk Gas Temperature Profiles

each location) are also plotted versus the distance from the entrance.

Figures 17 and 18 show local heat transfer coefficients for batch fluidization of fine glass spheres (D_p = 0.0052 inch). The data are for static bed heights of four and nine inches and mass velocities of 1540 and 1860 $lb_m/hr\ ft^2$.

For G = 1540 particles were fluidized to a height of approximately 30 inches. Above this height tube location had no significant effect on local heat transfer coefficients except for tube location 4 at a static bed height of nine inches. Coefficients are lower in this case because the mass velocity was significantly less than 1540 (1020). In the fluidized part of the test section heat transfer coefficients at tube locations 1 and 2 are the smallest and largest in magnitude respectively over most of the bed. The heat transfer coefficients at tube location 3 and 4 do not vary significantly from each other.

For G = 1860 the entire test section was fluidized. The local heat transfer coefficients at tube locations 1 and 2 are the smallest and largest in magnitude respectively over most of the bed. Heat transfer coefficients for the tube locations 3 and 4 are usually of an intermediate value, and do not vary significantly from each other.

For static bed heights of four inches heat transfer coefficient profiles are of Type I, as described by Toomey and Johnstone (31), except for the coefficient profile at tube location 2. At this location a Type II heat transfer coefficient profile is observed. For a static

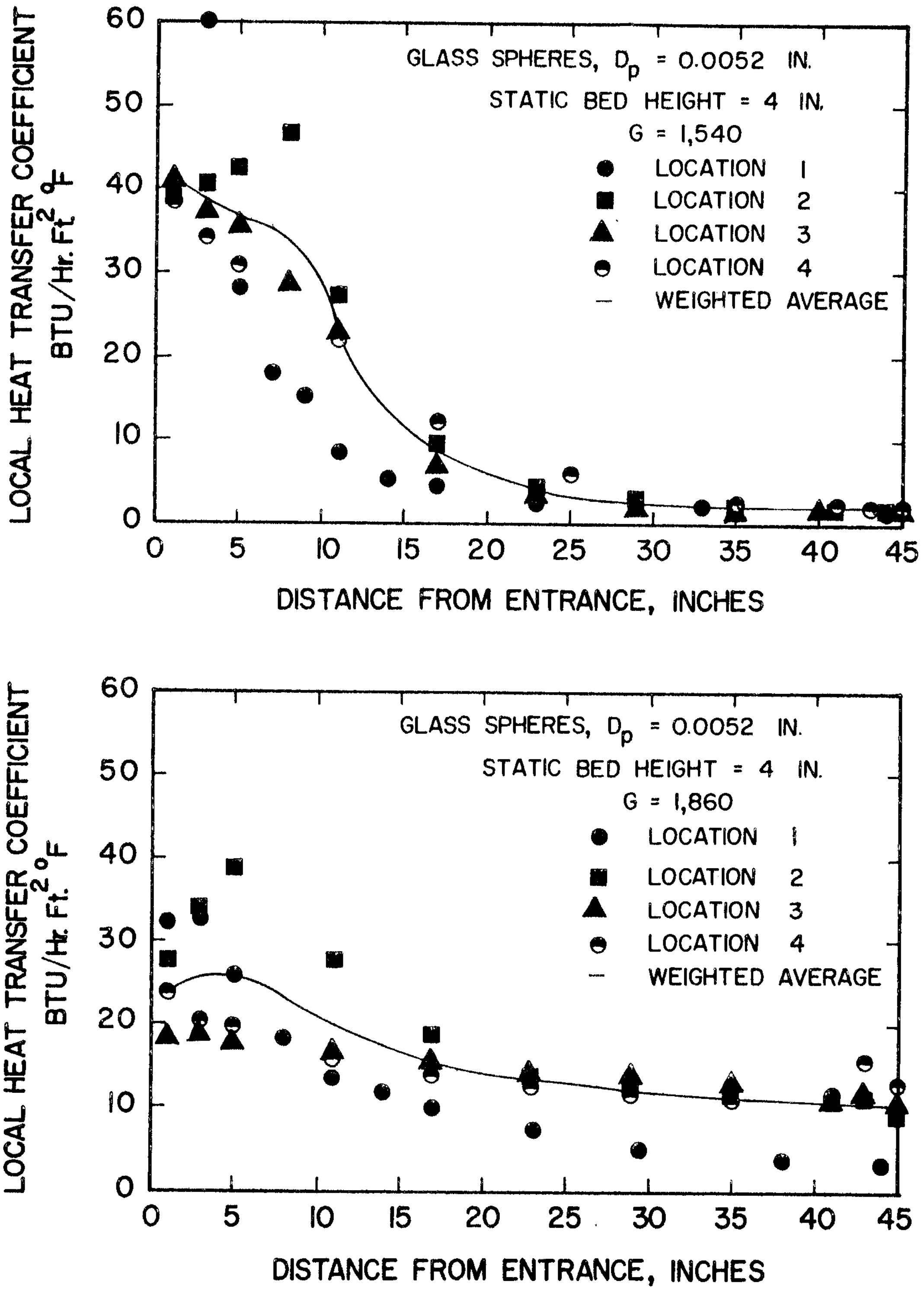

Figure 17. Local Heat Transfer Coefficients for Batch Fluidization

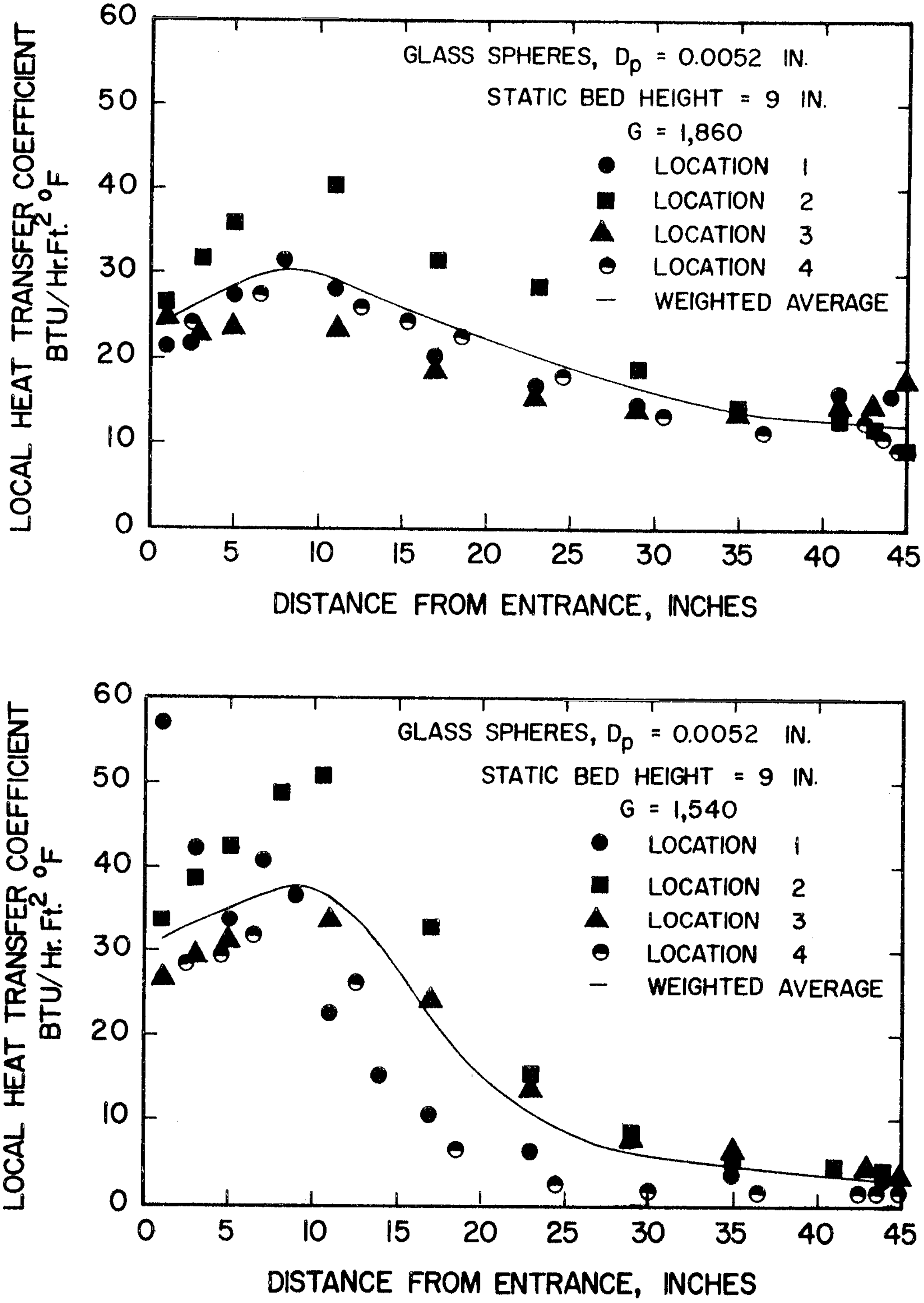

Figure 18. Local Heat Transfer Coefficients for Batch Fluidization

bed height of nine inches, heat transfer profiles are of Type II.

Figures 19 and 20 show local heat transfer coefficients for batch fluidization of coarse glass spheres (D_p = 0.0151 inch). The data are for static bed heights of four and nine inches and mass velocities of 2740 and 3210 $lb_m/hr\ ft^2$.

For G = 2740 particles were fluidized to heights of approximately 30 to 35 inches for the four and nine-inch static bed height cases respectively. Above this height tube location has no significant effect on heat transfer coefficients. In the fluidized part of the bed, heat transfer coefficients for tube location 1 are the lowest in magnitude over most of the bed.

For G = 3210 the entire test section was fluidized. For a static bed height of nine inches, the heat transfer coefficients observed at tube location 1 are lower than the coefficients for other tube locations. For this static bed height heat transfer coefficients at tube locations 2, 3, and 4 do not vary significantly from each other. Heat transfer coefficient profiles at this static bed height are of Type II. For a four-inch static bed height heat transfer coefficients at tube location 1, in the dense part of the bed, seem somewhat inconsistent since they are larger in magnitude than those of the other tube locations. At this static bed height coefficient profiles are of Type I.

Local heat transfer coefficients at tube locations 2 and 3 for fluidization with aluminum particles (D_p = 0.0306 inch) are shown

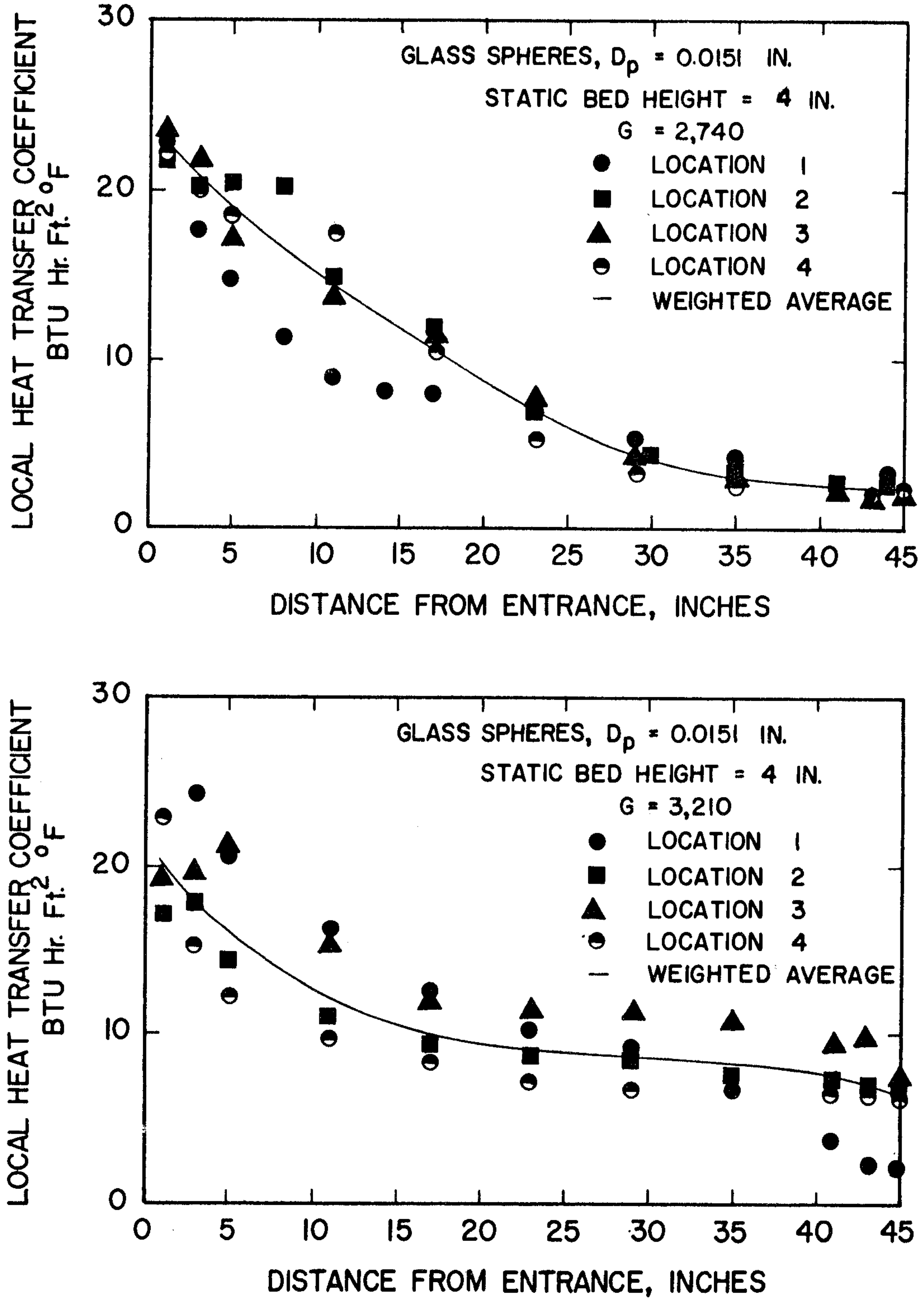

Figure 19. Local Heat Transfer Coefficients for Batch Fluidization

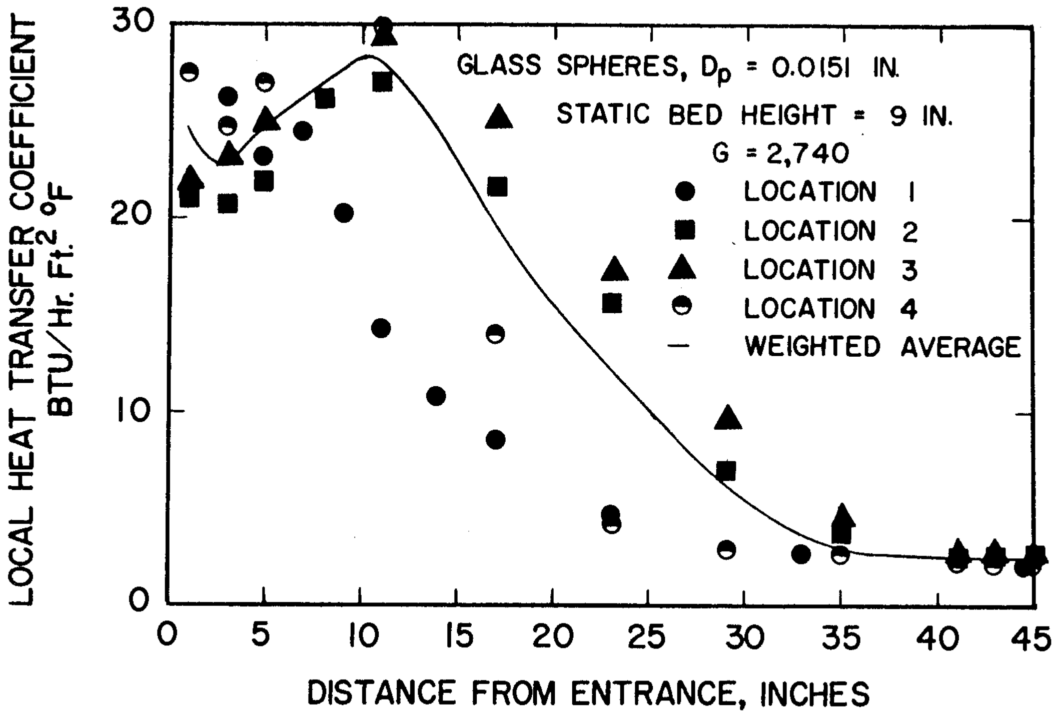

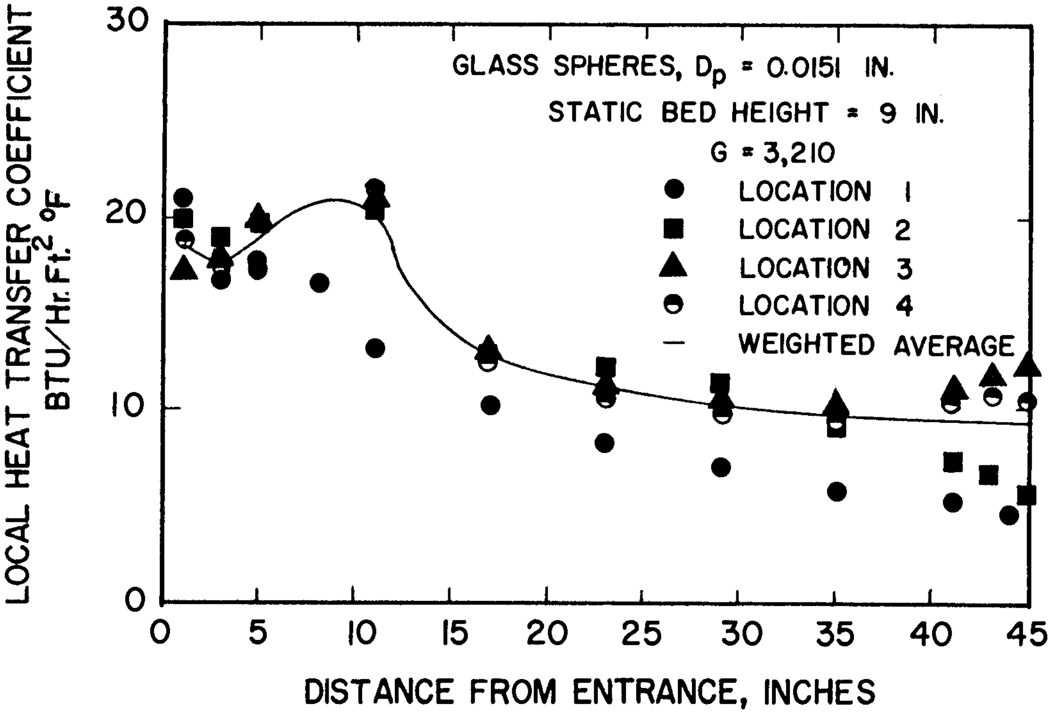

Figure 20. Local Heat Transfer Coefficients for Batch Fluidization

in Figures 21 and 22. The data are for static bed heights of four and nine inches and mass velocities of 2800 and 4300 $lb_m/hr\ ft^2$. For a static bed height of four inches, no significant differences in local heat transfer coefficients at locations 2 and 3 are observed. The heat transfer profiles are of Type I. For a static bed height of nine inches, no significant differences between coefficients at tube locations 2 and 3 are observed for the less dense part of the bed. For the dense part of the bed the local coefficients of tube location 3 are higher than those of location 2 up to a vertical height of about 12 inches. For vertical heights greater than 12 inches and less than 30 inches, the coefficients of tube location 2 are greater in magnitude. This results because the coefficients of tube location 2 have a maximum at a greater distance from the entrance than do the coefficients of location 3.

The criterion based on the dimensionless group, L_fD_p/A, proposed by Toomey and Johnstone (31) to determine the heat transfer coefficient profile type, indicates that an increase in the fluidization height and particle size will increase the tendency to produce a Type I profile. The results of the present investigation indicate that particle diameter has little influence on the profile type. Increases in the fluidization height and static bed height tend to decrease the tendency for Type I profiles. With this in mind the group, D_t^2/L_fS_b, should indicate a tendency toward Type I profiles. At each static height and

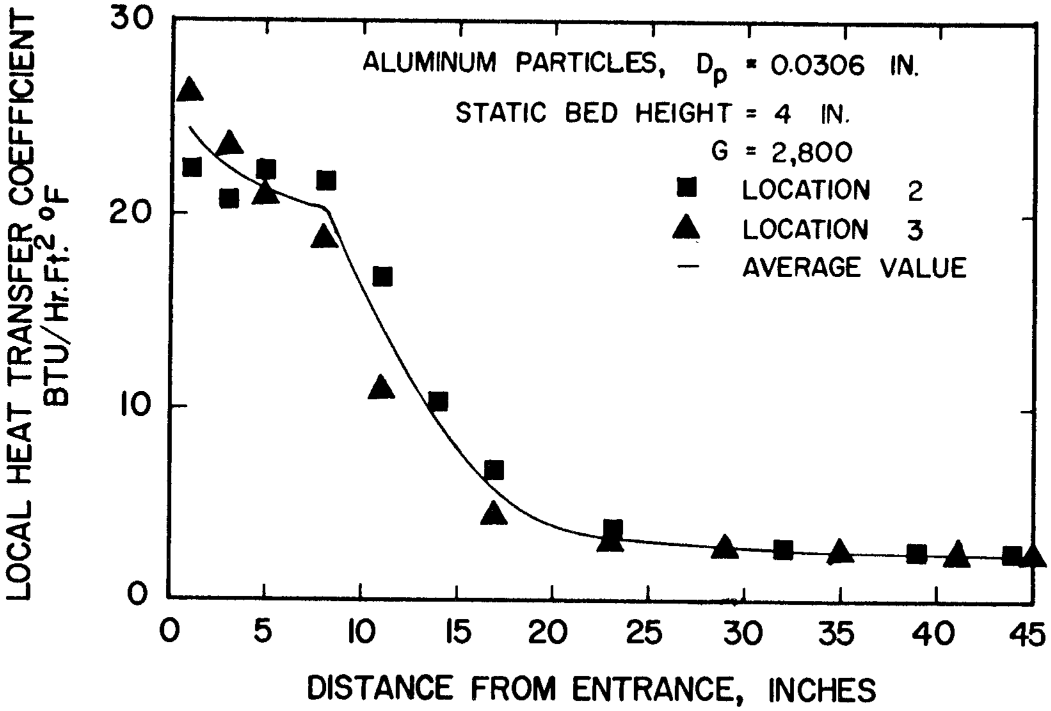

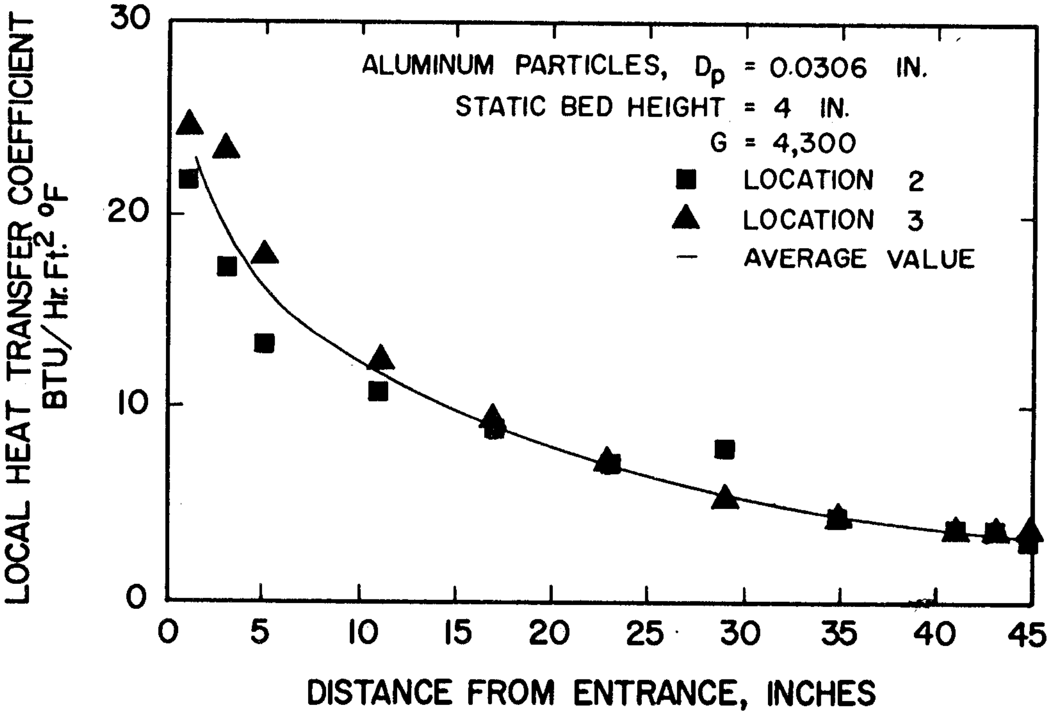

Figure 21. Local Heat Transfer Coefficients for Batch Fluidization

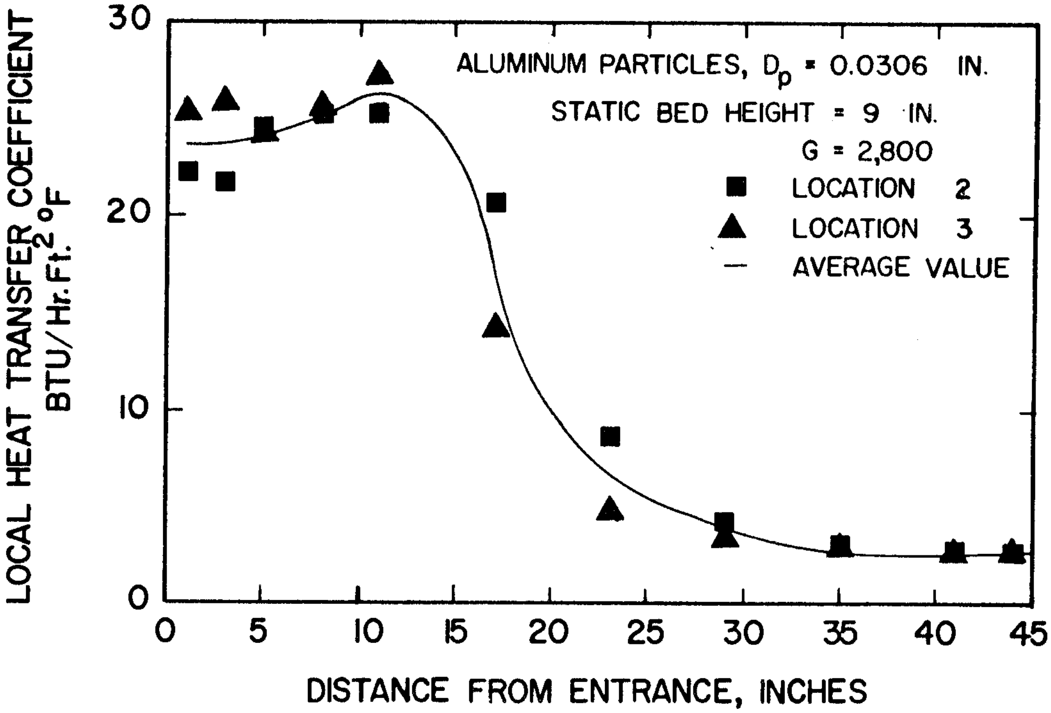

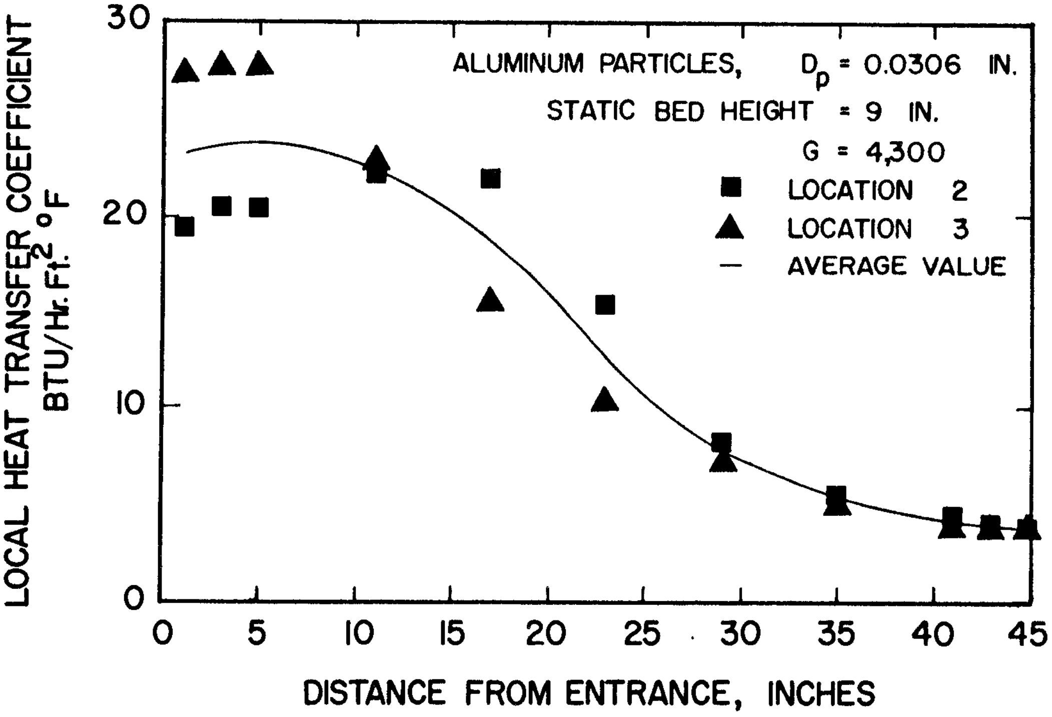

Figure 22. Local Heat Transfer Coefficients
for Batch Fluidization

fluidization height there were ten local coefficient profiles measured. The percent of these ten that are Type I is tabulated in Table I along with the group, D_t^2/L_fS_b. Increases in the magnitude of this group appear to increase the tendency toward Type I profiles. The tube location also seems to have an effect on the profile type. Tube location 2 exhibits Type II profiles more often than do the other locations.

Table I. Percent Occurrence of Type I Profiles

$\frac{D_t^2}{L_fS_b}$	Percent of Type I Profiles
.0689	90
.0459	50
.0306	20
.0204	0

Local heat transfer coefficients for fluidization with coarse glass spheres are approximately 40 percent lower in magnitude than coefficients for fluidization with fine glass spheres. Heat transfer coefficients for fluidization with aluminum particles and with coarse glass spheres are about the same magnitude even though the aluminum particles are larger in average diameter. The increase in effective surface area of the irregular aluminum particles may account for the fact that heat transfer coefficients did not decrease for fluidization using aluminum particles.

Average Sectional Coefficients for Batch Fluidization

With experimentally determined average particle fractions and average Nusselt numbers over the 11-inch sections of the fluidized bed, average particle contact times, $\bar{\theta}$, were calculated from Equation 48. Calculated contact times averaged 0.1, 0.4, and 1.3 seconds for the fine glass spheres, coarse glass spheres, and aluminum particles respectively. These values are in the range reported in the literature (32; 40).

To obtain a correlation for the contact times, $\bar{\theta}$, the dimensionless quantities $\bar{\theta}\, g^{1/2}/D_p^{\,1/2}$, G_{mf}/G, ρ_s/ρ_g and Re_p were calculated. Equation 49 was used to calculate G_{mf}. These quantities are plotted on logarithm scales in Figure 23. The following correlation represents the data:

$$\bar{\theta} \left(\frac{g}{D_p}\right)^{1/2} \left(\frac{\rho_s}{\rho_g}\right)^{1.1} Re_p = 97\left(\frac{G_{mf}}{G}\right)^{4/3} \qquad (67)$$

By substituting $\bar{\theta}$, as expressed in Equation 67, into Equation 48, the following correlation for average Nusselt numbers can be obtained:

$$Nu_p = \frac{5\,\phi\,(1-\epsilon)^{0.48}}{\left[1 + \frac{580}{Re_p}\left(\frac{k_g}{D_p^{\,3/2} C_s \rho_s g^{1/2}}\right)\left(\frac{\rho_s}{\rho_g}\right)^{1.1}\left(\frac{G_{mf}}{G}\right)^{4/3}\right]^2} \qquad (68)$$

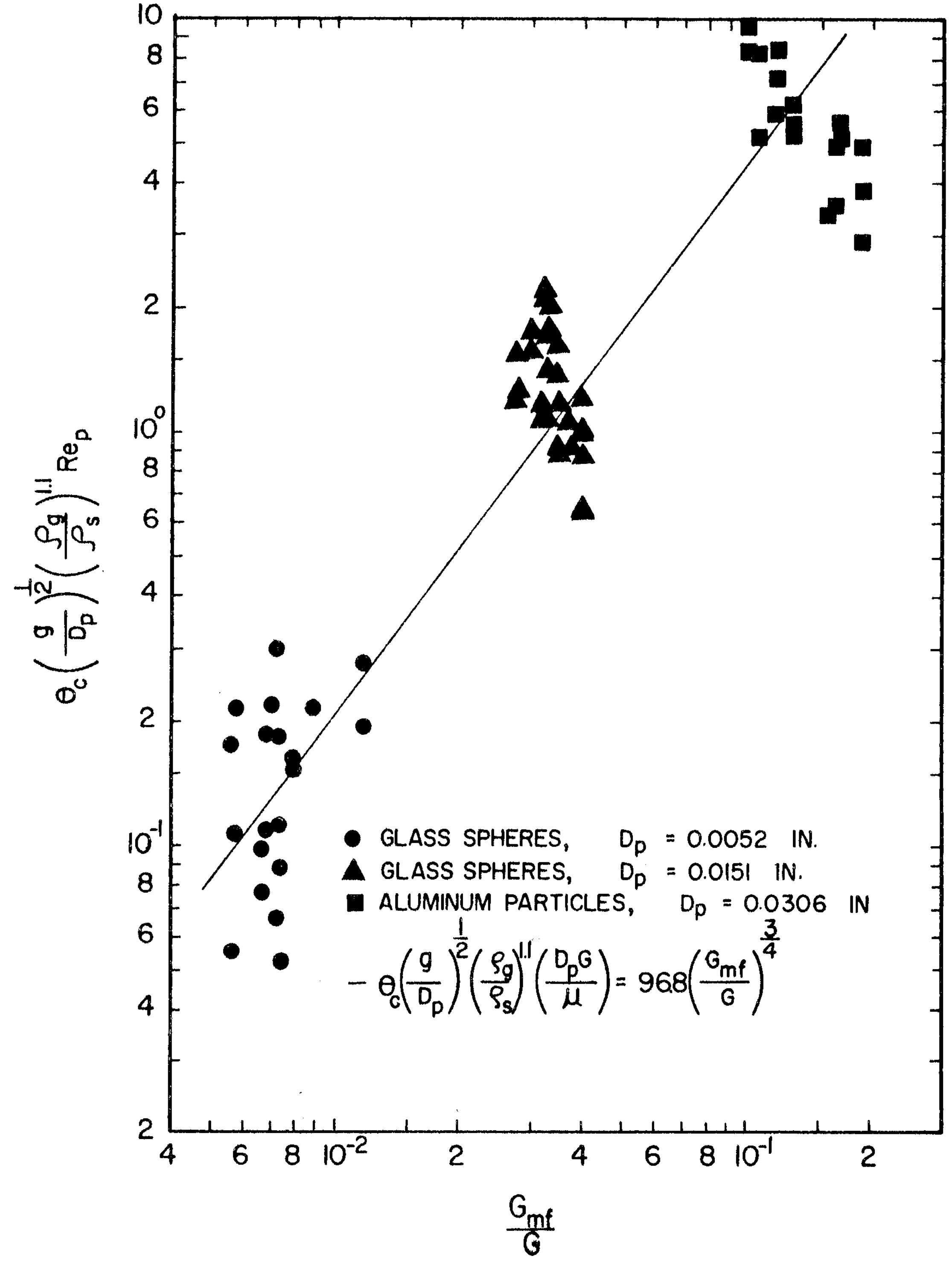

Figure 23. Correlation for Average Contact Time

where ϕ is the ratio of the surface area of the particle to the surface area of a sphere of the same average diameter.

Microscope enlargements (see Figure 13) of aluminum particles show many cracks and crevices on the particle surface. As a result of this observation, $\phi = 2$ was assumed for the aluminum particles. For the spherical glass particles $\phi = 1$ was used. Equation 68, as well as the experimental data, are shown in Figure 24. Most of the data for fluidization with the coarse glass spheres and the aluminum particles are within ± 20 percent of Equation 68. A wider scatter exists for fluidization with fine glass spheres; this scatter is attributed to less accurate measurement of the section pressure drops (and thus ϵ) for the fine glass particles. The fine glass particles had a tendency to plug the pressure taps on the test section.

The correlation based on the modified form of Ziegler, Koppel and Brazelton's model agrees with several experimental observations. The thermal conductivity of aluminum is 200 times larger than that of glass, yet no increase in heat transfer coefficients is observed for fluidization of aluminum particles. This is in agreement with the proposed mechanism and with published data (22, p. 303). The exponent 0.48 for $(1 - \epsilon)$ cited by other investigators, as has been previously noted, agrees with the present investigation. Back-calculated average contact times correlate with the proposed dimensionless groups and are in agreement with other workers (32; 40).

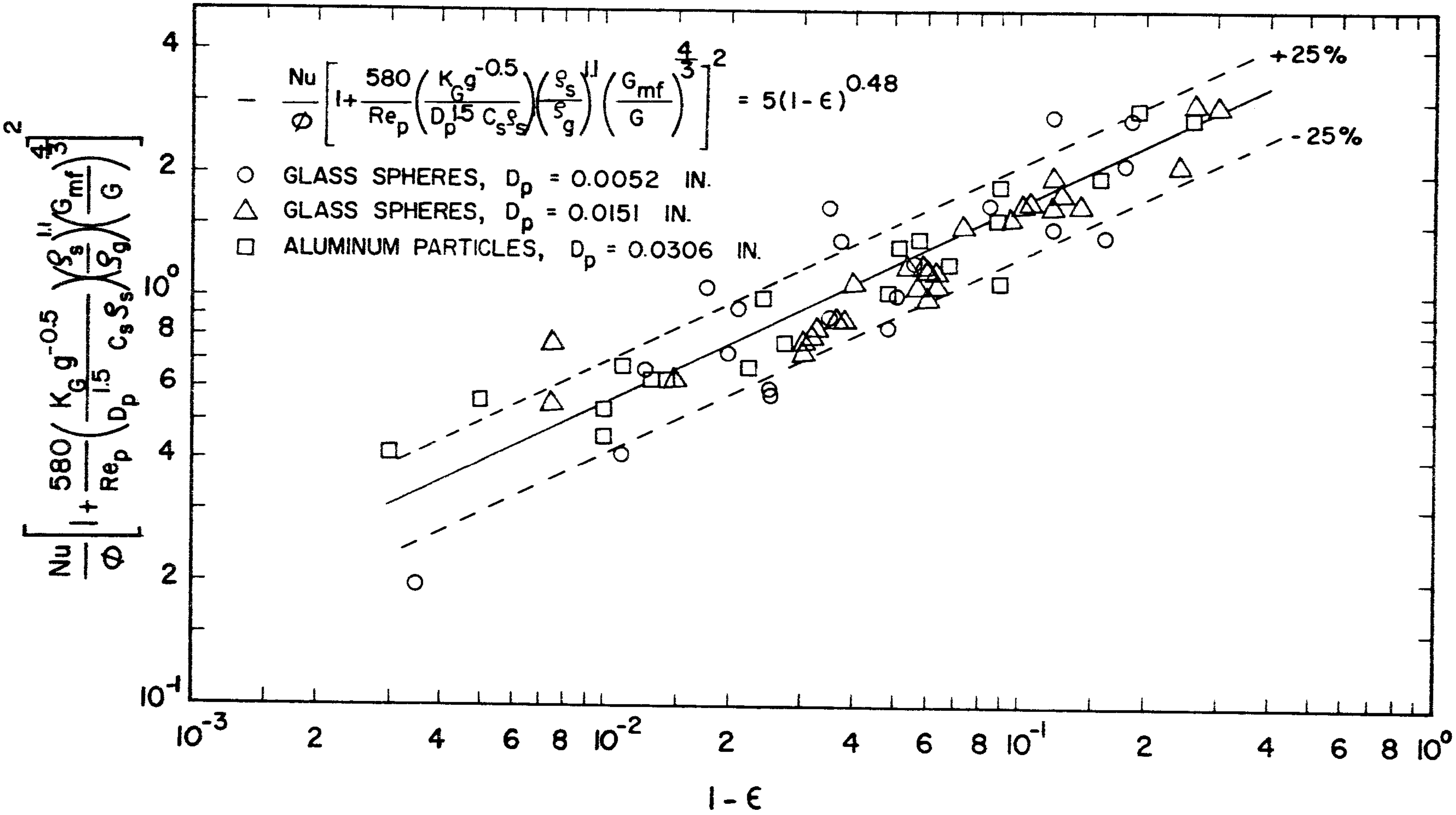

Figure 24. Correlation for Average Sectional Nusselt Numbers

All tube locations are represented in the data shown in Figure 24. Average sectional heat transfer coefficients for mass velocities studied in this investigation did not have a significant dependency on tube location. This is in agreement with the results of Toomey and Johnstone (31) as shown in Figure 4. These workers observed little difference in heat transfer coefficients simultaneously measured at the outer tube wall and at an internal tube located at the center of the bed for mass velocities above 1000.

In Figure 25 Noë's data for fluidization in a verticle tube bundle is shown. The line shown in this figure is the present correlation. A wider scatter is observed for his data than for the data of the present investigation; however, acceptable agreement exists. Most of Noë's data fall with ± 50 percent. Noë assumed that plug flow of gas existed in the test section. The present investigation has shown that backmixing is a more correct model. Coefficients calculated by a plug flow model are larger than those calculated with a backmix model. This would account for the fact that the calculated average Nusselt numbers for Noë's data are greater than for the present correlation.

Agreement of the present investigation with Equation 28 is poor. Details of experimental conditions were not presented in the review article where the results of Gel'perin, Ainshtein and Romanova were translated. Since a substantial dependency on tube location in the bed

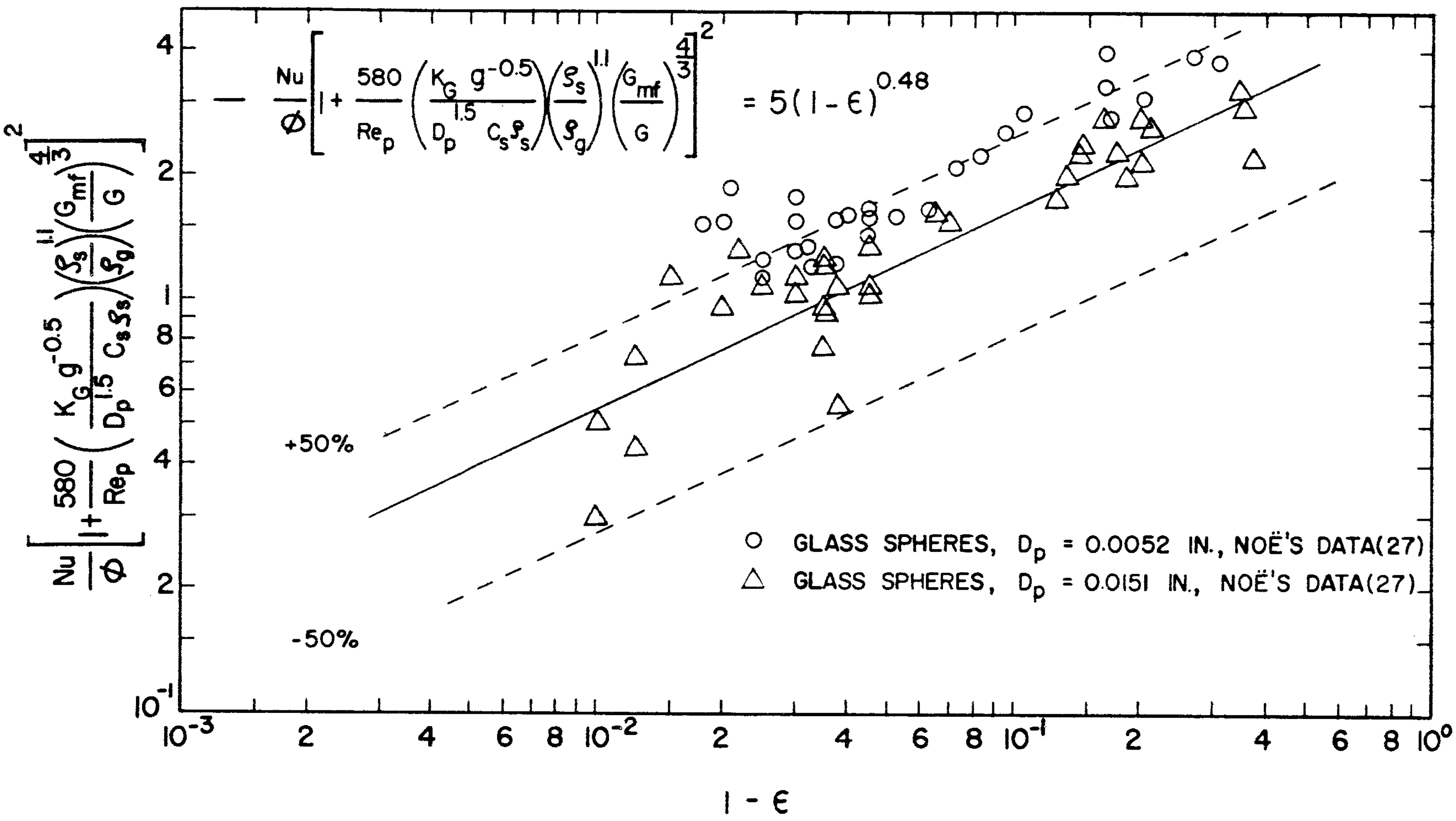

Figure 25. Comparison of the Correlation for Average Sectional Nusselt Numbers with Nöe's Data

was noted by these workers, it appears, based on the results of Toomey and Johnstone (see Figure 4), that the mass velocities investigated were less than 500.

Figure 26 compares Gamson's correlation (10) for a single vertical tube at the center of a fluidized bed with the results of this investigation. The solid line is Gamson's correlation. The j_H factors of the present investigation are about 20 percent lower than Gamson's correlation. These lower values could be attributed to the effect that the tube bundle has on fluidization. Particle dynamics would be different with a tube bundle than without a bundle. Contact times for a single vertical tube geometry would probably be smaller for similar operating conditions. The characteristic -0.3 slope was observed in this investigation. It might be well to point out that the particle surface area per unit of bed volume, a, is proportional to $(1 - \epsilon)$. For spherical particles $a = 6 \frac{(1 - \epsilon)}{D_p}$, and for aluminum particles $a = 12 \frac{(1 - \epsilon)}{D_p}$ was assumed.

A comparison of the results of this investigation with the correlation of Gel'perin, Kruglikov, and Ainshtein is shown in Figure 27. The solid line is Equation 26 which represents their correlation. The data of the present investigation fall above this line and show a great deal of scatter. Equation 26 shows a large tube location dependency which indicates that low mass velocities were probably used.

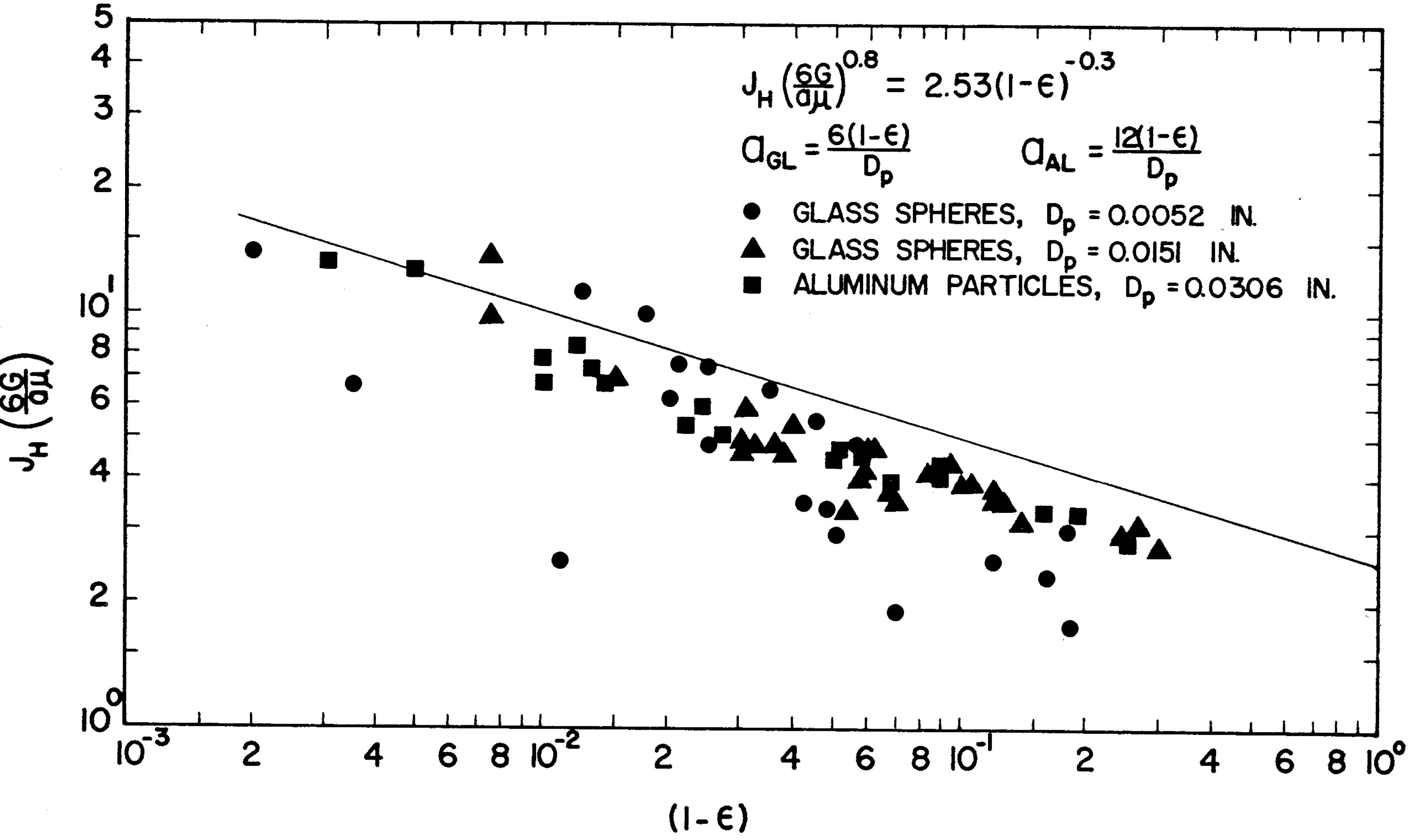

Figure 26. Comparison of Average Sectional Nusselt Numbers with Gamson's Correlation for a Single Vertical Tube

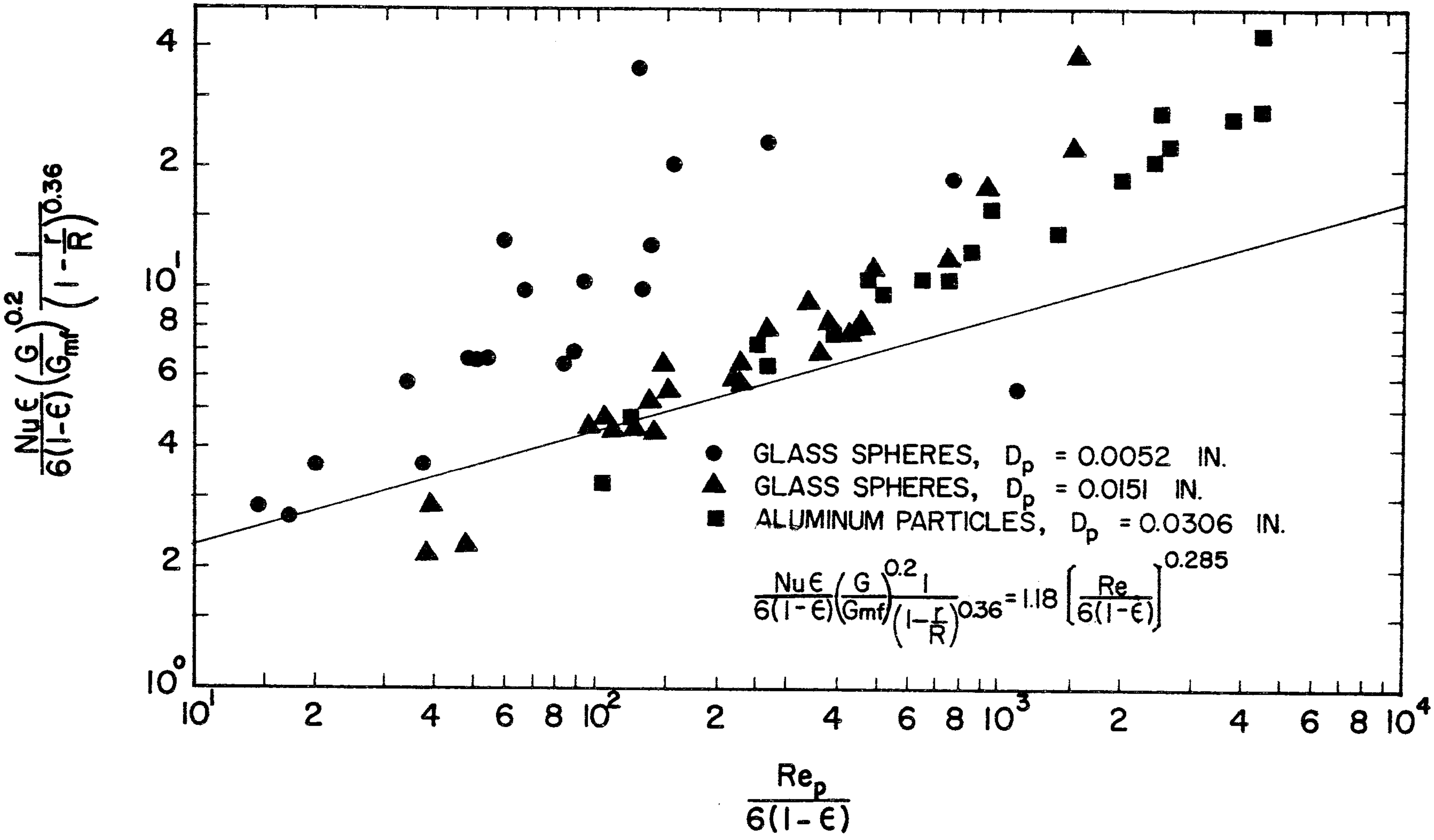

Figure 27. Comparison of Average Sectional Nusselt Numbers with Kruglikov and Ainshtein's Correlation for a Single Vertical Tube

Local Heat Transfer Coefficients for Fluidization with Particulate Reflux

Local heat transfer coefficients are plotted versus the distance from the entrance of the test section for the various tube locations and for four and nine-inch static bed heights. Weighted average local coefficients for the entire tube bundle are also shown.

Local heat transfer coefficients for fluidization with fine glass spheres are shown in Figures 28 and 29. All four tube locations were investigated at a static bed height of four inches. At a static bed height of nine inches only locations 3 and 4 were investigated. Local heat transfer coefficients for fluidization with coarse glass spheres are shown in Figures 30 and 31. All tube locations were investigated except location 1 for G = 6860 at a static bed height of nine inches. Figures 32 and 33 show local heat transfer coefficients for fluidization with aluminum particles. Tube locations 2 and 3 were investigated.

The same general shape of the coefficient profiles are observed for all static bed heights and mass velocities investigated. The heat transfer coefficient decreases in magnitude over the first five to ten inches of the test section; a constant value is then observed to heights between 35 and 40 inches from the entrance; and an increase in the

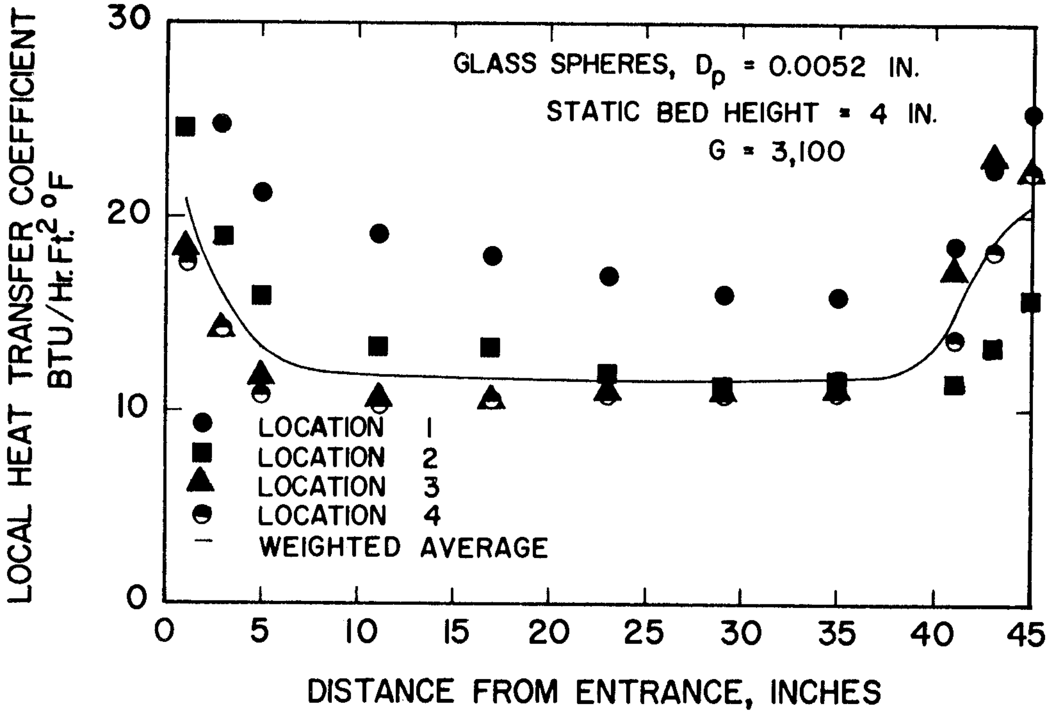

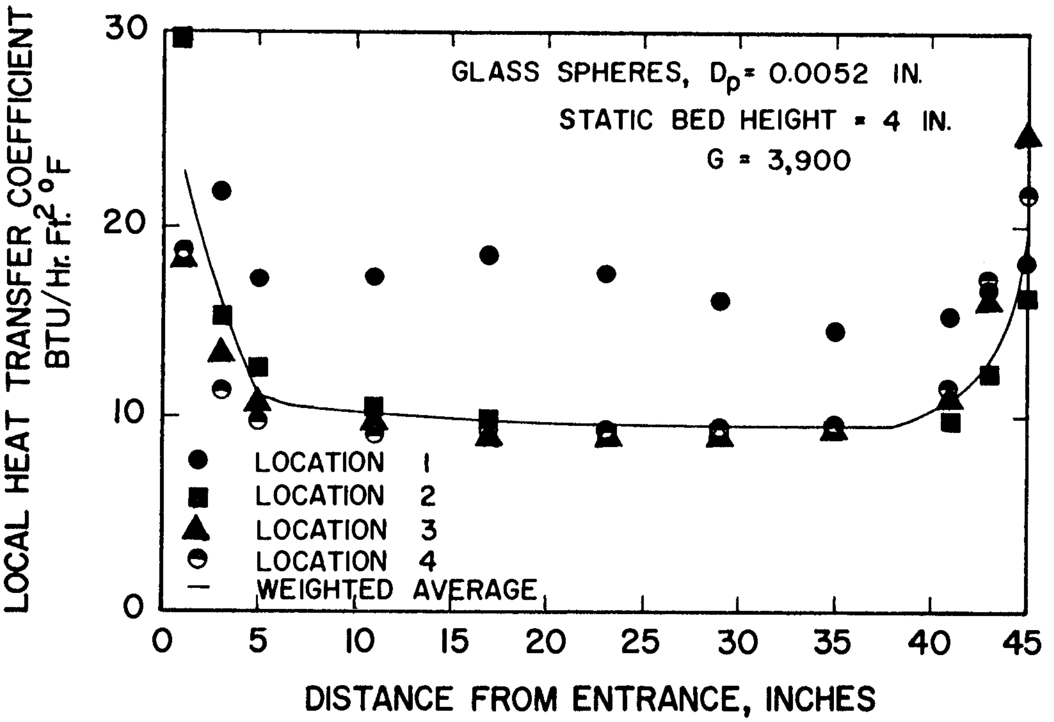

Figure 28. Local Heat Transfer Coefficients for Particulate Reflux Fluidization

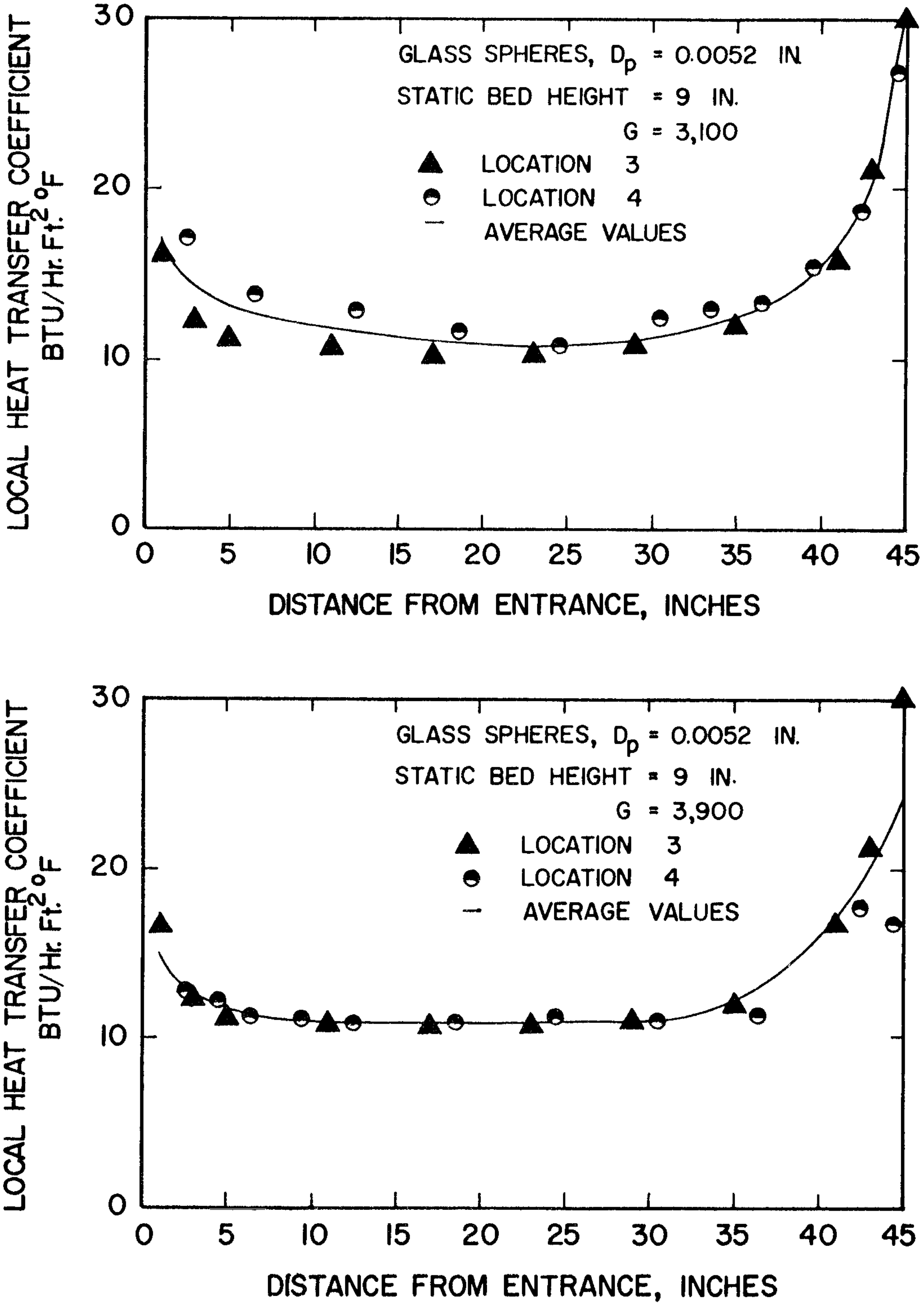

Figure 29. Local Heat Transfer Coefficients for Particulate Reflux Fluidization

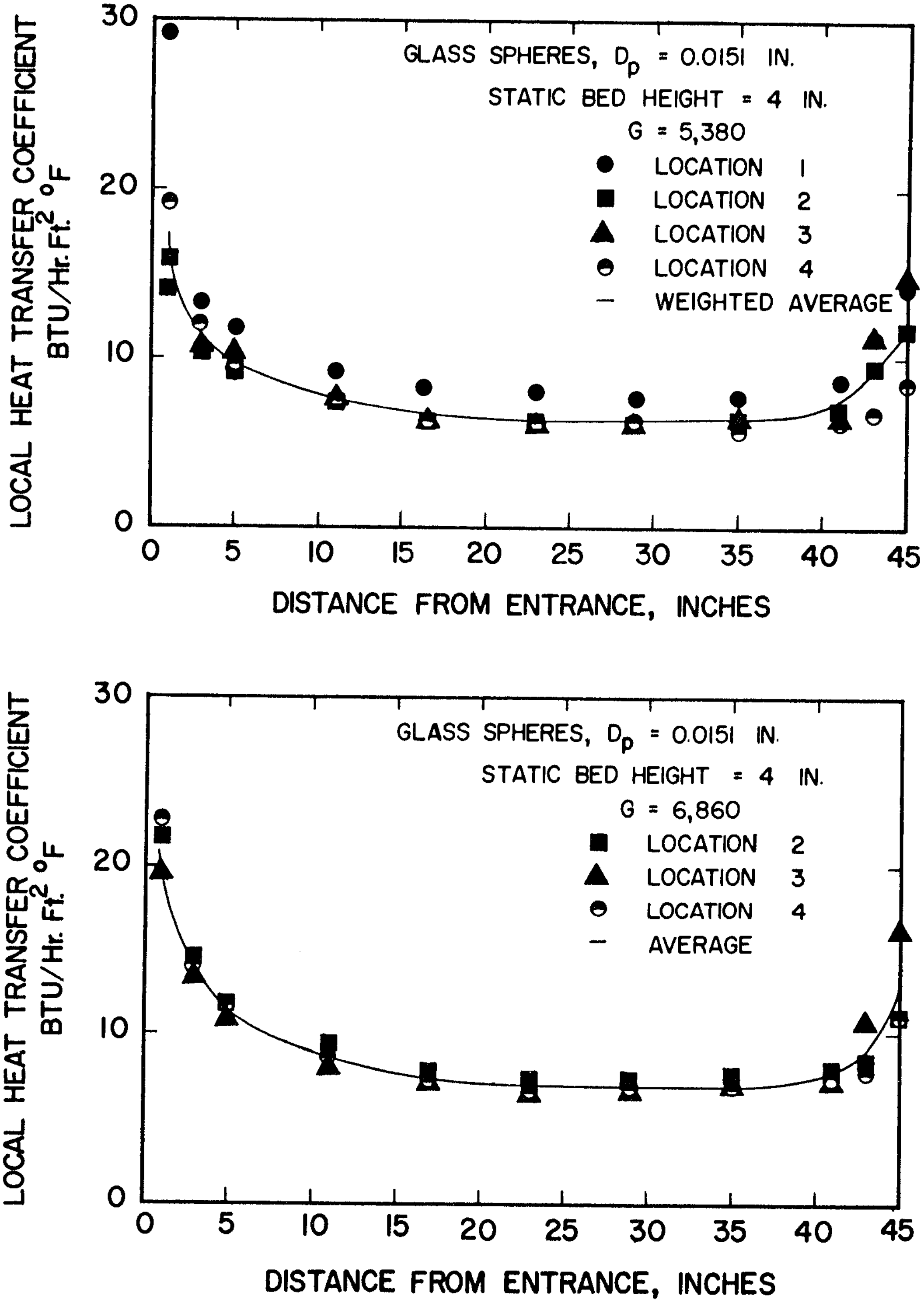

Figure 30. Local Heat Transfer Coefficients for Particulate Reflux Fluidization

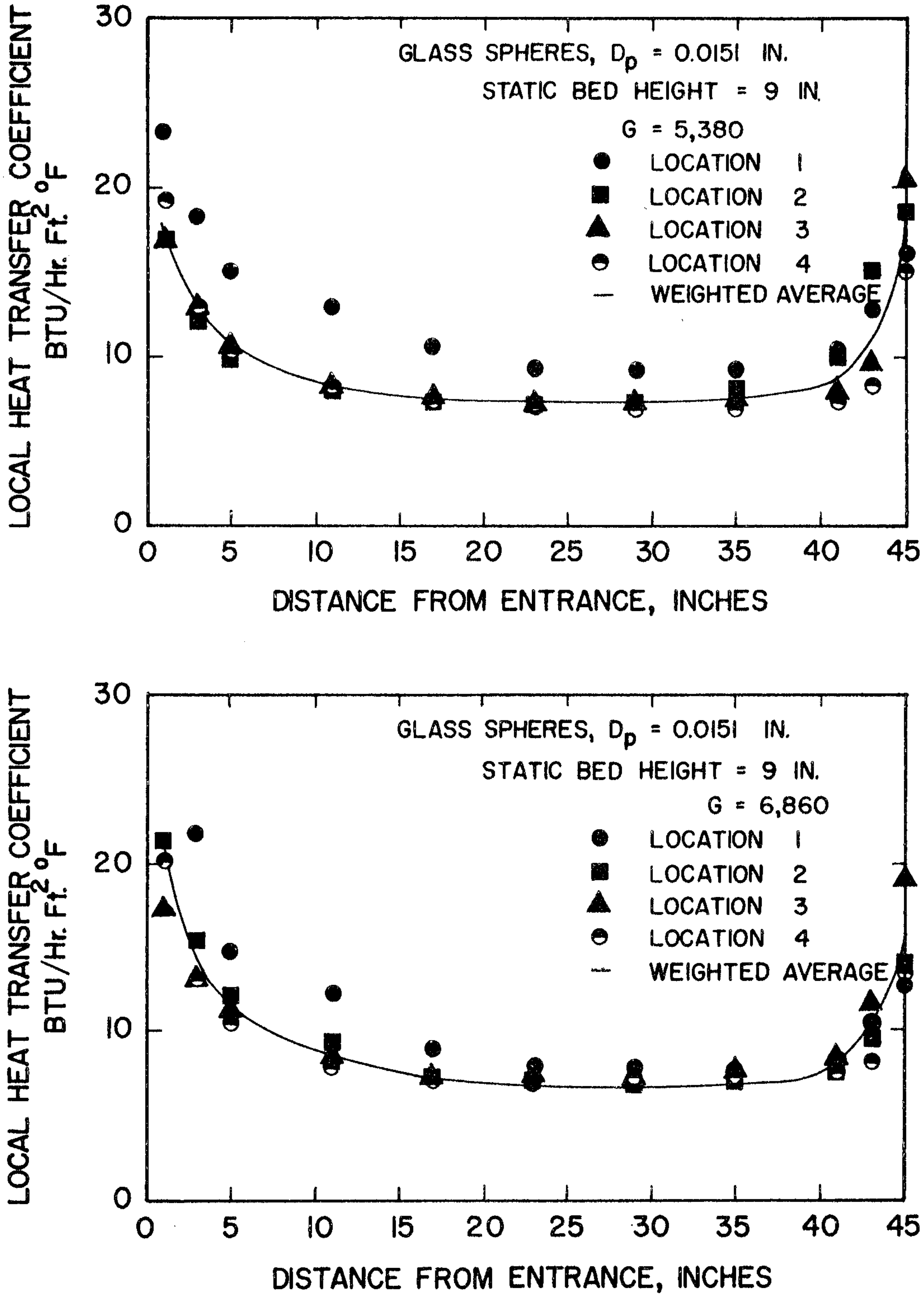

Figure 31. Local Heat Transfer Coefficients for Particulate Reflux Fluidization

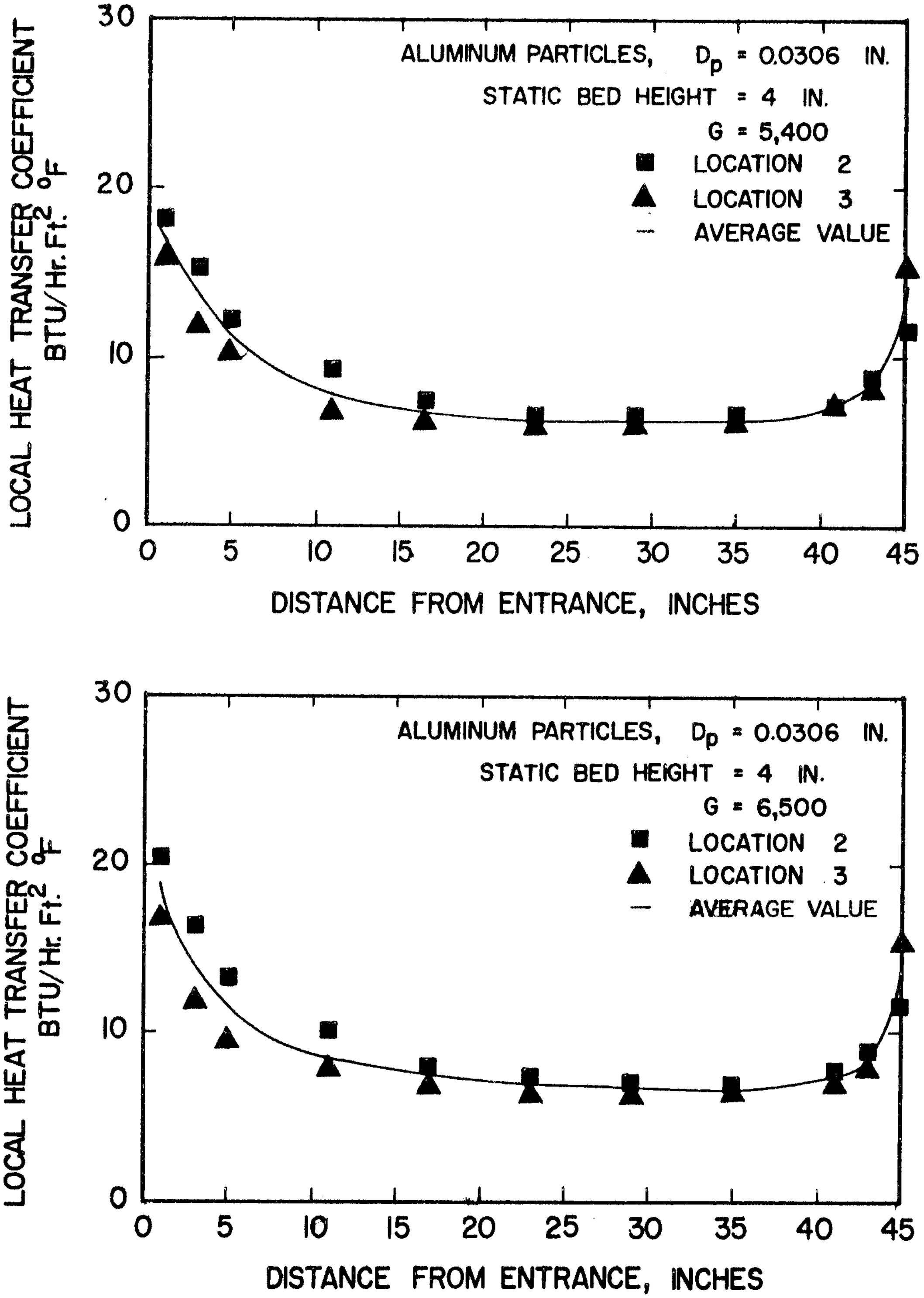

Figure 32. Local Heat Transfer Coefficients for Particulate Reflux Fluidization

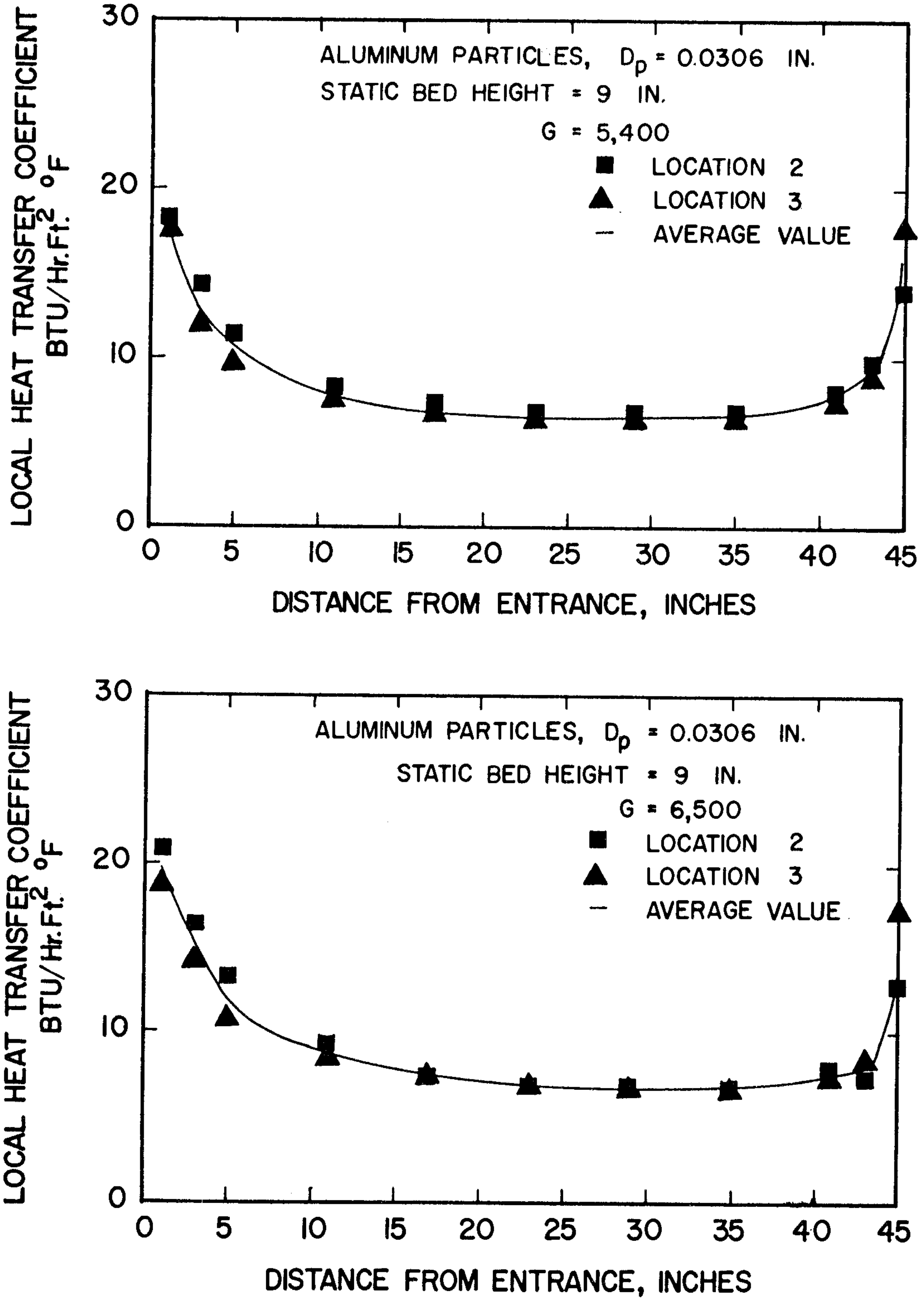

Figure 33. Local Heat Transfer Coefficients for Particulate Reflux Fluidization

heat transfer coefficient is observed over the last five to ten inches of the bed. At mass velocities discussed here, particles concentrate in the top part of the test section and in the disengaging section; thus explaining the increase in heat transfer coefficients in the latter part of the test section.

Coefficients for the coarse glass spheres are about 40 percent smaller in magnitude than those of the fine glass spheres. No significant difference in magnitude of heat transfer coefficients for fluidization with coarse glass and aluminum particles is observed. This fact is again attributed to the greater surface area per unit volume that the irregular aluminum particles have.

Only slightly larger heat transfer coefficients are observed at the nine-inch static bed height than at the four-inch static bed height. At the mass velocities investigated, an increase in the amount of particulate present in the model heat exchanger only slightly increases the particle concentration in the test section. Most of the extra particles were located in the top part of the test section and in the disengaging section. An increase in local heat transfer coefficient is observed near the top of the test section for an increase in static bed height.

Heat transfer coefficients measured at tube location 1 are greater than those at other tube locations. For fluidization with fine glass spheres heat transfer coefficients at location 1 are about 1.5

times greater than the weighted average; however, for fluidization with coarse glass spheres coefficients at location 1 are about 1.3 times greater. For one phase flow through unbaffled heat exchangers coefficients at a center location are also greater (27, p. 41). At the high velocities investigated here, the two phase flow in the test section approaches one phase flow. Heat transfer coefficients at the locations 2, 3, and 4 differ only slightly from each other. In most cases coefficients at location 2 are slightly greater than those at locations 3 and 4.

Average Heat Transfer Coefficients for Fluidization with Particulate Reflux

The average heat transfer coefficient over the entire heat exchanger is calculated from Equation 58. Using Pr = 0.7 and calculated values of the particle Reynolds and particle Nusselt numbers, j factors for heat transfer are calculated. Particle Reynolds numbers are correlated with j factors for heat transfer as shown in Figure 34. The following dimensionless equation fits most of the data with a scatter of ± 10 percent.

$$j_H = \frac{Nu_p}{Re_p Pr^{1/3}} = 0.14 \left(\frac{Re_p}{\phi}\right)^{-0.68} \qquad (69)$$

where ϕ is the ratio of the surface area of the particle to the surface area of a sphere of the same diameter. The solid symbols in

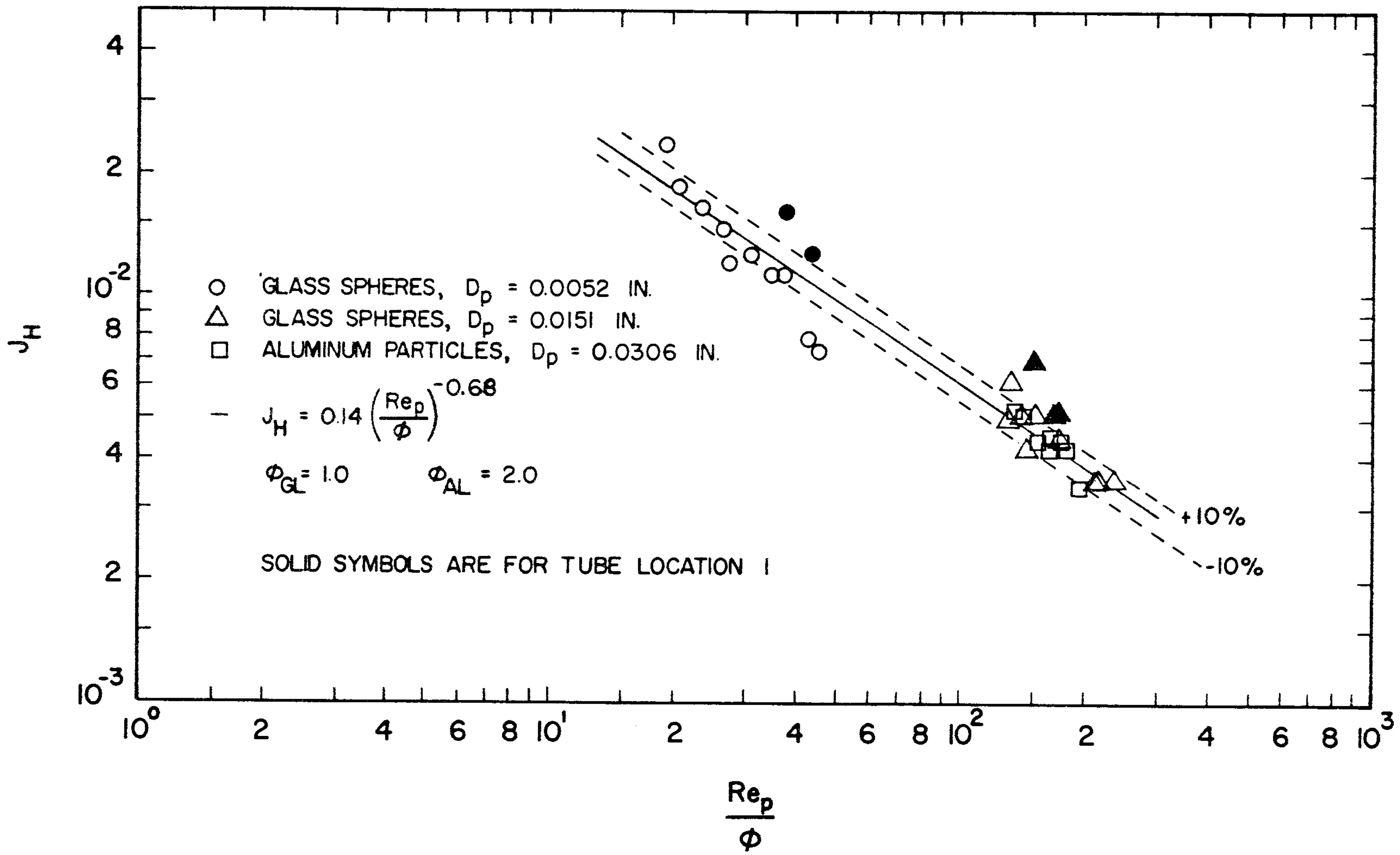

Figure 34. j_H vs. Re_p/ϕ for Particulate Reflux Fluidization

Figure 34 represent data measured at tube location 1. As noted in the previous section, coefficients at tube location 1 are greater than those of the other tube locations. From Equation 69 one can observe that the average heat transfer coefficient is proportional to $G^{0.32}$ and $D_p^{0.68}$.

Power and Space Considerations

Except for specific cases where costs are not the most important consideration or where a fluidized bed already exists for reasons other than increasing heat transfer coefficients, the fluidized bed heat exchanger must be at least as economical as other heat exchangers if it is to be used industrially.

Because of low heat transfer coefficients, unbaffled tubular heat exchangers require large surface areas to obtain desired heat transfer capacities. Costs of heat exchangers increase with increases in the needed surface area. Baffles have been used in tubular heat exchangers to reduce surface area requirements at the expense of pumping costs. The baffled tubular heat exchanger is the most widely used industrial heat exchanger, and for this reason it will be compared here with a fluidized bed tubular heat exchanger.

For each particle size four mass velocities were investigated at each tube location. Arithmetic averages of the average heat transfer coefficient and pressure drop at each tube location were calculated for all mass velocities. Pressure drop through a baffled heat exchanger of the same heat transfer capacity, $h_{av}A_s$, was calculated. The tube configuration and shell diameter of the fluidized unit and segmental baffles with 20 percent openings were used in the hypothetical baffled exchanger. Flow rates through both exchangers were the same. The baffle spacing was chosen to make the mean mass velocity, G_e, in the baffled exchanger equal to 5800 $lb_m/hr\ ft^2$. The number of baffles was chosen to give the same heat transfer capacity as the fluidized unit. Pressure drop and heat transfer coefficients for the baffled exchanger were calculated as described by Donohue (7).

The ratio of the pressure drop for the baffled heat exchanger to the pressure drop for the fluidized exchanger at the same heat transfer capacity, $h_{av}A_s$, was calculated. This ratio is plotted versus static bed height in Figure 35 for batch fluidization and in Figure 36 for fluidization with particulate recycle. When this pressure drop ratio is greater than one, the fluidized bed heat exchanger is advantageous in terms of pumping costs.

The plot at the top of Figure 35 describes this ratio at velocities where fluidization heights were approximately 30 inches. The ratio is greater than one for fluidization with fine glass particles for static bed heights less than seven inches. The ratio for fluidization with coarse glass particles and aluminum particles is significantly less

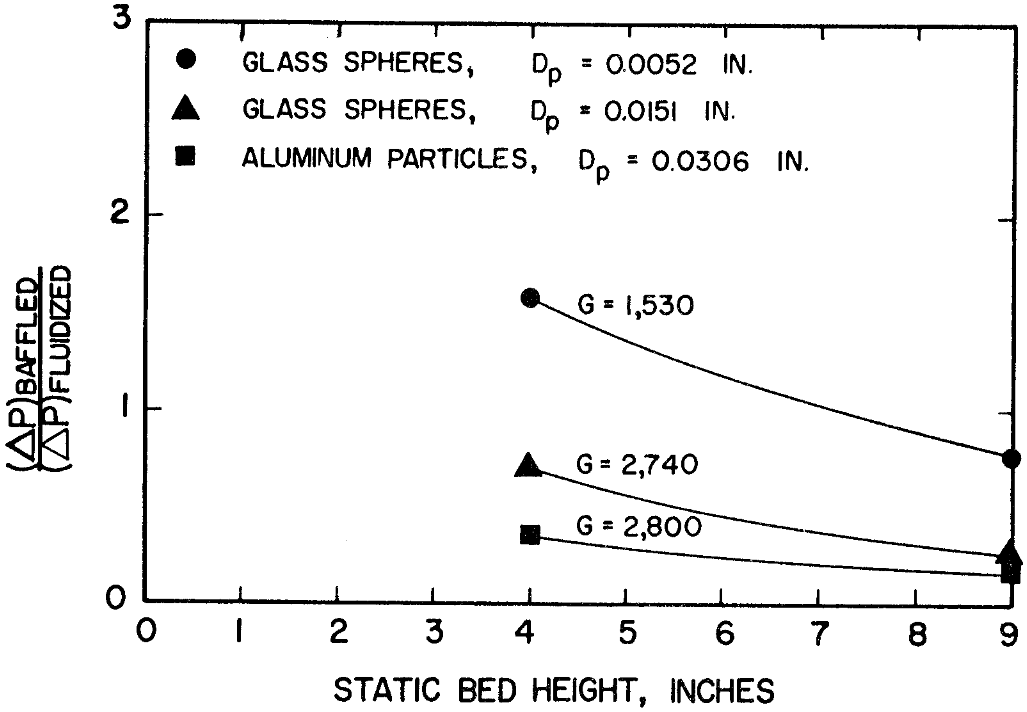

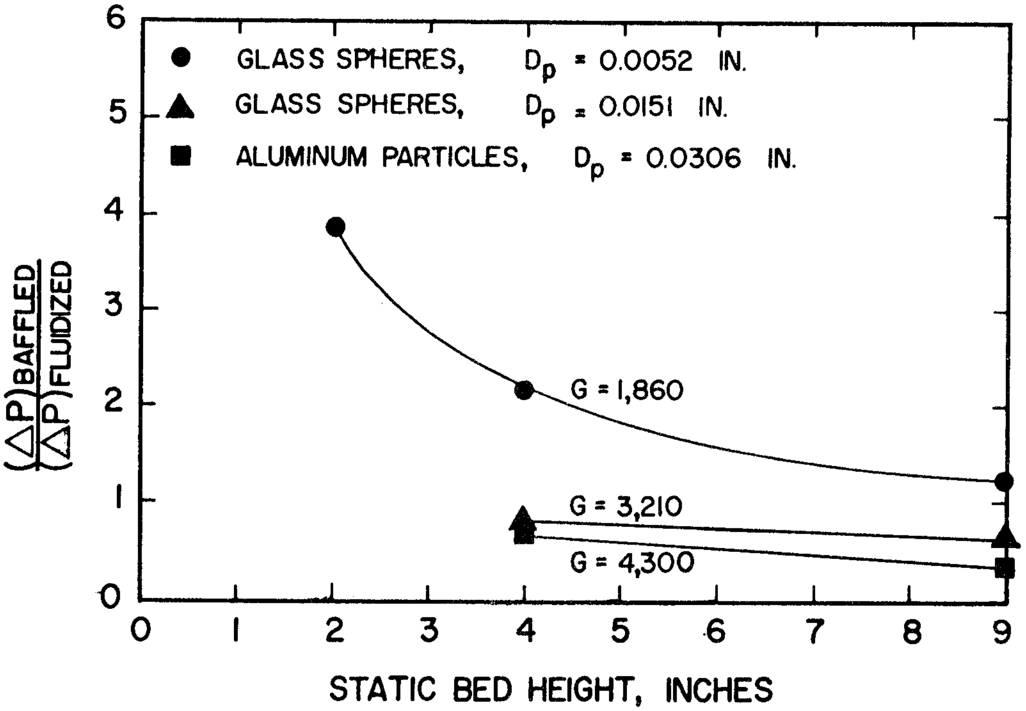

Figure 35. Comparison of Pressure Drops in Baffled and Fluidized Bed Exchangers for Batch Fluidization

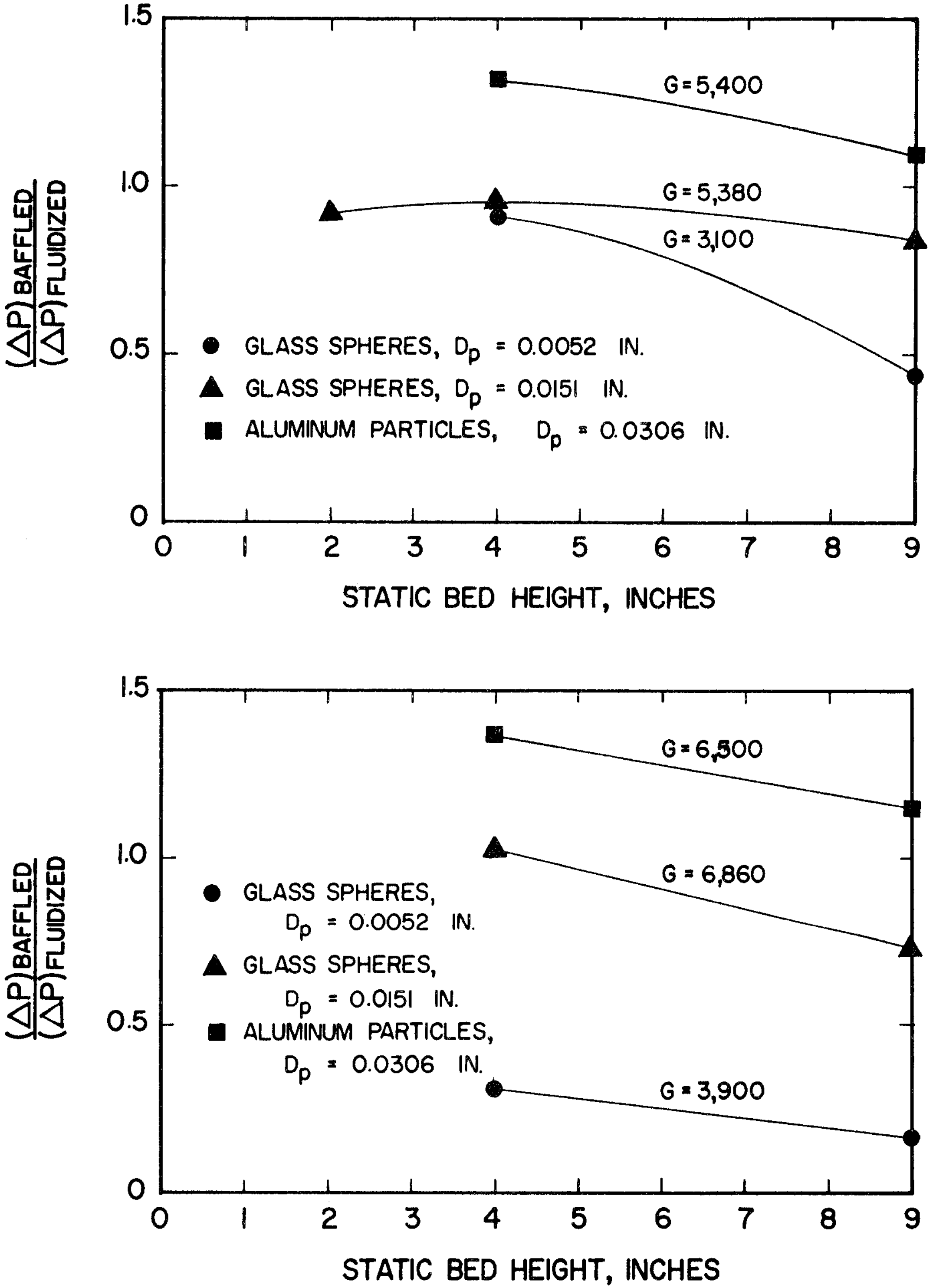

Figure 36. Comparison of Pressure Drops in Baffled and Fluidized Bed Exchangers for Particulate Reflux Fluidization

than one.

The lower plot of Figure 35 describes the pressure drop ratio at velocities where the entire heat exchanger is fluidized. The ratio is greater than one for fluidization with fine glass spheres for the static bed heights that were studied. The ratio for fluidization with coarse glass spheres and aluminum particles is again less than one.

The pressure drop ratio for fluidization with particle circulation, as is described in Figure 36, is greater than one for aluminum particles. The ratio for fluidization with coarse glass spheres is slightly less than one; whereas the ratio for fluidization with fine glass spheres is substantially less than one.

For the high mass velocities used in circulating the coarse glass and aluminum particles, calculated pressure drops through baffle openings are high. If a 30 percent baffle opening had been used, the pressure drop ratio at these velocities would have been less than one.

One additional pressure drop that should be considered for fluidization with particulate recycle is the pressure drop through the cyclone separator and connecting conduit. If this pressure drop was added to the pressure drop through the test section, the pressure drop ratio would be less than one for fluidization with all three particle types.

Since the shell diameter of the fluidized exchanger was used in the hypothetical baffled exchanger, a comparison of exchanger lengths will give an indication of surface area requirements for the two exchangers. For fluidization with fine glass spheres the baffled exchanger was longer than the fluidized exchanger except for G = 1540. The baffled exchangers ranged from 1.04 to 1.61 times greater in length. For fluidization with coarse glass and aluminum particles the baffled exchangers were always shorter.

Estimation of Experimental Errors

The errors involved in the determination of local heat transfer coefficients are:

1. errors in measurement of thermocouple emf values
2. errors in measurement of heating element voltage drop
3. errors in measurement of heating element current
4. errors in calculating local bulk temperatures

The values of emf from thermocouples were read to ± 0.002 millivolts. Over the range of temperature covered this error in temperature units is ± 0.07° F. Including a small computational error for calculating temperatures from emf values using Equations 52 or 53, the error is close to ± 0.1° F. Error involved in determining the local bulk gas temperature from temperatures at thermocouple locations by using Equation 54 is estimated to be ± 0.2° F. The total error in the local bulk gas temperature is felt to be close to ± 0.3° F.

The Simpson ammeter and the Simpson voltmeter used to measure the current and voltage drop respectively in the heating element had an accuracy of ± 2 percent at full scale. Both instruments were read at nearly full scale.

Errors involved in determining the heat flux are estimated by using Equation 56a, i. e.

$$q = 3.475\,(IV - I^2R_L) \tag{56a}$$

$$q \pm \text{error} = 3.475[(1 \pm 0.02)\,I(1 \pm 0.02)V - (1 \pm 0.02)^2 I^2 R_L]$$

$$q \pm \text{error} = 3.475\,(1 \pm 0.0404)(IV - I^2R_L)$$

$$q \pm \text{error} = (1 \pm 0.0404)q \tag{70}$$

Errors involved in determining ΔT_{loc} are estimated by using Equation 55, i. e.

$$\Delta T_{loc} = T_w - T_b \tag{55}$$

$$\Delta T_{loc} \pm \text{error} = (T_w \pm 0.1) - (T_b \pm 0.3)$$

$$\Delta T_{loc} \pm \text{error} = \Delta T_{loc} \pm 0.4 \tag{71}$$

By using Equation 56b, errors in the local heat transfer coefficient can be estimated as follows:

$$h_{loc} = \frac{q}{\Delta T_{loc}} \tag{56b}$$

$$h_{loc} \pm \text{error} = \frac{q(1 \pm 0.0404)}{\Delta T_{loc} \pm 0.4}$$

$$h_{loc} \pm \text{error} = h_{loc}(1 \pm 0.0404)(1 \pm \frac{\pm 0.4}{\Delta T_{loc} \pm 0.4}) \tag{72}$$

In this study local temperature differences, ΔT_{loc}, varied from 7° F to 188° F. Calculated percent error for local temperature differences, ΔT_{loc}, in this range are shown in Table II. For batch fluidization the smallest measured values for ΔT_{loc} are 7, 12, and 14° F for fluidization with fine glass, coarse glass, and aluminum particles respectively. For fluidization with fine glass particles ΔT_{loc} was less than ten for only three cases. For fluidization with particulate recycle ΔT_{loc} was greater than 20° F in almost all cases.

Table II. Percent Error in Local Heat Transfer Coefficients

ΔT_{loc} °F	Percent Error
7	10.3
10	8.4
15	6.9
20	6.2
30	5.4
40	5.1
60	4.7
90	4.5
140	4.3
190	4.3

Manometer readings for the section bed pressure drops were read to approximately ± 0.4 cm of fluid. Except for a few readings section bed pressure drops were greater than 3 cm of fluid. For 3 cm of fluid the estimated error would be ± 13 percent. For fluidization with fine glass spheres, particles would at times plug the pressure taps on the test section which would cause incorrect readings. The line pressure was read to ± 0.2 cm of Hg. The manometer reading for the orifice pressure drop was read to ± 0.4 cm of fluid. For fluidization with fine glass, coarse glass and aluminum particles, the smallest recorded readings for orifice pressure drops were 3.1, 8.1, and 8.0 respectively. This would result in maximum percent errors in orifice pressure drops of 13.0, 5.0, and 4.9 for the fine glass, coarse glass, and aluminum particles respectively.

A correctly constructed square edged orifice meter has a reproducibility of about two percent (29, sec. 5, p. 11). This assumes that the correct coefficient of discharge, density, and pressure drop are used. With this in mind, a maximum error of the order of ± 10 percent is estimated for the gas flow rate.

RESULTS AND CONCLUSIONS

Local and average heat transfer coefficients for shell-side heat transfer from a fluidized bed tubular heat exchanger were investigated. Batch fluidization and fluidization with particle recycle were investigated, using air as the fluid phase and glass or aluminum particles as the particulate phase. Heat transfer coefficients for air flowing through the heat exchanger without fluidization were also investigated.

Average Nusselt Numbers without Fluidization

The average heat transfer coefficients for air alone agree with those calculated from accepted correlations (2, p. 93; 7); therefore, it is concluded that correct values of coefficients were obtained by the procedure followed.

Bed Thermal Gradients

From measurements of radial and vertical temperature profiles, bed thermal gradients are shown to be small in the fluidized bed except for the first few inches of the test section. A one to three degree increase of temperature is observed over the first few inches of the bed. Since thermal gradients in the bed are small, coefficients for a fluidized heat exchanger with all of the tubes in the bundle heated would not differ substantially from the coefficients for an exchanger with one tube heated in the bundle.

Heat Transfer with Batch Fluidization

For batch fluidization local heat transfer coefficient profiles were of two types. For a Type I profile coefficients are high at the bottom of the bed and decrease at higher levels in the bed. Type II profiles have a maximum. For increasing values of the group $D_t^2/L_f S_b$, there is a greater tendency to have Type I profiles. When fine glass particles are the fluidized medium, the local heat transfer coefficients are in the range 25 - 40 Btu/hr ft^2 °F for the most dense part of the bed. When coarse glass or aluminum particles are the fluidized medium, the local heat transfer coefficients are in the range 15 - 30 Btu/hr ft^2 °F for the most dense part of the bed.

Nusselt numbers averaged over 11-inch sections of the fluidized bed are correlated with Equation 68, an equation developed from a modified form of the Ziegler, Koppel, and Brazelton model for fluidization heat transfer, i. e.

$$Nu_p = \frac{5\,\phi\,(1-\epsilon)^{0.48}}{\left[1 + \frac{580}{Re_p}\left(\frac{k_g}{D_p^{3/2} C_s \rho_s g^{1/2}}\right)\left(\frac{\rho_s}{\rho_g}\right)^{1.1}\left(\frac{G_{mf}}{G}\right)^{4/3}\right]^2} \qquad (68)$$

Several conclusions can be drawn from this correlation:

1. Particle Nusselt numbers are independent of particle thermal conductivity.
2. Particle Nusselt numbers are proportional to $(1 - \epsilon)^{0.48}$. (This result agrees with previously published data (10; 23; 24; 27, p. 47).)
3. Particle Nusselt numbers are proportional to average particle surface area.
4. Particle Nusselt numbers become less dependent on mass velocity as mass velocities are increased. (This fact was also concluded by Leva (18, p. 197) when discussing Dow and Jakob's results.)

Particle Nusselt numbers, Nu_p, are about 20 percent lower than those calculated from Gamson's correlation (10) for a single vertical heating tube in a fluidized bed. This agreement leads one to believe that tube configuration and tube spacing affects heat transfer coefficients only slightly.

Local coefficients did vary slightly with tube location for batch fluidization. In most cases coefficients measured at tube location 2 were the largest and coefficients measured at tube location 1 were the smallest. Coefficients measured at tube locations 3 and 4 were usually of an intermediate value. Average coefficients did not vary significantly with tube location. It is concluded from the results of Toomey and Johnstone (31), Vreedenberg (34), and the present investigation that the effect of tube location on heat transfer coefficients is a function of the mass velocity. At mass velocities greater than 1000 $lb_m/hr\ ft^2$, tube location affects heat transfer coefficients only slightly. At mass velocities below 700 $lb_m/hr\ ft^2$, it is believed that tube location will significantly affect heat transfer coefficients.

Heat Transfer with Particle Recycle Fluidization

For fluidization with particulate recycle, local heat transfer coefficients decrease in magnitude over the first few inches of the test section; the coefficient then remains constant to heights between 35 and 40 inches from the entrance; and an increase in heat transfer coefficient is observed over the remaining five to ten inches.

Equation 69 correlates the average particle Nusselt number within ± ten percent, i. e.

$$j_H = \frac{Nu_p}{Re_p Pr^{1/3}} = 0.14 \left(\frac{Re_p}{\phi}\right)^{-0.68} \qquad (69)$$

Except at tube location 1, local heat transfer coefficients are only slightly affected by tube location. Average coefficients at location 1 are 10 to 20 percent larger than coefficients measured at locations 2, 3, and 4.

Comparisons of the Fluidized Bed Exchanger to a Typical Baffled Exchanger

For batch fluidization with fine glass spheres (D_p = 0.0052 inch) a fluidized bed heat exchanger, having a static bed height of less than seven inches, and operating at a fluidized bed height of 30 inches, has a smaller pumping requirement than does a baffled exchanger of the same heat transfer capacity. When the fluidized bed exchanger is completely fluidized, the fluidized exchanger is advantageous in terms of pumping requirements when using fine glass spheres. For fluidization with coarse glass spheres (D_p = 0.0151 inch) or aluminum particles (D_p = 0.0306 inch), the baffled exchanger is advantageous in terms of pumping requirements.

For fluidization with particle recycle, pumping costs are less for the fluidized exchanger when fluidized with aluminum particles. Calculated pressure drops through the baffle openings were large at the velocities used for the aluminum and coarse glass particles. The pressure drop through the baffled heat exchanger could be reduced by using larger baffle openings. Pressure drops through the cyclone separator and connecting conduit were not considered.

At the same heat transfer capacity, $h_{av} A_s$, the fluidized bed heat exchanger was advantageous in terms of surface area requirement when completely fluidized with fine glass spheres for all static bed heights studied.

RECOMMENDATIONS FOR FURTHER STUDY

1. More experimental information is needed for heat transfer from a vertical tube bundle to a gas fluidized bed for mass velocities less than 800 $lb_m/hr\ ft^2$. For velocities in this range it is expected that tube location will have a significant effect on heat transfer coefficients. It is suggested when studying the effect of tube location that tubes of interest be heated simultaneously. In this manner heat transfer coefficients at different tube locations can be determined at identical conditions.

2. A study of heat transfer to a bed fluidized with nonspherical particles of known surface area is recommended. A study of this type will help to further substantiate the theory presented here and will determine quantitatively the effect that particle shape has on heat transfer. Such particle shapes as cubes, discs, and pyramids are suggested.

3. Baffles made of wire cloth could be used to more evenly distribute the particles over the entire heat exchanger. In effect the heat exchanger would consist of several fluidized beds stacked on top of each other. In this manner the high heat transfer coefficients of dense phase fluidization could be obtained for an exchanger of any length. Power requirements of such an operation should be determined.

4. An increase in the effective area of the heating tubes can be obtained by adding fins to the tubes. It appears that longitudinal fins would be more feasible since transverse fins on a vertical tube would probably increase particle hold-up. The effects of fin spacing and fin widths on heat transfer coefficients should be determined. Local heat transfer coefficients on the fins and the tube should also be determined.

5. It is recommended that the study of a gas fluidized bed tubular heat exchanger be extended to a liquid fluidized bed exchanger. Since the mathematical model proposed in the present study is valid only for $k_f/k_s < 0.2$ a fluidizing medium such as water, $k_f/k_s \cong 0.6$, would further test the proposed mechanism. The particle thermal conductivity in fluidized beds with $k_f/k_s > 0.2$ is expected to have an effect on heat transfer coefficients. Several particle types having different thermal conductivities should be investigated.

6. Gases or liquids that normally cause excessive fouling should be used in a fluidized bed heat exchanger to study the effecttiveness of the particle scrubbing action in eliminating fouling.

BIBLIOGRAPHY

1. Ainshtein, V. G. and N. I. Gel'perin. Heat transfer between a fluidized bed and a surface. International Chemical Engineering 6:67-74. 1966.

2. Ambrose, Tommy W. Local shell-side heat transfer coefficients in baffled tubular heat exchangers. Ph. D. Thesis. Corvallis, Oregon State College, 1957. 185 numb. leaves.

3. Baddour, R. F. and C. Y. Yoon. Local radial effective conductivity and the wall effect in packed beds. American Institute of Chemical Engineers, Chemical Engineering Progress Symposium Series no. 32, p. 35-50. 1961. (Supplement to Chemical Engineering Progress v. 57)

4. Baskakov, A. P. The mechanism of heat transfer between a fluidized bed and a surface. International Chemical Engineering 4:320-323. 1964.

5. Botterill, J. S. M. and J. R. Williams. The mechanism of heat transfer to gas-fluidized beds. Transactions of the Institute of Chemical Engineers 41:217-230. 1963.

6. Carslaw, H. S. and J. S. Jaeger. Conduction of heat in solids. London, Oxford University, 1959. 510 p.

7. Donohue, Daniel A. Heat transfer and pressure drop in heat exchangers. Industrial and Engineering Chemistry 41:2499-2511. 1949.

8. Dow, Willard M. and Max Jakob. Heat transfer between a vertical tube and a fluidized air-solid mixture. Chemical Engineering Progress 47:637-648. 1951.

9. Eichhorn, J. and R. R. White. Particle-to-fluid heat transfer in fixed and fluidized beds. American Institute of Chemical Engineers, Chemical Engineering Progress Symposium Series no. 4, p. 11-18. 1952. (Supplement to Chemical Engineering Progress v. 48)

10. Gamson, Bernard W. Heat and mass transfer. Chemical Engineering Progress 47:19-28. 1951.

11. Harriott, Peter and L. A. Barnstone. Heat transfer in fluidized beds. Industrial and Engineering Chemistry 59(4):55-60. 1967.

12. Heertjes, P. M. and S. W. McKibbins. The partial coefficient of heat transfer in a drying fluidized bed. Chemical Engineering Science 5:161-167. 1956.

13. Holman, J. P., T. W. Moore and V. M. Wong. Particle-to-fluid heat transfer in water-fluidized systems. Industrial and Engineering Chemistry Fundamentals 4:21-31. 1965.

14. Juveland, A. C., H. P. Deinken and J. E. Dougherty. Particle-to-gas heat transfer in fluidized beds. Industrial and Engineering Chemistry Fundamentals 3:329-333. 1964.

15. Ketternring, K. N., E. L. Manderfield and J. M. Smith. Heat and mass transfer in fluidized systems. Chemical Engineering Progress 46:139-145. 1950.

16. Knudsen, James G. and Donald L. Katz. Fluid dynamics and heat transfer. New York, McGraw-Hill, 1958. 576 p.

17. Lemlich, Robert and Isidoro Caldas, Jr. Heat transfer to a liquid fluidized bed. A. I. Ch. E. Journal 4:376-380. 1958.

18. Leva, Max. Fluidization. New York, McGraw-Hill, 1959. 327 p.

19. Leva, Max, M. Weintraub and M. Grummer. Heat transmission through fluidized beds of fine particles. Chemical Engineering Progress 45:563-572. 1949.

20. Levenspiel, O. and J. S. Walton. Bed-wall heat transfer in fluidized systems. American Institute of Chemical Engineers, Chemical Engineering Progress Symposium Series no. 9, p. 1-13. 1954. (Supplement to Chemical Engineering Progress v. 50)

21. Lewis, W. K., E. R. Gilliland and H. Girouard. Heat transfer and solid mixing in beds of fluidized solids. American Institute of Chemical Engineers, Chemical Engineering Progress Symposium Series no. 38, p. 87-97. 1962. (Supplement to Chemical Engineering Progress v. 58)

22. McAdams, William H. Heat transmission. 3d ed. New York, McGraw-Hill, 1954. 532 p.

23. Mickley, H. S. and D. F. Fairbanks. Mechanisms of heat transfer to fluidized beds. A. I. Ch. E. Journal 1:374-384. 1955.

24. Mickley, Harold S. and Charles A. Trilling. Heat transfer characteristics of fluidized beds. Industrial and Engineering Chemistry 41:1135-1147. 1949.

25. Miller, C. O. and A. K. Logwinuk. Fluidization studies of solid particles. Industrial and Engineering Chemistry 43:1220-1226. 1951.

26. Milne, William Edmund. Numerical calculus. Princeton, N. J., Princeton University, 1949. 393 p.

27. Noë, Alphonse Roman. Local and average heat transfer coefficients in a fluidized bed heat exchanger. M. S. Thesis. Corvallis, Oregon State University, 1964. 88 numb. leaves.

28. Perry, John H. et al. Chemical engineers' handbook. 3d ed. New York, McGraw-Hill, 1956. 1942 p.

29. Perry, Robert H. et al. Chemical engineers' handbook. 4th ed. New York, McGraw-Hill, 1963. Various paging.

30. Richardson, J. F. and P. Ayers. Heat transfer between particles and a gas in a fluidised bed. Transactions of the Institute of Chemical Engineers 37:314-322. 1959.

31. Toomey, Robert D. and H. F. Johnstone. Heat transfer between beds of fluidized solids and the walls of the container. American Institute of Chemical Engineers, Chemical Engineering Progress Symposium Series no. 5, p. 51-63. 1953. (Supplement to Chemical Engineering Progress v. 49)

32. Van Heerden, C., A. P. Nobel and D. Krevelen. Mechanism of heat transfer in fluidized beds. Industrial and Engineering Chemistry 45:1237-1242. 1953.

33. Vreedenberg, H. A. Heat transfer between a fluidized bed and a horizontal tube. Chemical Engineering Science 9:52-60. 1958.

34. ________________ Heat transfer between fluidized beds and vertically inserted tubes. Journal of Applied Chemistry 2(sup.): S26-S33. 1952.

35. Walton, J. S., R. L. Olson and Octave Levenspiel. Gas-solid film coefficients of heat transfer in fluidized coal beds. Industrial and Engineering Chemistry 44:1474-1480. 1952.

36. Wamsley, W. W. and L. N. Johanson. Fluidized bed heat transfer. Chemical Engineering Progress 50:347-355. 1954.

37. Wender, Leonard and George T. Cooper. Heat transfer between fluidized-solids beds and boundary surfaces - correlation of data. A. I. Ch. E. Journal 4:15-23. 1958.

38. Zenz, F. A. and D. F. Othmer. Fluidization and fluid-particle systems. New York, Reinhold, 1960. 513 p.

39. Ziegler, Edward N. and William T. Brazelton. Mechanism of heat transfer to a fixed surface in a fluidized bed. Industrial and Engineering Chemistry Fundamentals 3:94-98. 1964.

40. Ziegler, E. N., L. B. Koppel and W. T. Brazelton. Effects of solid thermal properties on heat transfer to gas fluidized beds. Industrial and Engineering Chemistry Fundamentals 3:324-328. 1964.

41. Gel'perin, N. I., V. G. Ainshtein and N. A. Romanova. Hydraulics and heat exchange in a fluidized bed with vertical tube bundles. Kimicheskaya Promyshlennost (11): 823-830.

APPENDICES

APPENDIX A

NOMENCLATURE

NOMENCLATURE

Symbol	Definition	Dimensions
a	effective area for heat transfer per unit volume of bed	ft^{-1}
A	cross sectional area of fluidized bed	ft^2
A_n	coefficients for the interpolating formula for the local bulk gas temperature	° F/inch
Ar	Archimedes number, $\frac{gD_p^3}{\nu^2} \frac{\rho_s - \rho_f}{\rho_f}$	dimensionless
b	coefficient for Equation 28	dimensionless
C	coefficient of discharge used in orifice meter calculations	dimensionless
C_f	heat capacity of the fluid	Btu/lb_m ° F
C_g	heat capacity of the gas	Btu/lb_m ° F
C_{qb}	quiescent bed heat capacity	Btu/lb_m ° F
C_s	heat capacity of solids	Btu/lb_m ° F
C_R	correction factor for tube location in the fluidized bed	dimensionless
d_t	tube diameter	ft
D	bed diameter	ft
D_e	equivalent diameter of a tubular heat exchanger	inches
D_p	particle diameter	inches, ft.
D_t	bed diameter	ft
D_{AB}	diffusivity	ft^2/sec

Symbol	Definition	Dimensions
emf	electromotive force produced by the thermocouples	millivolts
$f(\theta)$	contact time distribution function	dimensionless
F_ϵ	velocity correction factor of Equation 6	dimensionless
g	acceleration due to gravity	ft/sec^2
g_c	gravitational constant	$\frac{lb_m\ ft}{lb_f sec^2}$
G	gas mass velocity	$lb_m/hr\ ft^2$
G_{mf}	gas mass velocity at minimum fluidization	$lb_m/hr\ ft^2$
h	heat transfer coefficient	$Btu/hr\ ft^2\ °F$
h_c	heat transfer coefficient for transfer to a particle near the wall	$Btu/hr\ ft^2\ °F$
h_{loc}	local heat transfer coefficient	$Btu/hr\ ft^2\ °F$
h_N	natural convection heat transfer coefficient	$Btu/hr\ ft^2\ °F$
Δh	manometer readings	cm
H_0	heat transfer surface height	ft
I	current flowing through the heating element	amperes
j_H	j factor for heat transfer, $Nu/Pr^{1/3}Re$	dimensionless
k_c	thermal conductivity of copper	Btu/hr ft ° F
k_f	thermal conductivity of the fluid	Btu/hr ft ° F
k_g, K_G	thermal conductivity of the gas	Btu/hr ft ° F
k_m	mean bed thermal conductivity	Btu/hr ft ° F

Symbol	Definition	Dimension
k_{qb}	quiescent bed thermal conductivity	Btu/hr ft ° F
k_s	thermal conductivity of the solids	Btu/hr ft ° F
K_m	mean mass transfer coefficient	ft/hr
L	length of test section	ft
L_f	fluidization height	ft
L_c	length of copper contacts in tube wall temperature probe	ft
M	exponent coefficient in Equation 36, $12k_g/\rho_s C_s D_p^2$	hr^{-1}
N	modified Nusselt number, $h_c D_p/2k_g$	dimensionless
Nu_p	particle Nusselt number, $h D_p/k_g$	dimensionless
Nu_{av}	average particle Nusselt number, $h_{av} D_p/k_g$	dimensionless
Nu_{max}	maximum Nusselt number, $h_{max} D_p/k_g$	dimensionless
P	Pressure	lb_f/ft^2
ΔP_o	orifice pressure drop	lb_f/ft^2
ΔP_b	pressure drop across a section of the fluidized bed	lb_f/ft^2
ΔP_t	total pressure drop across the test section	lb_f/ft^2
Pr	Prandtl number, $C_g \mu/k_g$	dimensionless
q	heat flux from heat transfer surface	Btu/hr ft^2
q_p	heat flux to a particle near the heat transfer surface	Btu/hr ft^2
r	radial distance from the center of the bed	ft

Symbol	Definition	Dimension
R	radius of the fluidized bed	ft
Re	Reynolds number	dimensionless
Re_p	particle Reynolds number, $D_p G/\mu$	dimensionless
Re_{opt}	particle Reynolds number when the particle Nusselt number is a maximum	dimensionless
s	stirring factor	hr^{-1}
S	tube spacing in tube bundle	ft
S_b	static bed height	inches
S_2	cross sectional area of orifice	ft^2
Sc	Schmidt number, $\mu/\rho_g D_{AB}$	dimensionless
T	temperature	° F
T_b	bulk bed gas temperature	° F
T_{b_n}	bulk bed gas temperature at the nth bulk gas thermocouple	° F
T_f	average temperature of air surrounding a particle near the heat transfer surface	° F
T_{in}	gas inlet temperature	° F
T_w	tube wall temperature	° F
T_c	temperature in the copper contact of the tube wall probe	° F
T_m	temperature in micarta surrounding the thermocouples in the tube wall probe	° F
ΔT_{loc}	local temperature difference	° F
ΔT_{av}	average temperature difference	° F

Symbol	Definition	Dimension
V	voltage drop across heating element	volts
x	distance into the copper contact of the tube wall temperature probe	inches
X	dimensionless distance into the copper contact of the tube wall temperature probe	dimensionless
Y	radial distance to the transverse thermocouple	inches
Y_o	expansion factor for the orifice meter	dimensionless
Z	vertical distance from the entrance of the test section	inches
Z_n	vertical distance to the nth bulk gas thermocouple	inches
α	shape factor for gamma distribution	dimensionless
β	ratio of the orifice diameter to the pipe diameter	dimensionless
γ_p	number of particles per unit surface area	particles/ft^2
ϵ	void fractions	dimensionless
η	dimensionless radius, $2r_p/D_p$	dimensionless
θ	contact time	hr
$\bar{\theta}, \theta_c$	average contact time	hr
ρ_b	bed density	lb_m/ft^3
ρ_g	gas density	lb_m/ft^3
ρ_f	fluid density	lb_m/ft^3

Symbol	Definition	Dimension
ρ_m	mean density	lb_m/ft^3
ρ_{qb}	quiescent bed density	lb_m/ft^3
ρ_s	solids density	lb_m/ft^3
ρ_1	gas density upstream from the orifice	lb_m/ft^3
μ	gas viscosity	$lb_m/hr\ ft$
ν	kinematic viscosity	ft^2/hr
Φ	dimensionless temperature	dimensionless
ϕ	ratio of the particle surface area to the area of a spherical particle of the same diameter	dimensionless
τ	dimensionless contact time, $\frac{4k_s\theta}{\rho_s C_s D_p^2}$	dimensionless
λ_n	eigenvalues	$hr^{-1/2}$

APPENDIX B

CALIBRATION OF THE ORIFICE METER

CALIBRATION OF THE ORIFICE METER

The orifice meter was calibrated with velocity profiles determined with a pitot tube. The pitot tube was placed in the three-inch diameter gas supply line. A location on the supply line was chosen where the velocity profile is fully developed. The pitot tube was constructed with a 1/16-inch stainless steel tube. A screw moving device with a mounted indicating dial was used to determine the radial location of the pitot tube in the pipe. Pitot tube pressure drops were measured with a manometer inclined at 30°.

For six flow rates in the range of interest, point velocities were determined at nine radial locations in the pipe. The resulting velocity profiles were integrated to determine the average velocities in the pipe. The temperature and pressure of the air in the pipe line were also measured. Gas density was calculated using the ideal gas law.

The average velocity in the pipe determined from the measured velocity profile is plotted versus the calculated quantity, $Y_o S_2/\rho_1 S_1 \sqrt{\frac{2g_c \Delta P_o \rho_1}{1 - \beta^2}}$, and is shown in Figure 37.

The slope of the line, 0.6024, determined by a least squares analysis (26, p. 242) is the coefficient of discharge, C, over the flow rates of interest.

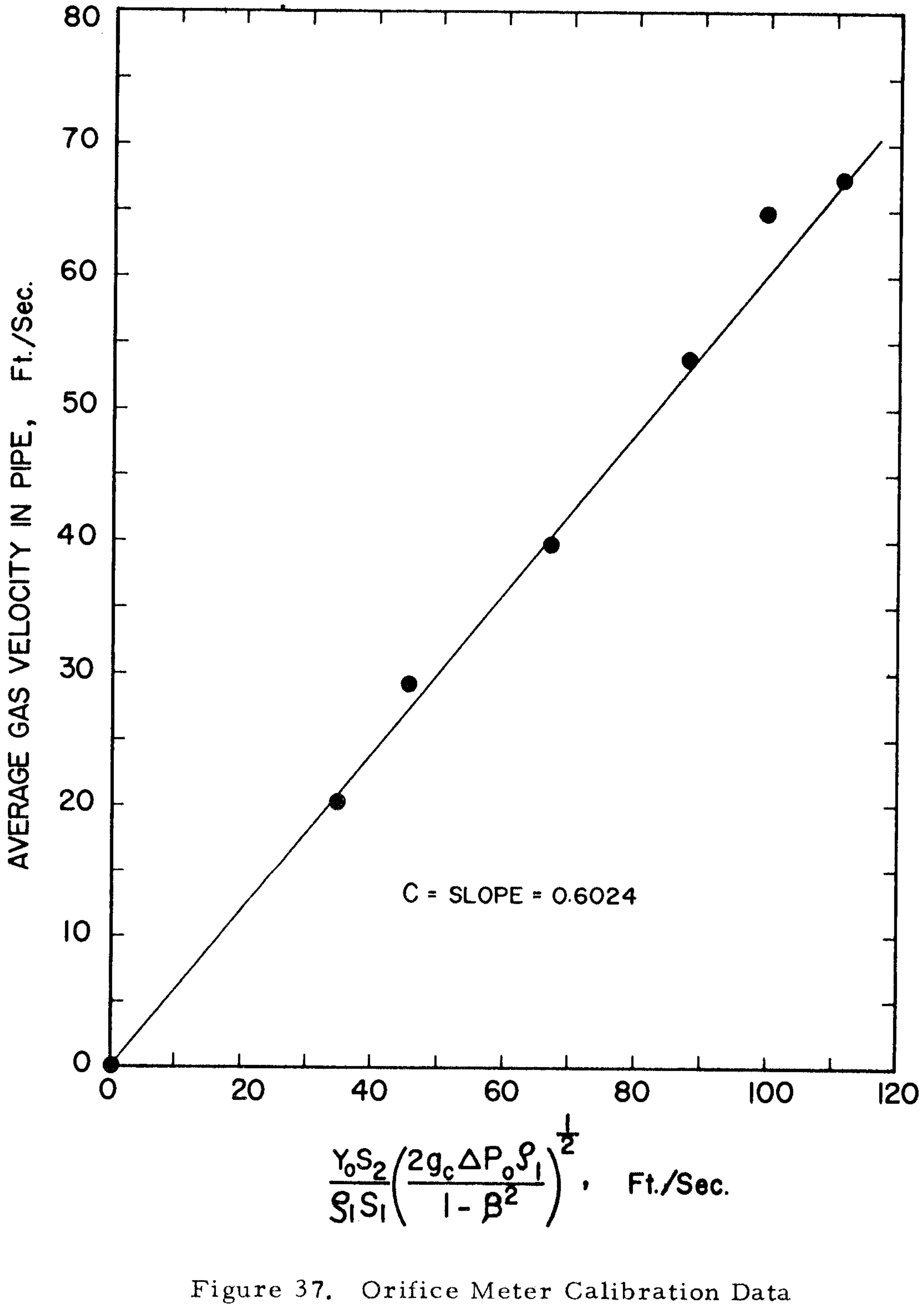

Figure 37. Orifice Meter Calibration Data

APPENDIX C

CALIBRATION OF THERMOCOUPLES AND THE TUBE WALL PROBE ANALYSIS

CALIBRATION OF THERMOCOUPLES AND THE TUBE WALL PROBE ANALYSIS

1. Thermocouple Calibrations

The copper-constantan thermocouples used in this investigation were calibrated with a mercury thermometer accurate to 0.1° F. Both the thermocouple to be calibrated and the thermometer were submerged in a well stirred water bath. The thermocouple emf and thermometer were simultaneously read for bath temperatures between 50 and 180° F.

The measured temperatures are plotted versus the measured emf's for the various thermocouples on Figure 38. The curve represents the Leeds and Northrup calibration for copper-constantan thermocouples[1]. Agreement between the present calibrations and the Leeds and Northrup calibration is excellent. The tabulated data of the Leeds and Northrup calibration were used to determine the coefficients for the interpolating formulas.

2. Tube Wall Probe Analysis

The tube wall probe consisted of two copper contacts rounded to the shape of the tube wall. A thermocouple was embedded in the

---

[1] The leeds and Northrup standard conversion tables for L and N thermocouples are available through the Leeds and Northrup Company of Philadelphia.

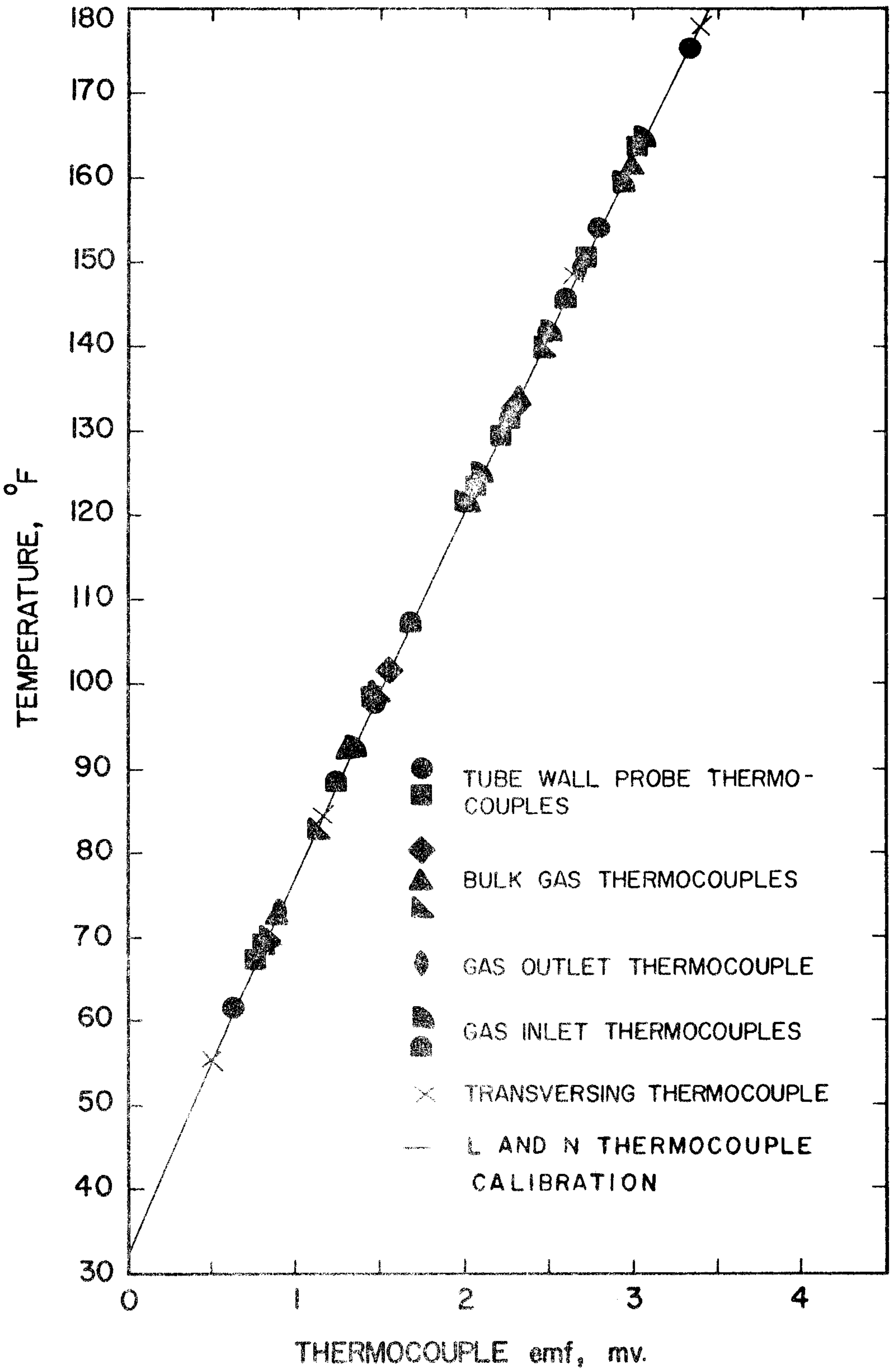

Figure 38. Thermocouple Calibration Data

copper contact, but electrically insulated from the copper with epoxy and micarta. Each copper contact is held in contact with the tube wall by a spring. The sides of the copper contacts are insulated with micarta; however, the spring ends of the contacts are adjacent to air. It is conceivable that steady state conduction through the copper and micarta would not be negligible.

If we consider the contact to be a 1/8-inch long cylinder, the first 1/16 inch being copper, and the remaining 1/16 inch being micarta, we can approximate the contact. Using a relation given by McAdams (22, p. 181), a natural convection heat transfer coefficient of 0.25 Btu/hr ft^2 °F was calculated. In this calculation a temperature difference of 10° F was assumed. A heat transfer coefficient representing the inverse of the resistance to heat transfer between the tube wall and the copper contact was assumed to be 1000 Btu/hr ft^2°F.

The differential equations and boundary conditions with the above assumptions are as follows:

$$\frac{d^2T_c}{dX^2} = 0 \qquad 0 \leq X \leq \frac{1}{2} \qquad (73a)$$

$$\frac{d^2T_m}{dX^2} = 0 \qquad \frac{1}{2} \leq X \leq 1 \qquad (73b)$$

$$\frac{-k_c}{L}\,\frac{dT_c}{dX}(0) = h_w(T_w - T_c(0)) \tag{73c}$$

$$T_c(\tfrac{1}{2}) = T_m(\tfrac{1}{2}) \tag{73d}$$

$$-k_c\,\frac{dT_c}{dX}(\tfrac{1}{2}) = -k_m\,\frac{dT_m}{dX}(\tfrac{1}{2}) \tag{73e}$$

$$\frac{-k_m}{L}\,\frac{dT_m}{dX}(1) = h_N(T_m(1) - T_A) \tag{73f}$$

where

$X = \frac{x}{L}$

T_A = air temperature inside probe, °F

h_w = 1000 Btu/hr ft^2 °F

h_N = 0.25 Btu/hr ft^2 °F

k_c = 218 Btu/hr ft °F

k_m = 0.1 Btu/hr ft °F

The solution to the above problem is:

$$T_c(X) = \frac{\left[\frac{L}{2}\left[1 + \frac{k_m}{k_c}(1 - X) + \frac{k_m}{h_N}\right]\right](T_w - T_A)}{\left[\frac{L}{2}\left(1 + \frac{k_m}{k_c}\right) + \frac{k_m}{h_N} + \frac{k_m}{h_w}\right]} + T_A \tag{74a}$$

$$T_m(X) = \frac{[L(1 - X) + \frac{k_m}{h_N}]\,(T_w - T_A)}{[\frac{L}{2}(1 + \frac{k_m}{k_c}) + \frac{k_m}{h_N} + \frac{k_m}{h_w}]} + T_A \tag{74b}$$

The largest errors in determining the local heat transfer coefficients for the heat exchanger occur when the wall temperature is about 90° F; therefore, for the present calculation, the tube wall temperature and the air temperature in the probe are assumed to be 90° F and 80° F respectively. By substituting numerical values into Equation 74b, the following equation for the temperature in the micarta is obtained:

$$T_m(X) = \frac{[0.40 + .0104\,(1 - X)]\,10}{0.40531} + 80 \tag{75}$$

The thermocouple junction is located at approximately X = 5/8; therefore, the temperature at the junction is

$$T_m(\tfrac{5}{8}) = 89.965°\ F \tag{76}$$

The error involved in the probe is

$$T_w - T_m(\tfrac{5}{8}) = 0.035°\ F \tag{77}$$

This calculated error is greater than would be expected in the operating probe, since the assumed values of the temperature difference between the contact and the enclosed air and the heat transfer resistance between the contact and the tube wall were purposely chosen large. The calculated error is less than the accuracy involved in reading the thermocouple emf; therefore, it is negligible.

APPENDIX D

SAMPLE RAW DATA SHEET

SAMPLE RAW DATA SHEET

RUN 9 F

Date 7/25/67

Tube Location 2

Static Bed Height 6 inches

Type of Particle Fine Glass Spheres

	Volt	Volt	Volt	Volt
Voltmeter Reading	2.78	2.78	2.77	2.77
	Amperes	Amperes	Amperes	Amperes
Ammeter Reading	39.1	38.9	38.9	38.9
	cm of fluid		cm of fluid	
Orifice Pressure Drop	5.3	5.3	5.3	5.3
	cm of Hg	cm of Hg	cm of Hg	cm of Hg
Inlet Pressure	3.8	3.8	3.8	3.8
	mv	mv	mv	mv
Inlet Thermocouple emf	2.065	2.047	2.052	2.066
Outlet Thermocouple emf	1.162	1.153	1.161	1.168

Transversing Thermocouple emf

Y, inches	Y/D		mv	mv	mv
0.575	0.1		1.188	1.165	1.163
1.75	0.4		1.178	1.157	1.158
4.00	0.8		1.101	1.094	1.112

	cm of fluid		cm of fluid	
Section 1, ΔP_b	25.0	25.0	25.0	25.0
Section 2, ΔP_b	23.0	23.3	23.3	23.4
Section 3, ΔP_b	4.7	5.2	5.0	6.3
Section 4, ΔP_b	40.0	40.0	40.0	40.0

Tube Wall Probe Thermocouple

Position, inches	1.0 mv	3.0 mv	5.0 mv	8.0 mv	11.0 mv
emf	2.704	2.808	2.803	2.763	2.949
Position, inches	17.0 mv	23.0 mv	29.0 mv	35.0 mv	41.0 mv
emf	2.948	3.218	3.765	4.183	4.512
Position, inches	45.0 mv				
emf	4.672				

Bulk bed Thermocouples, emf

height, inches	mv	mv	mv	mv
9.5	1.188	1.212	1.173	1.205
17.5	1.191	1.172	1.179	1.181
27.5	1.183	1.158	1.167	1.178
38.5	1.188	1.168	1.172	1.164

APPENDIX E

TABLE III. RADIAL BULK BED TEMPERATURE DATA

Table III. Radial Bulk Bed Temperature Data

Run	$\frac{Y}{D}$	Radial Temperature, °F
1B	0.1	75.0
	0.4	73.2
	0.8	71.8
1C	0.1	73.4
	0.4	71.1
	0.8	70.6
1D	0.1	70.7
	0.4	71.1
	0.8	71.0
1E	0.1	71.4
	0.4	69.8
	0.8	69.8
1F	0.1	73.6
	0.4	73.0
	0.8	72.7
1G	0.1	71.5
	0.4	71.2
	0.8	71.6
1H	0.1	71.8
	0.4	71.6
	0.8	71.3
1I	0.1	70.3
	0.4	70.3
	0.8	70.2
1J	0.1	77.5
	0.4	77.4
	0.8	77.0
3A	0.1	72.2
	0.4	72.1
	0.8	72.2

Table III. Continued

Run	$\frac{Y}{D}$	Radial Temperature, °F
3B	0.1	68.2
	0.4	67.7
	0.8	68.5
3C	0.1	67.1
	0.4	68.2
	0.8	68.1
3E	0.1	68.5
	0.4	68.1
	0.8	67.8
3F	0.1	68.2
	0.4	68.3
	0.8	68.2
3G	0.1	65.1
	0.4	64.8
	0.8	64.8
3H	0.1	63.3
	0.4	63.3
	0.8	63.3
4H	0.1	78.5
	0.4	78.9
	0.8	78.8
4I	0.1	80.8
	0.4	80.8
	0.8	80.9
5A	0.1	76.6
	0.4	76.7
	0.8	76.8
5B	0.1	79.8
	0.4	79.1
	0.8	78.9

Table III. Continued

Run	$\frac{Y}{D}$	Radial Temperature, °F
5C	0.1	77.0
	0.4	77.0
	0.8	76.9
5E	0.1	76.1
	0.4	75.8
	0.8	75.8
5F	0.1	76.8
	0.4	76.5
	0.8	76.3
5G	0.1	67.4
	0.4	67.6
	0.8	67.4
5H	0.1	70.6
	0.4	70.8
	0.8	71.0
9H	0.1	85.5
	0.3	85.6
	0.7	85.2
10A	0.1	96.9
	0.3	97.4
	0.7	97.2
10B	0.1	102.9
	0.3	103.1
	0.7	102.8

APPENDIX F

TABLE IV. EXPERIMENTAL AND CALCULATED DATA

```
RUN 1B         FINE GLASS SPHERES           STATIC BED HEIGHT= 9 INCHES      HEAT TUBE LOC. NO.=4

PROBE LOCATION        TUBE WALL TEMPERATURE        TEMPERATURE DIFFERENCE      LOCAL HEAT TRANSFER COEFFICIENT
   INCHES             DEGREES FAHRENHEIT           DEGREES FAHRENHEIT              BTU/HR. SQ. FT.  F
    2.5                      85.3                         12.4                          29.1
    4.5                      86.2                         12.1                          29.8
    6.5                      86.4                         11.3                          31.9
   12.5                      90.6                         13.9                          26.0
   18.5                     134.7                         55.9                           6.5
   24.5                     228.5                        148.3                           2.4
   30.5                     278.0                        198.1                           1.8
   36.5                     307.7                        228.4                           1.6
   42.5                     326.6                        246.2                           1.5
   43.5                     327.7                        246.2                           1.5
   44.5                     328.8                        247.9                           1.5
INLET TEMPERATURE         GAS DENSITY       HEAT FLUX          MASS FLOW RATE        AVG. HT. TRANS. COEFFICIENT
DEGREES FAHRENHEIT        LBS./CU. FT.    BTU/HR. SQ. FT.     LBS./HR. SQ. FT.          BTU/HR. SQ. FT.  F
     71.0                   .0788             361.2                 1023                       3.10

RUN 1C         FINE GLASS SPHERES           STATIC BED HEIGHT= 9 INCHES      HEAT TUBE LOC. NO.=4

PROBE LOCATION        TUBE WALL TEMPERATURE        TEMPERATURE DIFFERENCE      LOCAL HEAT TRANSFER COEFFICIENT
   INCHES             DEGREES FAHRENHEIT           DEGREES FAHRENHEIT              BTU/HR. SQ. FT.  F
    2.5                      82.7                         14.3                          24.2
    6.5                      83.1                         12.6                          27.5
   12.5                      85.8                         13.3                          26.0
   15.5                      86.9                         14.4                          24.2
   18.5                      87.7                         15.5                          22.3
   24.5                      91.7                         19.4                          17.9
   30.5                      99.2                         26.4                          13.1
   36.5                     105.0                         32.1                          10.8
   42.5                     103.3                         30.5                          11.4
   43.5                     106.9                         33.9                          10.2
   44.5                     110.5                         37.4                           9.3
INLET TEMPERATURE         GAS DENSITY       HEAT FLUX          MASS FLOW RATE        AVG. HT. TRANS. COEFFICIENT
DEGREES FAHRENHEIT        LBS./CU. FT.    BTU/HR. SQ. FT.     LBS./HR. SQ. FT.          BTU/HR. SQ. FT.  F
     66.3                   .0792             347.2                 1536                      17.60

RUN 1D         FINE GLASS SPHERES           STATIC BED HEIGHT= 9 INCHES      HEAT TUBE LOC. NO.=4

PROBE LOCATION        TUBE WALL TEMPERATURE        TEMPERATURE DIFFERENCE      LOCAL HEAT TRANSFER COEFFICIENT
   INCHES             DEGREES FAHRENHEIT           DEGREES FAHRENHEIT              BTU/HR. SQ. FT.  F
    2.5                      95.3                         27.0                          12.8
    4.5                      97.9                         28.7                          12.1
    6.5                     100.2                         30.7                          11.3
    9.5                     100.7                         31.1                          11.1
   12.5                     101.3                         31.7                          10.9
   18.5                     100.8                         31.7                          10.9
   24.5                      99.9                         30.8                          11.2
   30.5                     100.9                         31.3                          11.1
   36.5                     100.9                         30.5                          11.4
   42.5                      90.1                         19.3                          17.9
   44.5                      91.4                         20.2                          17.2
INLET TEMPERATURE         GAS DENSITY       HEAT FLUX          MASS FLOW RATE        AVG. HT. TRANS. COEFFICIENT
DEGREES FAHRENHEIT        LBS./CU. FT.    BTU/HR. SQ. FT.     LBS./HR. SQ. FT.          BTU/HR. SQ. FT.  F
     66.0                   .0827             346.3                 2525                      12.30
```

```
RUN 1E          FINE GLASS SPHERES                STATIC BED HEIGHT= 9 INCHES       HEAT TUBE LOC. NO.=4

PROBE LOCATION         TUBE WALL TEMPERATURE        TEMPERATURE DIFFERENCE       LOCAL HEAT TRANSFER COEFFICIENT
   INCHES              DEGREES FAHRENHEIT           DEGREES FAHRENHEIT               BTU/HR. SQ. FT.  F
    2.5                       87.8                         20.3                            17.0
    6.5                       93.9                         25.2                            13.7
   12.5                       96.0                         27.0                            12.8
   18.5                       99.0                         30.1                            11.5
   24.5                      101.2                         32.0                            10.8
   30.5                       97.2                         27.6                            12.5
   33.5                       96.8                         26.8                            12.9
   36.5                       96.3                         25.9                            13.3
   39.5                       92.9                         22.3                            15.5
   42.5                       89.5                         18.5                            18.7
   44.5                       83.8                         12.9                            26.9
INLET TEMPERATURE        GAS DENSITY       HEAT FLUX            MASS FLOW RATE        AVG. HT. TRANS. COEFFICIENT
DEGREES FAHRENHEIT      LBS./CU. FT.   BTU/HR. SQ. FT.        LBS./HR. SQ. FT.          BTU/HR. SQ. FT.  F
    65.7                 .0806             345.9                   2076                      14.40

RUN 1F          FINE GLASS SPHERES                STATIC BED HEIGHT= 9 INCHES       HEAT TUBE LOC. NO.=4

PROBE LOCATION         TUBE WALL TEMPERATURE        TEMPERATURE DIFFERENCE       LOCAL HEAT TRANSFER COEFFICIENT
   INCHES              DEGREES FAHRENHEIT           DEGREES FAHRENHEIT               BTU/HR. SQ. FT.  F
    2.5                       95.5                         21.5                            17.1
    3.5                       95.3                         20.3                            18.0
    4.5                       94.3                         18.6                            19.7
    6.5                       93.5                         16.7                            22.0
    8.5                      112.6                         30.8                            11.9
   10.5                      146.5                         57.3                             6.4
   12.5                      179.4                         84.6                             4.3
   18.5                      295.5                        203.2                             1.8
   24.5                      329.2                        244.7                             1.5
   30.5                      361.4                        278.5                             1.3
   44.5                      358.1                        272.5                             1.3
INLET TEMPERATURE        GAS DENSITY       HEAT FLUX            MASS FLOW RATE        AVG. HT. TRANS. COEFFICIENT
DEGREES FAHRENHEIT      LBS./CU. FT.   BTU/HR. SQ. FT.        LBS./HR. SQ. FT.          BTU/HR. SQ. FT.  F
    70.8                 .0790             366.9                    679                       2.04

RUN 1G          FINE GLASS SPHERES                STATIC BED HEIGHT= 4 INCHES       HEAT TUBE LOC. NO.=4

PROBE LOCATION         TUBE WALL TEMPERATURE        TEMPERATURE DIFFERENCE       LOCAL HEAT TRANSFER COEFFICIENT
   INCHES              DEGREES FAHRENHEIT           DEGREES FAHRENHEIT               BTU/HR. SQ. FT.  F
    1.0                       82.5                         14.6                            24.0
    3.0                       87.2                         17.3                            20.2
    5.0                       88.9                         17.8                            19.6
   11.0                       94.3                         22.3                            15.7
   17.0                       96.5                         25.2                            13.9
   23.0                       98.9                         27.9                            12.5
   29.0                      101.6                         30.1                            11.6
   35.0                      104.9                         32.7                            10.7
   41.0                      103.4                         30.2                            11.6
   43.0                       95.1                         22.2                            15.7
   45.0                      102.0                         28.9                            12.1
INLET TEMPERATURE        GAS DENSITY       HEAT FLUX            MASS FLOW RATE        AVG. HT. TRANS. COEFFICIENT
DEGREES FAHRENHEIT      LBS./CU. FT.   BTU/HR. SQ. FT.        LBS./HR. SQ. FT.          BTU/HR. SQ. FT.  F
    67.2                 .0791             349.3                   1664                      13.96
```

```
RUN 1H       FINE GLASS SPHERES            STATIC BED HEIGHT= 4 INCHES     HEAT TUBE LOC. NO.=4

PROBE LOCAITON       TUBE WALL TEMPERATURE        TEMPERATURE DIFFERENCE       LOCAL HEAT TRANSFER COEFFICIENT
   INCHES            DEGREES FAHRENHEIT           DEGREES FAHRENHEIT               BTU/HR. SQ. FT.  F
    1.0                    79.2                          9.3                              38.7
    3.0                    81.2                         10.5                              34.1
    5.0                    83.0                         11.6                              31.1
    8.0                    83.6                         11.5                              31.3
   11.0                    88.4                         16.1                              22.4
   17.0                   104.9                         32.4                              11.1
   25.0                   134.2                         61.1                               5.9
   35.0                   198.9                        124.4                               2.9
   41.0                   225.4                        150.4                               2.4
   43.0                   251.3                        175.9                               2.0
   45.0                   251.3                        175.0                               2.0
INLET TEMPERATURE       GAS DENSITY       HEAT FLUX         MASS FLOW RATE        AVG. HT. TRANS. COEFFICIENT
DEGREES FAHRENHEIT     LBS./CU. FT.   BTU/HR. SQ. FT.     LBS./HR. SQ. FT.          BTU/HR. SQ. FT.  F
    69.3                 .0790            360.0                1333                      5.30

RUN 1I       FINE GLASS SPHERES            STATIC BED HEIGHT= 4 INCHES     HEAT TUBE LOC. NO.=4

PROBE LOCAITON       TUBE WALL TEMPERATURE        TEMPERATURE DIFFERENCE       LOCAL HEAT TRANSFER COEFFICIENT
   INCHES            DEGREES FAHRENHEIT           DEGREES FAHRENHEIT               BTU/HR. SQ. FT.  F
    1.0                    85.3                         19.7                              17.6
    3.0                    91.3                         24.3                              14.2
    5.0                   100.3                         32.2                              10.8
   11.0                   102.1                         33.4                              10.3
   17.0                   101.1                         33.0                              10.5
   23.0                   100.4                         32.4                              10.7
   29.0                   100.6                         32.3                              10.7
   35.0                   100.7                         31.7                              10.9
   41.0                    94.8                         25.3                              13.7
   43.0                    88.4                         18.9                              18.3
   45.0                    85.3                         15.5                              22.4
INLET TEMPERATURE       GAS DENSITY       HEAT FLUX         MASS FLOW RATE        AVG. HT. TRANS. COEFFICIENT
DEGREES FAHRENHEIT     LBS./CU. FT.   BTU/HR. SQ. FT.     LBS./HR. SQ. FT.          BTU/HR. SQ. FT.  F
    64.7                 .0816            346.1                2200                     11.94

RUN 1J       FINE GLASS SPHERES            STATIC BED HEIGHT= 4 INCHES     HEAT TUBE LOC. NO.=4

PROBE LOCAITON       TUBE WALL TEMPERATURE        TEMPERATURE DIFFERENCE       LOCAL HEAT TRANSFER COEFFICIENT
   INCHES            DEGREES FAHRENHEIT           DEGREES FAHRENHEIT               BTU/HR. SQ. FT.  F
    1.0                    96.1                         18.8                              18.8
    3.0                   110.3                         31.1                              11.3
    5.0                   116.1                         35.9                               9.8
   11.0                   119.4                         38.8                               9.1
   17.0                   117.5                         37.8                               9.3
   23.0                   116.9                         37.5                               9.4
   29.0                   116.9                         37.3                               9.5
   35.0                   116.5                         36.4                               9.7
   41.0                   111.3                         30.6                              11.5
   43.0                   101.0                         20.5                              17.2
   45.0                    96.9                         16.3                              21.7
INLET TEMPERATURE       GAS DENSITY       HEAT FLUX         MASS FLOW RATE        AVG. HT. TRANS. COEFFICIENT
DEGREES FAHRENHEIT     LBS./CU. FT.   BTU/HR. SQ. FT.     LBS./HR. SQ. FT.          BTU/HR. SQ. FT.  F
    76.4                 .0889            352.6                2973                     10.57
```

```
RUN 3A      COARSE GLASS SPHERES          STATIC BED HEIGHT= 4 INCHES      HEAT TUBE LOC. NO.=4

PROBE LOCAITON      TUBE WALL TEMPERATURE       TEMPERATURE DIFFERENCE      LOCAL HEAT TRANSFER COEFFICIENT
   INCHES           DEGREES FAHRENHEIT          DEGREES FAHRENHEIT              BTU/HR. SQ. FT.  F
     1.0                   88.4                        15.5                          22.8
     3.0                   98.9                        23.4                          15.1
     5.0                  107.2                        29.3                          12.1
    11.0                  115.0                        36.4                           9.7
    17.0                  120.1                        43.3                           8.2
    23.0                  125.6                        50.0                           7.1
    29.0                  128.1                        52.7                           6.7
    35.0                  130.0                        54.1                           6.6
    41.0                  131.8                        55.3                           6.4
    43.0                  131.7                        55.3                           6.4
    45.0                  135.5                        59.3                           6.0
INLET TEMPERATURE     GAS DENSITY      HEAT FLUX          MASS FLOW RATE       AVG. HT. TRANS. COEFFICIENT
DEGREES FAHRENHEIT    LBS./CU. FT.   BTU/HR. SQ. FT.     LBS./HR. SQ. FT.         BTU/HR. SQ. FT.  F
      72.1              .0893           354.1                3209                       8.11

RUN 3B      COARSE GLASS SPHERES          STATIC BED HEIGHT= 4 INCHES      HEAT TUBE LOC. NO.=4

PROBE LOCAITON      TUBE WALL TEMPERATURE       TEMPERATURE DIFFERENCE      LOCAL HEAT TRANSFER COEFFICIENT
   INCHES           DEGREES FAHRENHEIT          DEGREES FAHRENHEIT              BTU/HR. SQ. FT.  F
     1.0                   79.7                        18.2                          19.2
     3.0                   92.3                        19.2                          12.0
     5.0                  100.2                        36.0                           9.7
    11.0                  110.0                        45.0                           7.8
    17.0                  118.9                        54.5                           6.4
    23.0                  120.8                        56.9                           6.1
    29.0                  121.4                        57.6                           6.1
    35.0                  123.7                        59.4                           5.9
    41.0                  120.7                        55.7                           6.3
    43.0                  116.5                        51.1                           6.8
    45.0                  106.4                        40.9                           8.5
INLET TEMPERATURE     GAS DENSITY      HEAT FLUX          MASS FLOW RATE       AVG. HT. TRANS. COEFFICIENT
DEGREES FAHRENHEIT    LBS./CU. FT.   BTU/HR. SQ. FT.     LBS./HR. SQ. FT.         BTU/HR. SQ. FT.  F
      60.5              .0821           349.7                4883                       7.16

RUN 3C      COARSE GLASS SPHERES          STATIC BED HEIGHT= 4 INCHES      HEAT TUBE LOC. NO.=4

PROBE LOCAITON      TUBE WALL TEMPERATURE       TEMPERATURE DIFFERENCE      LOCAL HEAT TRANSFER COEFFICIENT
   INCHES           DEGREES FAHRENHEIT          DEGREES FAHRENHEIT              BTU/HR. SQ. FT.  F
     1.0                   91.5                        15.4                          22.7
     3.0                   92.5                        24.9                          14.0
     5.0                   98.2                        29.9                          11.7
    11.0                  110.6                        41.2                           8.5
    17.0                  115.1                        46.5                           7.5
    23.0                  118.5                        50.5                           6.9
    29.0                  120.2                        52.3                           6.7
    35.0                  119.5                        51.3                           6.8
    41.0                  117.3                        48.4                           7.2
    43.0                  114.9                        45.6                           7.6
    45.0                  100.2                        31.3                          11.1
INLET TEMPERATURE     GAS DENSITY      HEAT FLUX          MASS FLOW RATE       AVG. HT. TRANS. COEFFICIENT
DEGREES FAHRENHEIT    LBS./CU. FT.   BTU/HR. SQ. FT.     LBS./HR. SQ. FT.         BTU/HR. SQ. FT.  F
      65.5              .0873           349.0                7843                       8.15
```

```
RUN 3D     COARSE GLASS SPHERES              STATIC BED HEIGHT= 4 INCHES     HEAT TUBE LOC. NO.=4

PROBE LOCATION      TUBE WALL TEMPERATURE      TEMPERATURE DIFFERENCE      LOCAL HEAT TRANSFER COEFFICIENT
    INCHES           DEGREES FAHRENHEIT         DEGREES FAHRENHEIT              BTU/HR. SQ. FT.  F
     1.0                    78.2                        15.1                          22.2
     3.0                    81.1                        16.9                          19.9
     5.0                    82.7                        17.7                          19.0
    11.0                    84.7                        19.6                          17.1
    17.0                    97.4                        32.3                          10.4
    23.0                   132.6                        65.8                           5.1
    29.0                   179.5                       109.9                           3.1
    35.0                   204.0                       132.8                           2.5
    41.0                   213.0                       141.1                           2.4
    43.0                   216.0                       143.4                           2.3
    45.0                   215.2                       142.7                           2.4
 INLET TEMPERATURE      GAS DENSITY      HEAT FLUX         MASS FLOW RATE      AVG. HT. TRANS. COEFFICIENT
 DEGREES FAHRENHEIT     LBS./CU. FT.   BTU/HR. SQ. FT.    LBS./HR. SQ. FT.         BTU/HR. SQ. FT.  F
      61.5                 .0825           356.5                3148                    4.65

RUN 3E     COARSE GLASS SPHERES              STATIC BED HEIGHT= 9 INCHES     HEAT TUBE LOC. NO.=4

PROBE LOCATION      TUBE WALL TEMPERATURE      TEMPERATURE DIFFERENCE      LOCAL HEAT TRANSFER COEFFICIENT
    INCHES           DEGREES FAHRENHEIT         DEGREES FAHRENHEIT              BTU/HR. SQ. FT.  F
     1.0                    77.9                        13.1                          27.5
     3.0                    80.7                        14.6                          24.7
     5.0                    80.4                        13.3                          27.0
    11.0                    79.5                        11.7                          30.7
    17.0                    93.7                        25.7                          14.0
    23.0                   155.1                        86.8                           4.3
    29.0                   192.9                       125.3                           2.9
    35.0                   208.8                       141.2                           2.6
    41.0                   224.6                       157.2                           2.3
    43.0                   229.8                       162.2                           2.2
    45.0                   232.9                       165.1                           2.2
 INLET TEMPERATURE      GAS DENSITY      HEAT FLUX         MASS FLOW RATE      AVG. HT. TRANS. COEFFICIENT
 DEGREES FAHRENHEIT     LBS./CU. FT.   BTU/HR. SQ. FT.    LBS./HR. SQ. FT.         BTU/HR. SQ. FT.  F
      64.0                 .0830           360.2                2565                    4.57

RUN 3F     COARSE GLASS SPHERES              STATIC BED HEIGHT= 9 INCHES     HEAT TUBE LOC. NO.=4

PROBE LOCATION      TUBE WALL TEMPERATURE      TEMPERATURE DIFFERENCE      LOCAL HEAT TRANSFER COEFFICIENT
    INCHES           DEGREES FAHRENHEIT         DEGREES FAHRENHEIT              BTU/HR. SQ. FT.  F
     1.0                    81.8                        18.8                          18.8
     3.0                    85.7                        20.5                          17.3
     5.0                    86.7                        19.9                          17.7
    11.0                    84.8                        16.6                          21.3
    17.0                    98.9                        28.6                          12.4
    23.0                   103.1                        34.0                          10.4
    29.0                    10.4                        36.4                           9.7
    35.0                      .2                        38.0                           9.3
    41.0                      .7                        34.9                          10.1
    43.0                      .8                        32.9                          10.7
    45.0                      .6                        34.0                          10.4
 INLET TEMPERATURE      GAS DENSITY      HEAT FLUX         MASS FLOW RATE      AVG. HT. TRANS. COEFFICIENT
 DEGREES FAHRENHEIT     LBS./CU. FT.   BTU/HR. SQ. FT.    LBS./HR. SQ. FT.         BTU/HR. SQ. FT.  F
      62.0                 .0822           353.4                3332                   12.40
```

RUN 3 G COARSE GLASS SPHERES STATIC BED HEIGHT= 9 INCHES HEAT TUBE LOC. NO.=4

PROBE LOCATION INCHES	TUBE WALL TEMPERATURE DEGREES FAHRENHEIT	TEMPERATURE DIFFERENCE DEGREES FAHRENHEIT	LOCAL HEAT TRANSFER COEFFICIENT BTU/HR. SQ. FT. F
1.0	78.1	18.2	19.2
3.0	88.5	27.2	12.9
5.0	96.1	33.8	10.4
11.0	106.4	43.1	8.1
17.0	110.6	48.2	7.3
23.0	112.4	50.5	6.9
29.0	113.3	51.2	6.8
35.0	113.7	51.0	6.9
41.0	111.3	47.7	7.3
43.0	106.4	42.6	8.2
45.0	86.2	23.3	15.0

INLET TEMPERATURE DEGREES FAHRENHEIT	GAS DENSITY LBS./CU. FT.	HEAT FLUX BTU/HR. SQ. FT.	MASS FLOW RATE LBS./HR. SQ. FT.	AVG. HT. TRANS. COEFFICIENT BTU/HR. SQ. FT. F
59.0	.0830	349.9	5228	8.10

RUN 3 H COARSE GLASS SPHERES STATIC BED HEIGHT= 9 INCHES HEAT TUBE LOC. NO.=4

PROBE LOCATION INCHES	TUBE WALL TEMPERATURE DEGREES FAHRENHEIT	TEMPERATURE DIFFERENCE DEGREES FAHRENHEIT	LOCAL HEAT TRANSFER COEFFICIENT BTU/HR. SQ. FT. F
1.0	78.9	17.2	20.2
3.0	90.0	26.7	13.0
5.0	97.4	33.2	10.5
11.0	109.3	44.1	7.9
17.0	112.7	48.5	7.2
23.0	114.2	50.5	6.9
29.0	113.2	49.5	7.0
35.0	112.1	47.9	7.3
41.0	110.0	45.8	7.6
43.0	108.2	42.8	8.1
45.0	90.4	25.7	13.5

INLET TEMPERATURE DEGREES FAHRENHEIT	GAS DENSITY LBS./CU. FT.	HEAT FLUX BTU/HR. SQ. FT.	MASS FLOW RATE LBS./HR. SQ. FT.	AVG. HT. TRANS. COEFFICIENT BTU/HR. SQ. FT. F
60.9	.0843	347.5	6505	8.17

RUN 4 A COARSE GLASS SPHERES STATIC BED HEIGHT= 9 INCHES HEATED TUBE LOC. NO.=3

PROBE LOCATION INCHES	TUBE WALL TEMPERATURE DEGREES FAHRENHEIT	TEMPERATURE DIFFERENCE DEGREES FAHRENHEIT	LOCAL HEAT TRANSFER COEFFICIENT BTU/HR. SQ. FT. F
1.3	90.2	20.5	17.1
3.0	91.6	19.9	17.6
5.0	90.6	17.7	19.7
11.0	91.4	16.5	21.2
17.0	104.5	27.7	12.7
23.0	107.0	31.7	11.0
29.0	106.6	32.5	10.8
35.0	107.0	33.8	10.3
41.0	104.0	31.5	11.1
43.0	101.6	29.3	11.9
45.0	100.9	28.5	12.3

INLET TEMPERATURE DEGREES FAHRENHEIT	GAS DENSITY LBS./CU. FT.	HEAT FLUX BTU/HR. SQ. FT.	MASS FLOW RATE LBS./HR. SQ. FT.	AVG. HT. TRANS. COEFFICIENT BTU/HR. SQ. FT. F
68.6	.0810	349.9	3100	13.38

RUN 4 B COARSE GLASS SPHERES STATIC BED HEIGHT= 9 INCHES HEATED TUBE LOC. NO.=3

PROBE LOCATION INCHES	TUBE WALL TEMPERATURE DEGREES FAHRENHEIT	TEMPERATURE DIFFERENCE DEGREES FAHRENHEIT	LOCAL HEAT TRANSFER COEFFICIENT BTU/HR. SQ. FT. F
1.0	88.7	21.0	16.7
3.0	96.8	27.7	12.6
5.0	102.8	32.8	10.7
11.0	113.8	42.9	8.2
17.0	117.4	47.3	7.4
23.0	118.4	48.9	7.2
29.0	118.8	49.1	7.1
35.0	118.1	47.9	7.3
41.0	114.9	43.9	8.0
43.0	108.0	37.0	9.5
45.0	87.1	17.1	20.5

INLET TEMPERATURE DEGREES FAHRENHEIT	GAS DENSITY LBS./CU. FT.	HEAT FLUX BTU/HR. SQ. FT.	MASS FLOW RATE LBS./HR. SQ. FT.	AVG. HT. TRANS. COEFFICIENT BTU/HR. SQ. FT. F
66.8	.0818	350.2	5541	200000000008.00

RUN 4 C COARSE GLASS SPHERES STATIC BED HEIGHT= 9 INCHES HEATED TUBE LOC. NO.=3

PROBE LOCATION INCHES	TUBE WALL TEMPERATURE DEGREES FAHRENHEIT	TEMPERATURE DIFFERENCE DEGREES FAHRENHEIT	LOCAL HEAT TRANSFER COEFFICIENT BTU/HR. SQ. FT. F
1.0	88.4	20.2	17.3
3.0	96.4	26.8	13.1
5.0	102.1	31.8	11.1
11.0	114.1	42.8	8.2
17.0	119.5	48.9	7.2
23.0	118.5	48.7	7.2
29.0	118.2	48.3	7.3
35.0	117.8	47.2	7.4
41.0	114.2	43.0	8.2
43.0	101.2	30.4	11.6
45.0	88.8	18.4	19.1

INLET TEMPERATURE DEGREES FAHRENHEIT	GAS DENSITY LBS./CU. FT.	HEAT FLUX BTU/HR. SQ. FT.	MASS FLOW RATE LBS./HR. SQ. FT.	AVG. HT. TRANS. COEFFICIENT BTU/HR. SQ. FT. F
67.3	.0826	351.2	6390	8.59

RUN 4D   COARSE GLASS SPHERES   STATIC BED HEIGHT= 9 INCHES   HEATED TUBE LOC. NO.=3

PROBE LOCATION INCHES	TUBE WALL TEMPERATURE DEGREES FAHRENHEIT	TEMPERATURE DIFFERENCE DEGREES FAHRENHEIT	LOCAL HEAT TRANSFER COEFFICIENT BTU/HR. SQ. FT. F
1.0	87.1	16.1	22.0
3.0	87.4	15.1	23.4
5.0	87.4	14.1	25.0
11.0	86.1	12.0	29.4
17.0	87.1	14.0	25.2
23.0	92.8	20.3	17.4
29.0	109.0	36.1	9.8
35.0	151.0	77.5	4.6
41.0	195.0	121.2	2.9
43.0	201.5	127.3	2.8
45.0	204.8	130.6	2.7

INLET TEMPERATURE DEGREES FAHRENHEIT	GAS DENSITY LBS./CU. FT.	HEAT FLUX BTU/HR. SQ. FT.	MASS FLOW RATE LBS./HR. SQ. FT.	AVG. HT. TRANS. COEFFICIENT BTU/HR. SQ. FT. F
70.1	.0814	353.1	2532	8.29

RUN 4E   COARSE GLASS SPHERES   STATIC BED HEIGHT= 4 INCHES   HEATED TUBE LOC. NO.=3

PROBE LOCATION INCHES	TUBE WALL TEMPERATURE DEGREES FAHRENHEIT	TEMPERATURE DIFFERENCE DEGREES FAHRENHEIT	LOCAL HEAT TRANSFER COEFFICIENT BTU/HR. SQ. FT. F
1.0	90.8	18.2	19.3
3.0	92.2	17.9	19.6
5.0	91.7	16.7	21.1
11.0	99.3	23.2	15.2
17.0	105.2	30.0	11.8
23.0	105.7	31.2	11.3
29.0	105.9	31.4	11.2
35.0	108.1	33.1	10.6
41.0	113.1	37.5	9.4
43.0	112.5	36.8	9.6
45.0	124.0	48.3	7.3

INLET TEMPERATURE DEGREES FAHRENHEIT	GAS DENSITY LBS./CU. FT.	HEAT FLUX BTU/HR. SQ. FT.	MASS FLOW RATE LBS./HR. SQ. FT.	AVG. HT. TRANS. COEFFICIENT BTU/HR. SQ. FT. F
71.6	.0806	352.0	2929	12.49

RUN 4F   COARSE GLASS SPHERES   STATIC BED HEIGHT= 4 INCHES   HEATED TUBE LOC. NO.=3

PROBE LOCATION INCHES	TUBE WALL TEMPERATURE DEGREES FAHRENHEIT	TEMPERATURE DIFFERENCE DEGREES FAHRENHEIT	LOCAL HEAT TRANSFER COEFFICIENT BTU/HR. SQ. FT. F
1.0	84.5	15.0	23.6
3.0	86.6	16.2	21.9
5.0	92.0	20.5	17.3
11.0	97.6	25.6	13.8
17.0	101.5	30.8	11.5
23.0	115.3	44.9	7.9
29.0	150.9	80.2	4.4
35.0	197.6	126.6	2.8
41.0	229.6	158.1	2.2
43.0	232.3	160.9	2.2
45.0	226.0	153.8	2.3

INLET TEMPERATURE DEGREES FAHRENHEIT	GAS DENSITY LBS./CU. FT.	HEAT FLUX BTU/HR. SQ. FT.	MASS FLOW RATE LBS./HR. SQ. FT.	AVG. HT. TRANS. COEFFICIENT BTU/HR. SQ. FT. F
68.8	.0814	355.0	2756	5.20

RUN 4G COARSE GLASS SPHERES STATIC RED HEIGHT= 2 INCHES HEATED TUBE LOC. NO.=3

PROBE LOCATION INCHES	TUBE WALL TEMPERATURE DEGREES FAHRENHEIT	TEMPERATURE DIFFERENCE DEGREES FAHRENHEIT	LOCAL HEAT TRANSFER COEFFICIENT BTU/HR. SQ. FT. F
1.0	96.0	28.4	12.3
3.0	109.6	39.8	8.8
5.0	114.6	44.0	7.9
11.0	123.1	51.7	6.8
17.0	129.1	58.7	5.9
23.0	130.1	60.5	5.8
29.0	131.5	61.9	5.6
35.0	131.4	61.4	5.7
41.0	128.4	57.7	6.0
43.0	109.5	39.2	8.9
45.0	106.9	36.1	9.7

INLET TEMPERATURE DEGREES FAHRENHEIT	GAS DENSITY LBS./CU. FT.	HEAT FLUX BTU/HR. SQ. FT.	MASS FLOW RATE LBS./HR. SQ. FT.	AVG. HT. TRANS. COEFFICIENT BTU/HR. SQ. FT. F
66.4	.0796	349.2	5310	6.67

RUN 4H COARSE GLASS SPHERES STATIC RED HEIGHT= 4 INCHES HEATED TUBE LOC. NO.=3

PROBE LOCATION INCHES	TUBE WALL TEMPERATURE DEGREES FAHRENHEIT	TEMPERATURE DIFFERENCE DEGREES FAHRENHEIT	LOCAL HEAT TRANSFER COEFFICIENT BTU/HR. SQ. FT. F
1.0	89.2	18.3	19.1
3.0	98.4	26.0	13.4
5.0	105.3	32.1	10.9
11.0	117.4	43.1	8.1
17.0	122.8	49.4	7.1
23.0	126.0	53.1	6.6
29.0	126.7	54.1	6.5
35.0	125.3	52.2	6.7
41.0	121.8	48.3	7.2
43.0	106.2	33.1	10.6
45.0	94.4	21.5	16.2

INLET TEMPERATURE DEGREES FAHRENHEIT	GAS DENSITY LBS./CU. FT.	HEAT FLUX BTU/HR. SQ. FT.	MASS FLOW RATE LBS./HR. SQ. FT.	AVG. HT. TRANS. COEFFICIENT BTU/HR. SQ. FT. F
70.1	.0828	349.1	7721	7.99

RUN 4I COARSE GLASS SPHERES STATIC RED HEIGHT= 4 INCHES HEATED TUBE LOC. NO.=3

PROBE LOCATION INCHES	TUBE WALL TEMPERATURE DEGREES FAHRENHEIT	TEMPERATURE DIFFERENCE DEGREES FAHRENHEIT	LOCAL HEAT TRANSFER COEFFICIENT BTU/HR. SQ. FT. F
1.0	95.6	24.8	14.0
3.0	104.5	32.0	10.8
5.0	106.3	33.3	10.4
11.0	120.0	45.8	7.6
17.0	126.1	52.7	6.6
23.0	129.6	56.7	6.1
29.0	129.9	57.1	6.1
35.0	127.4	54.3	6.4
41.0	123.4	49.6	7.0
43.0	103.8	30.6	11.3
45.0	97.0	23.7	14.6

INLET TEMPERATURE DEGREES FAHRENHEIT	GAS DENSITY LBS./CU. FT.	HEAT FLUX BTU/HR. SQ. FT.	MASS FLOW RATE LBS./HR. SQ. FT.	AVG. HT. TRANS. COEFFICIENT BTU/HR. SQ. FT. F
69.7	.0792	346.6	5087	7.52

RUN 5A FINE GLASS SPHERES STATIC BED HEIGHT= 9 INCHES HEATED TUBE LOC. NO.=3

PROBE LOCATION INCHES	TUBE WALL TEMPERATURE DEGREES FAHRENHEIT	TEMPERATURE DIFFERENCE DEGREES FAHRENHEIT	LOCAL HEAT TRANSFER COEFFICIENT BTU/HR. SQ. FT. F
1.0	87.9	13.2	26.9
3.0	88.0	12.1	29.3
5.0	88.2	11.4	31.0
11.0	88.4	10.5	33.7
17.0	92.3	14.7	24.1
23.0	103.6	26.3	13.5
29.0	120.3	42.5	8.4
35.0	135.6	57.3	6.2
41.0	155.7	76.8	4.6
43.0	157.2	78.1	4.5
45.0	179.4	100.1	3.5

INLET TEMPERATURE DEGREES FAHRENHEIT	GAS DENSITY LBS./CU. FT.	HEAT FLUX BTU/HR. SQ. FT.	MASS FLOW RATE LBS./HR. SQ. FT.	AVG. HT. TRANS. COEFFICIENT BTU/HR. SQ. FT. F
73.9	.0819	355.0	1788	10.36

RUN 5B FINE GLASS SPHERES STATIC BED HEIGHT= 9 INCHES HEATED TUBE LOC. NO.=3

PROBE LOCATION INCHES	TUBE WALL TEMPERATURE DEGREES FAHRENHEIT	TEMPERATURE DIFFERENCE DEGREES FAHRENHEIT	LOCAL HEAT TRANSFER COEFFICIENT BTU/HR. SQ. FT. F
1.0	89.4	14.3	24.5
3.0	91.8	15.3	22.9
5.0	92.5	14.8	23.6
11.0	94.2	15.0	23.2
17.0	96.4	18.5	18.9
23.0	100.1	22.9	15.2
29.0	102.5	15.2	13.9
35.0	103.0	25.3	13.8
41.0	102.6	24.6	14.2
43.0	102.5	24.5	14.3
45.0	98.3	20.0	17.5

INLET TEMPERATURE DEGREES FAHRENHEIT	GAS DENSITY LBS./CU. FT.	HEAT FLUX BTU/HR. SQ. FT.	MASS FLOW RATE LBS./HR. SQ. FT.	AVG. HT. TRANS. COEFFICIENT BTU/HR. SQ. FT. F
74.2	.0814	349.8	2110	17.52

RUN 5C FINE GLASS SPHERES STATIC BED HEIGHT= 9 INCHES HEATED TUBE LOC. NO.=3

PROBE LOCATION INCHES	TUBE WALL TEMPERATURE DEGREES FAHRENHEIT	TEMPERATURE DIFFERENCE DEGREES FAHRENHEIT	LOCAL HEAT TRANSFER COEFFICIENT BTU/HR. SQ. FT. F
1.0	92.8	21.2	16.2
3.0	101.5	28.3	12.2
5.0	104.5	30.7	11.2
11.0	106.4	32.2	10.7
17.0	107.4	33.8	10.2
23.0	107.3	33.8	10.2
29.0	105.8	32.1	10.7
35.0	103.2	28.9	11.9
41.0	96.3	21.6	15.9
43.0	90.8	16.1	21.4
45.0	85.4	10.8	31.9

INLET TEMPERATURE DEGREES FAHRENHEIT	GAS DENSITY LBS./CU. FT.	HEAT FLUX BTU/HR. SQ. FT.	MASS FLOW RATE LBS./HR. SQ. FT.	AVG. HT. TRANS. COEFFICIENT BTU/HR. SQ. FT. F
70.6	.0810	344.1	2857	12.20

RUN 5 D FINE GLASS SPHERES STATIC BED HEIGHT= 9 INCHES HEATED TUBE LOC. NO.=3

PROBE LOCATION INCHES	TUBE WALL TEMPERATURE DEGREES FAHRENHEIT	TEMPERATURE DIFFERENCE DEGREES FAHRENHEIT	LOCAL HEAT TRANSFER COEFFICIENT BTU/HR. SQ. FT. F
1.0	89.8	20.7	16.7
3.0	98.5	27.9	12.4
5.0	102.2	30.9	11.2
11.0	103.5	32.0	10.8
17.0	103.6	32.7	10.6
23.0	102.9	32.3	10.7
29.0	102.1	31.3	11.0
35.0	100.3	29.0	11.9
41.0	91.9	20.3	17.0
43.0	87.8	16.2	21.3
45.0	83.0	11.5	30.1

INLET TEMPERATURE DEGREES FAHRENHEIT	GAS DENSITY LBS./CU. FT.	HEAT FLUX BTU/HR. SQ. FT.	MASS FLOW RATE LBS./HR. SQ. FT.	AVG. HT. TRANS. COEFFICIENT BTU/HR. SQ. FT. F
68.1	.0892	345.7	3752	12.54

RUN 5 E FINE GLASS SPHERES STATIC BED HEIGHT= 4 INCHES HEATED TUBE LOC. NO.=3

PROBE LOCATION INCHES	TUBE WALL TEMPERATURE DEGREES FAHRENHEIT	TEMPERATURE DIFFERENCE DEGREES FAHRENHEIT	LOCAL HEAT TRANSFER COEFFICIENT BTU/HR. SQ. FT. F
1.0	83.0	8.7	41.1
3.0	84.6	9.5	37.5
5.0	85.7	10.1	35.3
8.0	89.0	12.5	28.6
11.0	92.4	15.9	22.5
17.0	128.5	52.0	6.9
23.0	194.7	118.1	3.0
29.0	254.5	177.4	2.0
35.0	294.4	217.2	1.6
40.0	296.9	218.4	1.6
45.0	299.5	220.9	1.6

INLET TEMPERATURE DEGREES FAHRENHEIT	GAS DENSITY LBS./CU. FT.	HEAT FLUX BTU/HR. SQ. FT.	MASS FLOW RATE LBS./HR. SQ. FT.	AVG. HT. TRANS. COEFFICIENT BTU/HR. SQ. FT. F
73.9	.0818	357.5	1736	3.17

RUN 5 F FINE GLASS SPHERES STATIC BED HEIGHT= 4 INCHES HEATED TUBE LOC. NO.=3

PROBE LOCATION INCHES	TUBE WALL TEMPERATURE DEGREES FAHRENHEIT	TEMPERATURE DIFFERENCE DEGREES FAHRENHEIT	LOCAL HEAT TRANSFER COEFFICIENT BTU/HR. SQ. FT. F
1.0	91.5	19.0	18.2
3.0	92.6	18.4	18.7
5.0	95.0	19.5	17.7
11.0	96.1	20.4	17.0
17.0	97.2	22.3	15.5
23.0	98.9	24.4	14.2
29.0	100.1	25.3	13.7
35.0	103.2	27.8	12.4
41.0	107.8	31.6	10.9
43.0	105.1	28.9	11.9
45.0	110.1	33.9	10.2

INLET TEMPERATURE DEGREES FAHRENHEIT	GAS DENSITY LBS./CU. FT.	HEAT FLUX BTU/HR. SQ. FT.	MASS FLOW RATE LBS./HR. SQ. FT.	AVG. HT. TRANS. COEFFICIENT BTU/HR. SQ. FT. F
71.4	.0819	345.0	2153	14.73

RUN 5 G FINE GLASS SPHERES STATIC BED HEIGHT= 4 INCHES HEATED TUBE LOC. NO.=3

PROBE LOCATION INCHES	TUBE WALL TEMPERATURE DEGREES FAHRENHEIT	TEMPERATURE DIFFERENCE DEGREES FAHRENHEIT	LOCAL HEAT TRANSFER COEFFICIENT BTU/HR. SQ. FT. F
1.0	80.3	18.4	18.5
3.0	87.1	23.9	14.2
5.0	92.6	28.7	11.8
11.0	95.8	31.3	10.8
17.0	96.3	32.4	10.5
23.0	94.6	31.0	10.9
29.0	92.4	28.7	11.8
35.0	92.3	28.2	12.0
41.0	83.9	19.6	17.3
43.0	79.0	14.7	23.1
45.0	79.7	15.0	22.6

INLET TEMPERATURE DEGREES FAHRENHEIT	GAS DENSITY LBS./CU. FT.	HEAT FLUX BTU/HR. SQ. FT.	MASS FLOW RATE LBS./HR. SQ. FT.	AVG. HT. TRANS. COEFFICIENT BTU/HR. SQ. FT. F
61.1	.0863	339.3	3365	12.84

RUN 5 H FINE GLASS SPHERES STATIC BED HEIGHT= 4 INCHES HEATED TUBE LOC. NO.=3

PROBE LOCATION INCHES	TUBE WALL TEMPERATURE DEGREES FAHRENHEIT	TEMPERATURE DIFFERENCE DEGREES FAHRENHEIT	LOCAL HEAT TRANSFER COEFFICIENT BTU/HR. SQ. FT. F
1.0	84.7	18.5	18.5
3.0	93.2	25.6	13.3
5.0	100.3	31.8	10.7
11.0	104.9	35.9	9.5
17.0	106.7	38.5	8.9
23.0	107.2	39.4	8.7
29.0	106.9	39.1	8.7
35.0	105.5	37.3	9.2
41.0	99.4	30.9	11.1
43.0	89.6	21.3	16.0
45.0	81.9	13.7	24.9

INLET TEMPERATURE DEGREES FAHRENHEIT	GAS DENSITY LBS./CU. FT.	HEAT FLUX BTU/HR. SQ. FT.	MASS FLOW RATE LBS./HR. SQ. FT.	AVG. HT. TRANS. COEFFICIENT BTU/HR. SQ. FT. F
65.3	.0908	341.8	4787	10.31

RUN 6A ALUMINUM PARTICLES STATIC BED HEIGHT= 9 INCHES HEATED TUBE LOC. NO.#3

PROBE LOCATION INCHES	TUBE WALL TEMPERATURE DEGREES FAHRENHEIT	TEMPERATURE DIFFERENCE DEGREES FAHRENHEIT	LOCAL HEAT TRANSFER COEFFICIENT BTU/HR. SQ. FT. F
1.0	95.5	16.3	23.5
3.0	96.6	16.3	23.5
5.0	97.6	16.6	23.0
8.0	96.7	14.9	25.5
11.0	96.1	14.1	27.1
17.0	108.5	26.6	14.4
23.0	161.3	79.7	4.8
29.0	194.8	113.1	3.4
35.0	212.1	130.0	2.9
41.0	223.7	140.7	2.7
45.0	224.1	140.4	2.7

INLET TEMPERATURE DEGREES FAHRENHEIT	GAS DENSITY LBS./CU. FT.	HEAT FLUX BTU/HR. SQ. FT.	MASS FLOW RATE LBS./HR. SQ. FT.	AVG. HT. TRANS. COEFFICIENT BTU/HR. SQ. FT. F
78.6	.0809	381.3	2496	5.26

RUN 6B ALUMINUM PARTICLES STATIC BED HEIGHT= 9 INCHES HEATED TUBE LOC. NO.#3

PROBE LOCATION INCHES	TUBE WALL TEMPERATURE DEGREES FAHRENHEIT	TEMPERATURE DIFFERENCE DEGREES FAHRENHEIT	LOCAL HEAT TRANSFER COEFFICIENT BTU/HR. SQ. FT. F
1.0	94.4	15.4	24.1
3.0	96.1	15.6	23.9
5.0	96.5	15.0	24.8
11.0	99.0	16.3	22.8
17.0	106.8	24.4	15.2
23.0	118.5	36.7	10.1
29.0	134.9	53.0	7.0
35.0	157.5	75.1	5.0
41.0	177.6	94.6	3.9
43.0	180.6	97.6	3.8
45.0	179.7	96.8	3.8

INLET TEMPERATURE DEGREES FAHRENHEIT	GAS DENSITY LBS./CU. FT.	HEAT FLUX BTU/HR. SQ. FT.	MASS FLOW RATE LBS./HR. SQ. FT.	AVG. HT. TRANS. COEFFICIENT BTU/HR. SQ. FT. F
78.1	.0901	371.9	4509	8.39

RUN 6C ALUMINUM PARTICLES STATIC BED HEIGHT= 4 INCHES HEATED TUBE LOC. NO.#3

PROBE LOCATION INCHES	TUBE WALL TEMPERATURE DEGREES FAHRENHEIT	TEMPERATURE DIFFERENCE DEGREES FAHRENHEIT	LOCAL HEAT TRANSFER COEFFICIENT BTU/HR. SQ. FT. F
1.0	93.5	14.6	24.9
3.0	95.8	16.1	22.5
5.0	97.8	17.7	20.5
8.0	99.7	19.4	18.7
11.0	116.2	35.9	10.1
17.0	164.2	84.5	4.3
23.0	193.6	114.3	3.2
29.0	208.8	129.2	2.8
35.0	222.1	141.7	2.6
41.0	131.8	150.5	2.4
45.0	224.2	142.9	2.5

INLET TEMPERATURE DEGREES FAHRENHEIT	GAS DENSITY LBS./CU. FT.	HEAT FLUX BTU/HR. SQ. FT.	MASS FLOW RATE LBS./HR. SQ. FT.	AVG. HT. TRANS. COEFFICIENT BTU/HR. SQ. FT. F
78.5	.0814	362.4	2930	3.92

RUN 6 D ALUMINUM PARTICLES STATIC BED HEIGHT= 4 INCHES HEATED TUBE LOC. NO.=3

PROBE LOCATION INCHES	TUBE WALL TEMPERATURE DEGREES FAHRENHEIT	TEMPERATURE DIFFERENCE DEGREES FAHRENHEIT	LOCAL HEAT TRANSFER COEFFICIENT BTU/HR. SQ. FT. F
1.0	92.2	15.5	22.6
3.0	94.2	16.3	21.5
5.0	98.9	20.2	17.3
11.0	107.6	28.5	12.3
17.0	116.3	37.9	9.2
23.0	127.5	49.4	7.1
29.0	145.5	66.7	5.2
35.0	161.5	81.4	4.3
41.0	175.5	94.5	3.7
43.0	179.3	98.5	3.6
45.0	177.3	97.1	3.6

INLET TEMPERATURE DEGREES FAHRENHEIT	GAS DENSITY LBS./CU. FT.	HEAT FLUX BTU/HR. SQ. FT.	MASS FLOW RATE LBS./HR. SQ. FT.	AVG. HT. TRANS. COEFFICIENT BTU/HR. SQ. FT. F
75.8	.0891	349.9	4768	6.65

RUN 6 E ALUMINUM PARTICLES STATIC BED HEIGHT= 4 INCHES HEATED TUBE LOC. NO.=3

PROBE LOCATION INCHES	TUBE WALL TEMPERATURE DEGREES FAHRENHEIT	TEMPERATURE DIFFERENCE DEGREES FAHRENHEIT	LOCAL HEAT TRANSFER COEFFICIENT BTU/HR. SQ. FT. F
1.0	93.6	21.4	16.3
3.0	103.2	30.1	11.6
5.0	110.4	36.9	9.4
11.0	126.7	52.9	6.6
17.0	130.3	56.9	6.1
23.0	131.4	58.2	6.0
29.0	132.5	58.9	5.9
35.0	130.1	55.7	6.3
41.0	123.8	48.9	7.1
43.0	117.8	43.1	8.1
45.0	97.5	23.0	15.1

INLET TEMPERATURE DEGREES FAHRENHEIT	GAS DENSITY LBS./CU. FT.	HEAT FLUX BTU/HR. SQ. FT.	MASS FLOW RATE LBS./HR. SQ. FT.	AVG. HT. TRANS. COEFFICIENT BTU/HR. SQ. FT. F
71.7	.0836	348.4	6946	7.13

RUN 6 F ALUMINUM PARTICLES STATIC BED HEIGHT= 4 INCHES HEATED TUBE LOC. NO.=3

PROBE LOCATION INCHES	TUBE WALL TEMPERATURE DEGREES FAHRENHEIT	TEMPERATURE DIFFERENCE DEGREES FAHRENHEIT	LOCAL HEAT TRANSFER COEFFICIENT BTU/HR. SQ. FT. F
1.0	95.3	23.7	14.6
3.0	104.2	31.2	11.0
5.0	109.4	35.4	9.7
11.0	119.2	44.1	7.8
17.0	126.3	51.5	6.7
23.0	129.2	55.0	6.3
29.0	130.6	56.5	6.1
35.0	130.3	55.9	6.2
41.0	126.4	51.6	6.7
43.0	118.5	43.6	7.9
45.0	97.0	22.2	15.5

INLET TEMPERATURE DEGREES FAHRENHEIT	GAS DENSITY LBS./CU. FT.	HEAT FLUX BTU/HR. SQ. FT.	MASS FLOW RATE LBS./HR. SQ. FT.	AVG. HT. TRANS. COEFFICIENT BTU/HR. SQ. FT. F
70.8	.0807	364.4	5657	7.41

RUN 6 G ALUMINUM PARTICLES STATIC BED HEIGHT= 9 INCHES HEATED TUBE LOC. NO.=3

PROBE LOCATION INCHES	TUBE WALL TEMPERATURE DEGREES FAHRENHEIT	TEMPERATURE DIFFERENCE DEGREES FAHRENHEIT	LOCAL HEAT TRANSFER COEFFICIENT BTU/HR. SQ. FT. F
1.0	108.9	19.9	17.6
3.0	118.7	29.7	11.8
5.0	124.6	35.6	9.8
11.0	134.6	46.5	7.5
17.0	140.1	53.0	6.6
23.0	143.2	56.5	6.2
29.0	143.4	56.5	6.2
35.0	142.5	54.7	6.4
41.0	137.1	48.1	7.3
43.0	129.1	39.9	8.8
45.0	109.9	20.5	17.1

INLET TEMPERATURE DEGREES FAHRENHEIT	GAS DENSITY LBS./CU. FT.	HEAT FLUX BTU/HR. SQ. FT.	MASS FLOW RATE LBS./HR. SQ. FT.	AVG. HT. TRANS. COEFFICIENT BTU/HR. SQ. FT. F
88.8	.0775	349.9	4871	7.54

RUN 6 H ALUMINUM PARTICLES STATIC BED HEIGHT= 9 INCHES HEATED TUBE LOC. NO.=3

PROBE LOCATION INCHES	TUBE WALL TEMPERATURE DEGREES FAHRENHEIT	TEMPERATURE DIFFERENCE DEGREES FAHRENHEIT	LOCAL HEAT TRANSFER COEFFICIENT BTU/HR. SQ. FT. F
1.0	92.3	20.2	16.9
3.0	100.1	26.4	12.9
5.0	107.9	33.0	10.3
11.0	116.5	40.6	8.4
17.0	121.7	46.4	7.4
23.0	124.6	50.1	6.8
29.0	126.4	52.2	6.5
35.0	126.6	52.1	6.6
41.0	122.0	46.9	7.3
43.0	116.2	41.2	8.3
45.0	94.4	19.6	17.4

INLET TEMPERATURE DEGREES FAHRENHEIT	GAS DENSITY LBS./CU. FT.	HEAT FLUX BTU/HR. SQ. FT.	MASS FLOW RATE LBS./HR. SQ. FT.	AVG. HT. TRANS. COEFFICIENT BTU/HR. SQ. FT. F
71.1	.0821	341.6	6341	8.02

RUN 7 A ALUMINUM PARTICLES STATIC BED HEIGHT= 9 INCHES HEATED TUBE LOC. NO.=2

PROBE LOCATION INCHES	TUBE WALL TEMPERATURE DEGREES FAHRENHEIT	TEMPERATURE DIFFERENCE DEGREES FAHRENHEIT	LOCAL HEAT TRANSFER COEFFICIENT BTU/HR. SQ. FT. F
1.0	93.7	17.8	20.1
3.0	95.7	18.2	19.6
5.0	93.8	15.4	23.2
8.0	93.4	14.2	25.0
11.0	93.4	14.2	25.1
17.0	95.8	17.4	20.4
23.0	119.2	41.6	8.6
29.0	164.9	87.3	4.1
35.0	192.5	113.7	3.1
41.0	207.2	126.6	2.8
45.0	211.0	129.6	2.8

INLET TEMPERATURE DEGREES FAHRENHEIT	GAS DENSITY LBS./CU. FT.	HEAT FLUX BTU/HR. SQ. FT.	MASS FLOW RATE LBS./HR. SQ. FT.	AVG. HT. TRANS. COEFFICIENT BTU/HR. SQ. FT. F
74.9	.0801	356.5	2849	6.09

RUN 7 B ALUMINUM PARTICLES STATIC BED HEIGHT= 9 INCHES HEATED TUBE LOC. NO.=2

PROBE LOCATION INCHES	TUBE WALL TEMPERATURE DEGREES FAHRENHEIT	TEMPERATURE DIFFERENCE DEGREES FAHRENHEIT	LOCAL HEAT TRANSFER COEFFICIENT BTU/HR. SQ. FT. F
1.0	96.6	21.2	16.6
3.0	97.8	22.9	15.4
5.0	97.8	21.8	16.1
11.0	96.5	16.1	21.9
17.0	100.1	16.3	21.6
23.0	107.5	23.6	15.0
29.0	124.5	43.6	8.1
35.0	140.8	64.4	5.5
41.0	159.6	95.3	4.1
43.0	164.0	88.9	4.0
45.0	170.7	93.7	3.8

INLET TEMPERATURE DEGREES FAHRENHEIT	GAS DENSITY LBS./CU. FT.	HEAT FLUX BTU/HR. SQ. FT.	MASS FLOW RATE LBS./HR. SQ. FT.	AVG. HT. TRANS. COEFFICIENT BTU/HR. SQ. FT. F
74.4	.0793	352.3	3712	9.17

RUN 7 C ALUMINUM PARTICLES STATIC BED HEIGHT= 9 INCHES HEATED TUBE LOC. NO.=2

PROBE LOCATION INCHES	TUBE WALL TEMPERATURE DEGREES FAHRENHEIT	TEMPERATURE DIFFERENCE DEGREES FAHRENHEIT	LOCAL HEAT TRANSFER COEFFICIENT BTU/HR. SQ. FT. F
1.0	95.9	21.0	16.7
3.0	103.0	26.7	13.2
5.0	109.6	32.3	10.9
11.0	120.8	42.5	8.3
17.0	127.2	49.2	7.1
23.0	129.4	51.8	6.8
29.0	129.4	51.8	6.8
35.0	130.1	52.0	6.8
41.0	122.6	44.1	8.0
43.0	114.5	36.0	9.8
45.0	103.6	25.4	13.8

INLET TEMPERATURE DEGREES FAHRENHEIT	GAS DENSITY LBS./CU. FT.	HEAT FLUX BTU/HR. SQ. FT.	MASS FLOW RATE LBS./HR. SQ. FT.	AVG. HT. TRANS. COEFFICIENT BTU/HR. SQ. FT. F
73.9	.0792	351.8	5070	8.18

```
RUN 7D         ALUMINUM PARTICLES          STATIC BED HEIGHT= 9 INCHES        HEATED TUBE LOC. NO.=2

PROBE LOCATION       TUBE WALL TEMPERATURE      TEMPERATURE DIFFERENCE     LOCAL HEAT TRANSFER COEFFICIENT
    INCHES            DEGREES FAHRENHEIT         DEGREES FAHRENHEIT           BTU/HR. SQ. FT.  F
      1.0                   94.6                        18.6                        18.7
      3.0                  101.1                        23.5                        14.8
      5.0                  106.1                        27.4                        12.7
     11.0                  117.2                        37.4                         9.3
     17.0                  126.1                        46.9                         7.4
     23.0                  129.0                        50.5                         6.9
     29.0                  130.2                        51.8                         6.7
     35.0                  130.4                        51.4                         6.8
     41.0                  124.1                        44.5                         7.8
     43.0                  117.8                        38.2                         9.1
     45.0                  107.7                        28.4                        12.3
 INLET TEMPERATURE      GAS DENSITY       HEAT FLUX        MASS FLOW RATE      AVG. HT. TRANS. COEFFICIENT
 DEGREES FAHRENHEIT   LBS./CU. FT.    BTU/HR. SQ. FT.    LBS./HR. SQ. FT.        BTU/HR. SQ. FT.  F
      76.9               .0807            349.0               6092                     8.41

RUN 7E         ALUMINUM PARTICLES          STATIC BED HEIGHT= 4 INCHES        HEATED TUBE LOC. NO.=2

PROBE LOCATION       TUBE WALL TEMPERATURE      TEMPERATURE DIFFERENCE     LOCAL HEAT TRANSFER COEFFICIENT
    INCHES            DEGREES FAHRENHEIT         DEGREES FAHRENHEIT           BTU/HR. SQ. FT.  F
      1.0                   98.5                        21.7                        16.1
      3.0                  104.2                        25.7                        13.7
      5.0                  110.4                        30.6                        11.5
     11.0                  119.3                        38.2                         9.2
     17.0                  130.5                        49.8                         7.0
     23.0                  133.7                        53.7                         6.5
     29.0                  134.7                        54.7                         6.4
     35.0                  134.5                        53.9                         6.5
     41.0                  131.0                        50.0                         7.0
     43.0                  120.9                        39.9                         8.8
     45.0                  111.0                        30.4                        11.5
 INLET TEMPERATURE      GAS DENSITY       HEAT FLUX        MASS FLOW RATE      AVG. HT. TRANS. COEFFICIENT
 DEGREES FAHRENHEIT   LBS./CU. FT.    BTU/HR. SQ. FT.    LBS./HR. SQ. FT.        BTU/HR. SQ. FT.  F
      75.6               .0797            350.2               5898                     7.95

RUN 7F         ALUMINUM PARTICLES          STATIC BED HEIGHT= 4 INCHES        HEATED TUBE LOC. NO.=2

PROBE LOCATION       TUBE WALL TEMPERATURE      TEMPERATURE DIFFERENCE     LOCAL HEAT TRANSFER COEFFICIENT
    INCHES            DEGREES FAHRENHEIT         DEGREES FAHRENHEIT           BTU/HR. SQ. FT.  F
      1.0                   96.7                        19.7                        17.7
      3.0                  103.6                        24.5                        14.2
      5.0                  108.3                        27.8                        12.5
     11.0                  116.8                        34.8                        10.0
     17.0                  125.0                        43.6                         8.0
     23.0                  127.8                        47.2                         7.4
     29.0                  130.5                        50.2                         6.9
     35.0                  131.4                        50.5                         6.9
     41.0                  127.2                        45.7                         7.6
     43.0                  120.8                        39.3                         8.9
     45.0                  111.4                        30.2                        11.5
 INLET TEMPERATURE      GAS DENSITY       HEAT FLUX        MASS FLOW RATE      AVG. HT. TRANS. COEFFICIENT
 DEGREES FAHRENHEIT   LBS./CU. FT.    BTU/HR. SQ. FT.    LBS./HR. SQ. FT.        BTU/HR. SQ. FT.  F
      75.8               .0810            348.3               6694                     8.69
```

RUN 7G ALUMINUM PARTICLES STATIC BED HEIGHT= 4 INCHES HEATED TUBE LOC. NO.=2

PROBE LOCATION INCHES	TUBE WALL TEMPERATURE DEGREES FAHRENHEIT	TEMPERATURE DIFFERENCE DEGREES FAHRENHEIT	LOCAL HEAT TRANSFER COEFFICIENT BTU/HR. SQ. FT. F
1.0	95.9	17.3	20.9
3.0	98.2	18.7	19.3
5.0	96.9	16.9	21.4
8.0	97.4	16.7	21.6
11.0	102.6	21.7	16.6
14.0	116.5	35.7	10.1
17.0	135.1	54.4	6.6
23.0	174.6	94.1	3.8
32.0	206.9	126.3	2.9
39.0	220.9	139.3	2.6
44.0	227.0	144.3	2.5

INLET TEMPERATURE DEGREES FAHRENHEIT	GAS DENSITY LBS./CU. FT.	HEAT FLUX BTU/HR. SQ. FT.	MASS FLOW RATE LBS./HR. SQ. FT.	AVG. HT. TRANS. COEFFICIENT BTU/HR. SQ. FT. F
78.1	.0793	360.9	3049	4.59

RUN 7H ALUMINUM PARTICLES STATIC BED HEIGHT= 4 INCHES HEATED TUBE LOC. NO.=2

PROBE LOCATION INCHES	TUBE WALL TEMPERATURE DEGREES FAHRENHEIT	TEMPERATURE DIFFERENCE DEGREES FAHRENHEIT	LOCAL HEAT TRANSFER COEFFICIENT BTU/HR. SQ. FT. F
1.0	93.8	17.9	19.8
3.0	99.9	22.6	15.7
5.0	104.9	26.5	13.4
11.0	111.9	32.8	10.9
17.0	118.9	40.7	8.8
23.0	127.5	50.1	7.1
29.0	122.1	44.6	8.0
35.0	161.4	83.1	4.3
41.0	175.1	95.7	3.7
43.0	178.8	99.3	3.6
45.0	184.0	104.6	3.4

INLET TEMPERATURE DEGREES FAHRENHEIT	GAS DENSITY LBS./CU. FT.	HEAT FLUX BTU/HR. SQ. FT.	MASS FLOW RATE LBS./HR. SQ. FT.	AVG. HT. TRANS. COEFFICIENT BTU/HR. SQ. FT. F
74.8	.0787	355.8	4104	6.84

RUN 8 A   COARSE GLASS SPHERES   STATIC BED HEIGHT= 9 INCHES   HEATED TUBE LOC. NO.=2

PROBE LOCATION INCHES	TUBE WALL TEMPERATURE DEGREES FAHRENHEIT	TEMPERATURE DIFFERENCE DEGREES FAHRENHEIT	LOCAL HEAT TRANSFER COEFFICIENT BTU/HR. SQ. FT. F
1.0	93.3	16.9	21.0
3.0	95.0	17.3	20.6
5.0	94.9	16.2	22.0
8.0	93.1	13.6	26.1
11.0	92.8	13.2	27.0
17.0	95.6	16.5	21.6
23.0	101.3	22.7	15.7
29.0	129.6	51.1	7.0
35.0	171.8	92.5	3.8
41.0	214.6	134.1	2.7
44.0	216.4	135.3	2.6

INLET TEMPERATURE DEGREES FAHRENHEIT	GAS DENSITY LBS./CU. FT.	HEAT FLUX BTU/HR. SQ. FT.	MASS FLOW RATE LBS./HR. SQ. FT.	AVG. HT. TRANS. COEFFICIENT BTU/HR. SQ. FT. F
75.5	.0803	356.1	2545	7.54

RUN 8 B   COARSE GLASS SPHERES   STATIC BED HEIGHT= 9 INCHES   HEATED TUBE LOC. NO.=2

PROBE LOCATION INCHES	TUBE WALL TEMPERATURE DEGREES FAHRENHEIT	TEMPERATURE DIFFERENCE DEGREES FAHRENHEIT	LOCAL HEAT TRANSFER COEFFICIENT BTU/HR. SQ. FT. F
1.0	94.5	16.3	21.4
3.0	102.4	22.7	15.4
5.0	109.6	28.9	12.1
11.0	119.2	38.0	9.2
17.0	127.9	47.7	7.3
23.0	129.7	50.4	6.9
29.0	130.3	50.9	6.9
35.0	129.9	49.5	7.1
41.0	127.2	45.9	7.6
43.0	118.5	37.2	9.4
45.0	105.8	24.9	14.0

INLET TEMPERATURE DEGREES FAHRENHEIT	GAS DENSITY LBS./CU. FT.	HEAT FLUX BTU/HR. SQ. FT.	MASS FLOW RATE LBS./HR. SQ. FT.	AVG. HT. TRANS. COEFFICIENT BTU/HR. SQ. FT. F
77.2	.0749	348.9	5558	8.46

RUN 8 C   COARSE GLASS SPHERES   STATIC BED HEIGHT= 9 INCHES   HEATED TUBE LOC. NO.=2

PROBE LOCATION INCHES	TUBE WALL TEMPERATURE DEGREES FAHRENHEIT	TEMPERATURE DIFFERENCE DEGREES FAHRENHEIT	LOCAL HEAT TRANSFER COEFFICIENT BTU/HR. SQ. FT. F
1.0	99.0	20.8	16.9
3.0	109.1	29.2	12.0
5.0	117.2	36.0	9.8
11.0	125.8	43.1	8.2
17.0	130.8	48.0	7.3
23.0	131.6	48.8	7.2
29.0	131.0	47.8	7.3
35.0	127.8	43.9	8.0
41.0	119.1	35.0	10.0
43.0	107.2	23.4	15.0
45.0	102.2	19.0	18.5

INLET TEMPERATURE DEGREES FAHRENHEIT	GAS DENSITY LBS./CU. FT.	HEAT FLUX BTU/HR. SQ. FT.	MASS FLOW RATE LBS./HR. SQ. FT.	AVG. HT. TRANS. COEFFICIENT BTU/HR. SQ. FT. F
77.2	.0873	351.3	4814	8.83

RUN 8D COARSE GLASS SPHERES STATIC BED HEIGHT= 9 INCHES HEATED TUBE LOC. NO.=2

PROBE LOCATION INCHES	TUBE WALL TEMPERATURE DEGREES FAHRENHEIT	TEMPERATURE DIFFERENCE DEGREES FAHRENHEIT	LOCAL HEAT TRANSFER COEFFICIENT BTU/HR. SQ. FT. F
1.0	95.0	17.7	19.9
3.0	97.8	18.9	18.6
5.0	97.9	18.0	19.6
11.0	98.2	17.3	20.3
17.0	107.8	27.6	12.7
23.0	108.4	29.0	12.1
29.0	110.8	31.3	11.2
35.0	118.4	38.2	9.2
41.0	128.8	47.8	7.4
43.0	134.1	53.1	6.6
45.0	144.4	63.6	5.5

INLET TEMPERATURE DEGREES FAHRENHEIT	GAS DENSITY LBS./CU. FT.	HEAT FLUX BTU/HR. SQ. FT.	MASS FLOW RATE LBS./HR. SQ. FT.	AVG. HT. TRANS. COEFFICIENT BTU/HR. SQ. FT. F
76.3	.0871	351.8	3653	11.90

RUN 8E COARSE GLASS SPHERES STATIC BED HEIGHT= 4 INCHES HEATED TUBE LOC. NO.=2

PROBE LOCATION INCHES	TUBE WALL TEMPERATURE DEGREES FAHRENHEIT	TEMPERATURE DIFFERENCE DEGREES FAHRENHEIT	LOCAL HEAT TRANSFER COEFFICIENT BTU/HR. SQ. FT. F
1.0	103.3	22.2	15.7
3.0	116.1	33.2	10.5
5.0	122.2	38.1	9.2
11.0	130.6	45.4	7.7
17.0	138.9	54.2	6.4
23.0	138.9	55.0	6.3
29.0	137.6	53.8	6.5
35.0	136.3	51.8	6.7
41.0	132.7	47.5	7.3
43.0	122.4	37.2	9.4
45.0	115.1	30.1	11.6

INLET TEMPERATURE DEGREES FAHRENHEIT	GAS DENSITY LBS./CU. FT.	HEAT FLUX BTU/HR. SQ. FT.	MASS FLOW RATE LBS./HR. SQ. FT.	AVG. HT. TRANS. COEFFICIENT BTU/HR. SQ. FT. F
79.9	.0903	348.7	5813	7.60

RUN 8F COARSE GLASS SPHERES STATIC BED HEIGHT= 4 INCHES HEATED TUBE LOC. NO.=2

PROBE LOCATION INCHES	TUBE WALL TEMPERATURE DEGREES FAHRENHEIT	TEMPERATURE DIFFERENCE DEGREES FAHRENHEIT	LOCAL HEAT TRANSFER COEFFICIENT BTU/HR. SQ. FT. F
1.0	105.8	16.5	21.6
3.0	114.7	24.6	14.4
5.0	120.8	30.3	11.7
11.0	128.5	37.6	9.4
17.0	136.6	46.3	7.7
23.0	139.0	49.1	7.2
29.0	139.2	49.3	7.2
35.0	138.7	48.2	7.4
41.0	136.7	45.6	7.8
43.0	133.4	42.1	8.4
45.0	123.1	31.8	11.2

INLET TEMPERATURE DEGREES FAHRENHEIT	GAS DENSITY LBS./CU. FT.	HEAT FLUX BTU/HR. SQ. FT.	MASS FLOW RATE LBS./HR. SQ. FT.	AVG. HT. TRANS. COEFFICIENT BTU/HR. SQ. FT. F
88.8	.0991	355.6	8582	8.69

```
RUN 8 G      COARSE GLASS SPHERES          STATIC BED HEIGHT= 4 INCHES       HEATED TUBE T.C. NO.=2

PROBE LOCATION      TUBE WALL TEMPERATURE      TEMPERATURE DIFFERENCE      LOCAL HEAT TRANSFER COEFFICIENT
   INCHES           DEGREES FAHRENHEIT         DEGREES FAHRENHEIT              BTU/HR. SQ. FT.  F
    1.0                   95.9                       16.4                            21.7
    3.0                   98.9                       17.7                            20.1
    5.0                   99.8                       17.5                            20.4
    8.0                  100.8                       17.6                            20.2
   11.0                  104.1                       20.6                            17.3
   17.0                  113.0                       29.8                            11.9
   23.0                  133.9                       51.2                             7.0
   29.0                  163.4                       80.6                             4.4
   35.0                  196.2                      112.5                             3.2
   41.0                  226.7                      141.9                             2.5
   44.0                  235.9                      150.9                             2.4
 INLET TEMPERATURE     GAS DENSITY      HEAT FLUX        MASS FLOW RATE      AVG. HT. TRANS. COEFFICIENT
 DEGREES FAHRENHEIT    LBS./CU. FT.   BTU/HR. SQ. FT.   LBS./HR. SQ. FT.        BTU/HR. SQ. FT.  F
     78.5                .0791           355.9              2892                    5.73

RUN 8 H      COARSE GLASS SPHERES          STATIC BED HEIGHT= 4 INCHES       HEATED TUBE T.C. NO.=2

PROBE LOCATION      TUBE WALL TEMPERATURE      TEMPERATURE DIFFERENCE      LOCAL HEAT TRANSFER COEFFICIENT
   INCHES           DEGREES FAHRENHEIT         DEGREES FAHRENHEIT              BTU/HR. SQ. FT.  F
    1.0                   98.9                       20.8                            17.1
    3.0                   99.7                       19.9                            17.8
    5.0                  106.0                       25.0                            14.2
   11.0                  114.2                       32.1                            11.0
   17.0                  120.2                       38.5                             9.2
   23.0                  122.3                       41.3                             8.6
   29.0                  123.8                       42.8                             8.3
   35.0                  128.3                       46.5                             7.6
   41.0                  131.1                       48.5                             7.3
   43.0                  132.3                       49.6                             7.1
   45.0                  136.4                       53.7                             6.6
 INLET TEMPERATURE     GAS DENSITY      HEAT FLUX        MASS FLOW RATE      AVG. HT. TRANS. COEFFICIENT
 DEGREES FAHRENHEIT    LBS./CU. FT.   BTU/HR. SQ. FT.   LBS./HR. SQ. FT.        BTU/HR. SQ. FT.  F
     77.0                .0793           354.1              3026                    9.40
```

RUN 9A FINE GLASS SPHERES STATIC BED HEIGHT= 9 INCHES HEATED TUBE LOC. NO.=2

PROBE LOCAITON INCHES	TUBE WALL TEMPERATURE DEGREES FAHRENHEIT	TEMPERATURE DIFFERENCE DEGREES FAHRENHEIT	LOCAL HEAT TRANSFER COEFFICIENT BTU/HR. SQ. FT. F
1.0	94.9	10.6	33.8
3.0	96.1	9.2	38.8
5.0	97.0	8.4	42.4
8.0	97.3	7.3	48.9
11.0	97.4	7.0	50.8
17.0	100.6	10.9	32.7
23.0	112.3	23.5	15.2
29.0	132.6	43.7	8.2
35.0	155.1	64.9	5.5
41.0	170.5	79.0	4.5
44.0	180.9	89.4	4.0

INLET TEMPERATURE DEGREES FAHRENHEIT	GAS DENSITY LBS./CU. FT.	HEAT FLUX BTU/HR. SQ. FT.	MASS FLOW RATE LBS./HR. SQ. FT.	AVG. HT. TRANS. COEFFICIENT BTU/HR. SQ. FT. F
82.7	.0800	357.7	1690	10.92

RUN 9 B FINE GLASS SPHERES STATIC BED HEIGHT= 9 INCHES HEATED TUBE LOC. NO.=2

PROBE LOCAITON INCHES	TUBE WALL TEMPERATURE DEGREES FAHRENHEIT	TEMPERATURE DIFFERENCE DEGREES FAHRENHEIT	LOCAL HEAT TRANSFER COEFFICIENT BTU/HR. SQ. FT. F
1.0	96.8	13.4	26.2
3.0	97.3	11.0	31.8
5.0	97.9	9.8	35.9
11.0	99.2	8.7	40.2
17.0	101.1	11.1	31.6
23.0	101.4	12.3	28.5
29.0	107.5	18.6	18.8
35.0	114.3	24.5	14.3
41.0	118.8	28.1	12.5
43.0	120.2	29.4	11.9
45.0	128.5	38.0	9.2

INLET TEMPERATURE DEGREES FAHRENHEIT	GAS DENSITY LBS./CU. FT.	HEAT FLUX BTU/HR. SQ. FT.	MASS FLOW RATE LBS./HR. SQ. FT.	AVG. HT. TRANS. COEFFICIENT BTU/HR. SQ. FT. F
81.7	.0799	350.8	1828	21.80

RUN 9 C FINE GLASS SPHERES STATIC BED HEIGHT= 4 INCHES HEATED TUBE LOC. NO.=2

PROBE LOCATION INCHES	TUBE WALL TEMPERATURE DEGREES FAHRENHEIT	TEMPERATURE DIFFERENCE DEGREES FAHRENHEIT	LOCAL HEAT TRANSFER COEFFICIENT BTU/HR. SQ. FT. F
1.0	95.2	12.5	27.8
3.0	95.7	10.3	34.0
5.0	96.2	8.9	39.4
11.0	102.1	12.5	27.9
17.0	108.0	18.9	18.4
23.0	113.1	25.1	13.9
29.0	115.6	27.8	12.5
35.0	118.2	29.6	11.8
41.0	120.4	30.8	11.3
43.0	121.4	31.8	11.0
45.0	128.3	38.9	9.0

INLET TEMPERATURE DEGREES FAHRENHEIT	GAS DENSITY LBS./CU. FT.	HEAT FLUX BTU/HR. SQ. FT.	MASS FLOW RATE LBS./HR. SQ. FT.	AVG. HT. TRANS. COEFFICIENT BTU/HR. SQ. FT. F
81.0	.0800	348.8	1882	16.22

RUN 9 D FINE GLASS SPHERES STATIC BED HEIGHT= 4 INCHES HEATED TUBE LOC. NO.=2

PROBE LOCATION INCHES	TUBE WALL TEMPERATURE DEGREES FAHRENHEIT	TEMPERATURE DIFFERENCE DEGREES FAHRENHEIT	LOCAL HEAT TRANSFER COEFFICIENT BTU/HR. SQ. FT. F
1.0	92.9	9.3	39.1
3.0	94.2	9.0	40.6
5.0	94.8	8.5	42.8
8.0	94.9	7.8	46.8
11.0	100.7	13.4	27.1
17.0	125.6	39.0	9.3
23.0	174.6	88.7	4.1
29.0	218.4	132.1	2.8
35.0	262.7	175.2	2.1
41.0	275.9	186.8	1.9
44.0	277.6	188.1	1.9

INLET TEMPERATURE DEGREES FAHRENHEIT	GAS DENSITY LBS./CU. FT.	HEAT FLUX BTU/HR. SQ. FT.	MASS FLOW RATE LBS./HR. SQ. FT.	AVG. HT. TRANS. COEFFICIENT BTU/HR. SQ. FT. F
82.5	.0800	364.1	1626	4.15

RUN 9 E FINE GLASS SPHERES STATIC BED HEIGHT= 2 INCHES HEATED TUBE LOC. NO.=2

PROBE LOCATION INCHES	TUBE WALL TEMPERATURE DEGREES FAHRENHEIT	TEMPERATURE DIFFERENCE DEGREES FAHRENHEIT	LOCAL HEAT TRANSFER COEFFICIENT BTU/HR. SQ. FT. F
1.0	90.9	13.5	26.3
3.0	95.2	15.7	22.7
5.0	99.5	18.6	19.1
8.0	104.5	22.4	15.9
11.0	108.8	26.3	13.5
17.0	114.0	31.9	11.2
23.0	118.1	36.6	9.7
29.0	121.1	39.5	9.0
35.0	123.9	41.4	8.6
41.0	127.7	44.5	8.0
44.0	128.4	45.4	7.8

INLET TEMPERATURE DEGREES FAHRENHEIT	GAS DENSITY LBS./CU. FT.	HEAT FLUX BTU/HR. SQ. FT.	MASS FLOW RATE LBS./HR. SQ. FT.	AVG. HT. TRANS. COEFFICIENT BTU/HR. SQ. FT. F
76.1	.0807	356.0	1853	10.98

RUN 9 F FINE GLASS SPHERES STATIC BED HEIGHT= 6 INCHES HEATED TUBE LOC. NO.=2

PROBE LOCATION INCHES	TUBE WALL TEMPERATURE DEGREES FAHRENHEIT	TEMPERATURE DIFFERENCE DEGREES FAHRENHEIT	LOCAL HEAT TRANSFER COEFFICIENT BTU/HR. SQ. FT. F
1.0	92.9	12.6	28.3
3.0	95.1	12.4	28.7
5.0	95.0	10.6	33.5
8.0	94.1	8.4	42.4
11.0	98.2	12.0	29.6
17.0	98.1	12.7	28.0
23.0	103.9	19.4	18.3
29.0	115.6	31.1	11.4
35.0	124.4	39.0	9.1
41.0	131.3	45.2	7.8
44.0	134.6	49.0	7.2

INLET TEMPERATURE DEGREES FAHRENHEIT	GAS DENSITY LBS./CU. FT.	HEAT FLUX BTU/HR. SQ. FT.	MASS FLOW RATE LBS./HR. SQ. FT.	AVG. HT. TRANS. COEFFICIENT BTU/HR. SQ. FT. F
78.7	.0806	354.8	1725	15.30

RUN 9G COARSE GLASS SPHERES STATIC BED HEIGHT= 6 INCHES HEATED TUBE LOC. NO.=2

PROBE LOCATION INCHES	TUBE WALL TEMPERATURE DEGREES FAHRENHEIT	TEMPERATURE DIFFERENCE DEGREES FAHRENHEIT	LOCAL HEAT TRANSFER COEFFICIENT BTU/HR. SQ. FT. F
1.0	104.2	21.9	16.2
3.0	106.7	23.1	15.4
5.0	106.4	21.9	16.2
8.0	107.0	21.9	16.2
11.0	112.0	26.8	13.2
17.0	114.6	30.1	11.8
23.0	115.5	31.7	11.2
30.0	126.6	42.9	8.3
35.0	147.0	62.8	5.7
41.0	183.0	98.1	3.6
44.0	198.1	113.0	3.1

INLET TEMPERATURE DEGREES FAHRENHEIT	GAS DENSITY LBS./CU. FT.	HEAT FLUX BTU/HR. SQ. FT.	MASS FLOW RATE LBS./HR. SQ. FT.	AVG. HT. TRANS. COEFFICIENT BTU/HR. SQ. FT. F
81.5	.0978	354.9	3957	8.28

RUN 9H COARSE GLASS SPHERES STATIC BED HEIGHT= 2 INCHES HEATED TUBE LOC. NO.=2

PROBE LOCATION INCHES	TUBE WALL TEMPERATURE DEGREES FAHRENHEIT	TEMPERATURE DIFFERENCE DEGREES FAHRENHEIT	LOCAL HEAT TRANSFER COEFFICIENT BTU/HR. SQ. FT. F
1.0	103.0	19.6	18.2
3.0	113.2	28.9	12.3
5.0	119.1	34.2	10.4
8.0	122.1	36.7	9.7
11.0	126.9	41.2	8.6
17.0	133.7	48.1	7.4
23.0	142.6	57.4	6.2
29.0	169.4	84.4	4.2
35.0	208.3	123.2	2.9
41.0	229.1	143.6	2.5
44.0	231.5	145.8	2.4

INLET TEMPERATURE DEGREES FAHRENHEIT	GAS DENSITY LBS./CU. FT.	HEAT FLUX BTU/HR. SQ. FT.	MASS FLOW RATE LBS./HR. SQ. FT.	AVG. HT. TRANS. COEFFICIENT BTU/HR. SQ. FT. F
82.9	.0981	356.0	4114	4.94

RUN 9I FINE GLASS SPHERES STATIC BED HEIGHT= 4 INCHES HEATED TUBE LOC. NO.=2

PROBE LOCATION INCHES	TUBE WALL TEMPERATURE DEGREES FAHRENHEIT	TEMPERATURE DIFFERENCE DEGREES FAHRENHEIT	LOCAL HEAT TRANSFER COEFFICIENT BTU/HR. SQ. FT. F
1.0	102.1	14.5	24.5
3.0	107.6	18.6	19.1
5.0	112.1	22.2	16.0
11.0	117.2	26.6	13.4
17.0	117.0	27.1	13.1
23.0	118.8	29.6	12.0
29.0	120.6	31.5	11.3
35.0	121.3	31.6	11.2
41.0	121.4	31.1	11.4
43.0	116.9	26.6	13.4
45.0	112.9	22.8	15.6

INLET TEMPERATURE DEGREES FAHRENHEIT	GAS DENSITY LBS./CU. FT.	HEAT FLUX BTU/HR. SQ. FT.	MASS FLOW RATE LBS./HR. SQ. FT.	AVG. HT. TRANS. COEFFICIENT BTU/HR. SQ. FT. F
86.7	.1050	355.4	4019	13.32

RUN 9J FINE GLASS SPHERES STATIC BED HEIGHT= 4 INCHES HEATED TUBE LOC. NO.=2

PROBE LOCATION INCHES	TUBE WALL TEMPERATURE DEGREES FAHRENHEIT	TEMPERATURE DIFFERENCE DEGREES FAHRENHEIT	LOCAL HEAT TRANSFER COEFFICIENT BTU/HR. SQ. FT. F
1.0	108.2	11.9	29.7
3.0	119.7	23.1	15.4
5.0	125.2	28.4	12.5
11.0	130.9	33.9	10.5
17.0	132.8	35.9	9.9
23.0	135.1	38.5	9.2
29.0	134.7	38.4	9.2
35.0	134.8	38.6	9.2
41.0	131.7	35.5	10.0
43.0	125.3	29.0	12.2
45.0	122.5	26.1	13.6

INLET TEMPERATURE DEGREES FAHRENHEIT	GAS DENSITY LBS./CU. FT.	HEAT FLUX BTU/HR. SQ. FT.	MASS FLOW RATE LBS./HR. SQ. FT.	AVG. HT. TRANS. COEFFICIENT BTU/HR. SQ. FT. F
96.0	.1112	354.8	4584	10.74

RUN 10 A FINE GLASS SPHERES STATIC BED HEIGHT= 2 INCHES HEATED TUBE LOC. NO. =1

PROBE LOCATION INCHES	TUBE WALL TEMPERATURE DEGREES FAHRENHEIT	TEMPERATURE DIFFERENCE DEGREES FAHRENHEIT	LOCAL HEAT TRANSFER COEFFICIENT BTU/HR. SQ. FT. F
1.0	103.5	10.3	34.5
3.0	110.2	17.2	20.7
5.0	117.0	24.0	14.8
6.5	121.7	28.8	12.3
8.0	126.4	33.6	10.6
9.5	130.5	37.7	9.4
11.0	134.6	41.8	8.5
17.0	142.2	49.3	7.2
23.0	167.7	74.7	4.6
35.0	197.2	103.5	3.4
44.0	268.6	174.8	2.0

INLET TEMPERATURE DEGREES FAHRENHEIT	GAS DENSITY LBS./CU. FT.	HEAT FLUX BTU/HR. SQ. FT.	MASS FLOW RATE LBS./HR. SQ. FT.	AVG. HT. TRANS. COEFFICIENT BTU/HR. SQ. FT. F
93.2	.0812	355.9	2777	4.86

RUN 10 B FINE GLASS SPHERES STATIC BED HEIGHT= 4 INCHES HEATED TUBE LOC. NO. =1

PROBE LOCATION INCHES	TUBE WALL TEMPERATURE DEGREES FAHRENHEIT	TEMPERATURE DIFFERENCE DEGREES FAHRENHEIT	LOCAL HEAT TRANSFER COEFFICIENT BTU/HR. SQ. FT. F
1.0	109.8	11.2	32.2
3.0	110.6	11.0	32.7
5.0	114.2	14.0	25.8
8.0	120.4	19.7	18.3
11.0	126.5	25.8	13.9
14.0	130.8	30.4	11.8
17.0	135.7	35.7	10.1
23.0	149.0	49.6	7.3
29.0	172.1	72.7	5.0
38.0	191.0	90.8	4.0
44.0	202.9	102.8	3.5

INLET TEMPERATURE DEGREES FAHRENHEIT	GAS DENSITY LBS./CU. FT.	HEAT FLUX BTU/HR. SQ. FT.	MASS FLOW RATE LBS./HR. SQ. FT.	AVG. HT. TRANS. COEFFICIENT BTU/HR. SQ. FT. F
97.9	.0805	360.1	2658	6.96

RUN 10 C FINE GLASS SPHERES STATIC BED HEIGHT= 4 INCHES HEATED TUBE LOC. NO. =1

PROBE LOCATION INCHES	TUBE WALL TEMPERATURE DEGREES FAHRENHEIT	TEMPERATURE DIFFERENCE DEGREES FAHRENHEIT	LOCAL HEAT TRANSFER COEFFICIENT BTU/HR. SQ. FT. F
1.0	104.7	4.6	80.1
3.0	106.3	6.0	62.2
5.0	113.4	13.1	28.3
7.0	120.7	20.5	18.1
9.0	129.2	29.4	12.6
11.0	142.1	42.8	8.7
14.0	166.4	67.8	5.5
17.0	183.1	85.1	4.4
23.0	226.3	130.9	2.8
33.0	272.4	174.0	2.1
44.0	290.1	190.5	1.9

INLET TEMPERATURE DEGREES FAHRENHEIT	GAS DENSITY LBS./CU. FT.	HEAT FLUX BTU/HR. SQ. FT.	MASS FLOW RATE LBS./HR. SQ. FT.	AVG. HT. TRANS. COEFFICIENT BTU/HR. SQ. FT. F
99.8	.0802	371.1	2552	3.44

RUN 10 D   FINE GLASS SPHERES   STATIC BED HEIGHT= 6 INCHES   HEATED TUBE LOC. NO. =1

PROBE LOCATION INCHES	TUBE WALL TEMPERATURE DEGREES FAHRENHEIT	TEMPERATURE DIFFERENCE DEGREES FAHRENHEIT	LOCAL HEAT TRANSFER COEFFICIENT BTU/HR. SQ. FT. F
1.0	107.0	10.1	35.6
3.0	108.7	10.7	33.4
5.0	108.9	10.2	35.2
8.0	112.4	13.1	27.3
11.0	115.4	16.0	22.4
17.0	122.2	23.3	15.4
23.0	126.2	27.7	12.9
29.0	129.6	31.2	11.5
35.0	131.9	33.2	10.8
41.0	131.4	32.5	11.0
44.0	134.8	36.1	9.9

INLET TEMPERATURE DEGREES FAHRENHEIT	GAS DENSITY LBS./CU. FT.	HEAT FLUX BTU/HR. SQ. FT.	MASS FLOW RATE LBS./HR. SQ. FT.	AVG. HT. TRANS. COEFFICIENT BTU/HR. SQ. FT. F
96.3	.0807	357.9	2943	14.90

RUN 10 E   FINE GLASS SPHERES   STATIC BED HEIGHT= 9 INCHES   HEATED TUBE LOC. NO. =1

PROBE LOCATION INCHES	TUBE WALL TEMPERATURE DEGREES FAHRENHEIT	TEMPERATURE DIFFERENCE DEGREES FAHRENHEIT	LOCAL HEAT TRANSFER COEFFICIENT BTU/HR. SQ. FT. F
1.0	115.2	16.6	21.4
3.0	116.6	16.1	22.0
5.0	114.8	13.1	27.2
8.0	113.8	11.1	31.8
11.0	115.4	12.7	28.0
17.0	119.2	17.4	20.4
23.0	122.1	21.2	16.7
29.0	124.9	24.3	14.6
35.0	125.0	23.7	15.0
41.0	123.7	21.9	16.2
44.0	123.8	22.3	15.9

INLET TEMPERATURE DEGREES FAHRENHEIT	GAS DENSITY LBS./CU. FT.	HEAT FLUX BTU/HR. SQ. FT.	MASS FLOW RATE LBS./HR. SQ. FT.	AVG. HT. TRANS. COEFFICIENT BTU/HR. SQ. FT. F
97.4	.0803	354.7	3137	19.32

RUN 10 F   FINE GLASS SPHERES   STATIC BED HEIGHT= 9 INCHES   HEATED TUBE LOC. NO. =1

PROBE LOCATION INCHES	TUBE WALL TEMPERATURE DEGREES FAHRENHEIT	TEMPERATURE DIFFERENCE DEGREES FAHRENHEIT	LOCAL HEAT TRANSFER COEFFICIENT BTU/HR. SQ. FT. F
1.0	98.9	6.3	58.2
3.0	102.2	8.7	42.1
5.0	104.8	10.8	33.8
7.0	103.2	8.9	40.9
9.0	104.2	9.9	36.6
11.0	110.3	16.2	22.5
14.0	117.8	24.0	15.2
17.0	127.4	34.1	10.7
23.0	151.4	58.8	6.2
35.0	187.0	94.2	3.9
44.0	206.9	113.6	3.2

INLET TEMPERATURE DEGREES FAHRENHEIT	GAS DENSITY LBS./CU. FT.	HEAT FLUX BTU/HR. SQ. FT.	MASS FLOW RATE LBS./HR. SQ. FT.	AVG. HT. TRANS. COEFFICIENT BTU/HR. SQ. FT. F
92.1	.0815	364.2	2541	6.76

```
RUN 10 G        FINE GLASS SPHERES             STATIC BED HEIGHT= 4 INCHES      HEATED TUBE LOC. NO. =1

PROBE LOCATION        TUBE WALL TEMPERATURE        TEMPERATURE DIFFERENCE     LOCAL HEAT TRANSFER COEFFICIENT
   INCHES             DEGREES FAHRENHEIT           DEGREES FAHRENHEIT               BTU/HR. SQ. FT.  F
     1.0                    114.8                        10.3                            34.3
     3.0                    118.4                        14.2                            24.9
     5.0                    120.7                        16.6                            21.2
    11.0                    121.8                        18.2                            19.4
    17.0                    122.7                        19.5                            18.0
    23.0                    123.5                        20.7                            17.0
    29.0                    124.5                        21.9                            16.1
    35.0                    124.6                        21.9                            16.1
    41.0                    122.1                        18.8                            18.8
    43.0                    119.2                        15.5                            22.7
    45.0                    117.9                        13.8                            25.5
 INLET TEMPERATURE      GAS DENSITY     HEAT FLUX         MASS FLOW RATE      AVG. HT. TRANS. COEFFICIENT
 DEGREES FAHRENHEIT     LBS./CU. FT.  BTU/HR. SQ. FT.     LBS./HR. SQ. FT.        BTU/HR. SQ. FT.  F
     104.6                .0837          352.7                 3976                    19.25

RUN 10 H        FINE GLASS SPHERES             STATIC BED HEIGHT= 4 INCHES      HEATED TUBE LOC. NO. =1

PROBE LOCATION        TUBE WALL TEMPERATURE        TEMPERATURE DIFFERENCE     LOCAL HEAT TRANSFER COEFFICIENT
   INCHES             DEGREES FAHRENHEIT           DEGREES FAHRENHEIT               BTU/HR. SQ. FT.  F
     1.0                    121.5                        11.5                            30.7
     3.0                    125.3                        16.2                            21.7
     5.0                    129.0                        20.3                            17.3
    11.0                    129.5                        20.2                            17.4
    17.0                    125.5                        19.0                            18.5
    23.0                    130.5                        20.1                            17.5
    29.0                    130.5                        21.7                            16.2
    35.0                    130.6                        24.1                            14.6
    41.0                    128.9                        23.3                            15.1
    43.0                    127.0                        20.8                            16.9
    45.0                    126.6                        19.2                            18.3
 INLET TEMPERATURE      GAS DENSITY     HEAT FLUX         MASS FLOW RATE      AVG. HT. TRANS. COEFFICIENT
 DEGREES FAHRENHEIT     LBS./CU. FT.  BTU/HR. SQ. FT.     LBS./HR. SQ. FT.        BTU/HR. SQ. FT.  F
     110.7                .0859          352.4                 4654                    17.74
```

```
RUN 11 A       COARSE GLASS SPHERES          STATIC BED HEIGHT= 4 INCHES      HEATED TUBE LOC. NO. =1

PROBE LOCATION       TUBE WALL TEMPERATURE       TEMPERATURE DIFFERENCE      LOCAL HEAT TRANSFER COEFFICIENT
   INCHES            DEGREES FAHRENHEIT          DEGREES FAHRENHEIT               BTU/HR. SQ. FT.  F
    1.0                   119.5                        16.2                             22.5
    3.0                   123.4                        20.8                             17.6
    5.0                   127.0                        24.8                             14.8
    8.0                   134.4                        32.4                             11.3
   11.0                   143.1                        41.1                              8.9
   14.0                   147.3                        45.3                              8.1
   17.0                   148.8                        46.5                              7.9
   23.0                   154.9                        52.7                              7.0
   29.0                   172.8                        71.0                              5.2
   35.0                   193.7                        92.5                              4.0
   44.0                   216.0                       114.8                              3.2
INLET TEMPERATURE       GAS DENSITY      HEAT FLUX          MASS FLOW RATE       AVG. HT. TRANS. COEFFICIENT
DEGREES FAHRENHEIT      LBS./CU. FT.   BTU/HR. SQ. FT.     LBS./HR. SQ. FT.         BTU/HR. SQ. FT.  F
    103.7                 .0775            366.1               4635                      6.15

RUN 11 B       COARSE GLASS SPHERES          STATIC BED HEIGHT= 4 INCHES      HEATED TUBE LOC. NO. =1

PROBE LOCATION       TUBE WALL TEMPERATURE       TEMPERATURE DIFFERENCE      LOCAL HEAT TRANSFER COEFFICIENT
   INCHES            DEGREES FAHRENHEIT          DEGREES FAHRENHEIT               BTU/HR. SQ. FT.  F
    1.0                   106.3                        11.1                             33.1
    3.0                   110.1                        15.2                             24.1
    5.0                   112.5                        17.9                             20.5
    7.0                   117.1                        22.7                             16.2
    9.0                   123.3                        29.2                             12.6
   11.0                   129.3                        35.4                             10.4
   13.0                   134.3                        40.6                              9.1
   17.0                   147.7                        54.3                              6.8
   23.0                   185.8                        92.8                              4.0
   33.0                   242.7                       150.6                              2.4
   44.0                   263.2                       171.2                              2.1
INLET TEMPERATURE       GAS DENSITY      HEAT FLUX          MASS FLOW RATE       AVG. HT. TRANS. COEFFICIENT
DEGREES FAHRENHEIT      LBS./CU. FT.   BTU/HR. SQ. FT.     LBS./HR. SQ. FT.         BTU/HR. SQ. FT.  F
     95.4                 .0792            367.5               4580                      4.15

RUN 11 C       COARSE GLASS SPHERES          STATIC BED HEIGHT= 6 INCHES      HEATED TUBE LOC. NO. =1

PROBE LOCATION       TUBE WALL TEMPERATURE       TEMPERATURE DIFFERENCE      LOCAL HEAT TRANSFER COEFFICIENT
   INCHES            DEGREES FAHRENHEIT          DEGREES FAHRENHEIT               BTU/HR. SQ. FT.  F
    1.0                   120.4                        21.0                             17.2
    3.0                   123.4                        24.0                             15.0
    5.0                   124.8                        25.3                             14.3
    8.0                   132.5                        32.9                             11.0
   11.0                   140.1                        40.4                              8.9
   14.0                   145.3                        45.5                              7.9
   17.0                   147.1                        47.2                              7.6
   23.0                   151.2                        51.5                              7.0
   29.0                   156.9                        57.6                              6.3
   35.0                   170.9                        72.2                              5.0
   44.0                   185.9                        88.4                              4.1
INLET TEMPERATURE       GAS DENSITY      HEAT FLUX          MASS FLOW RATE       AVG. HT. TRANS. COEFFICIENT
DEGREES FAHRENHEIT      LBS./CU. FT.   BTU/HR. SQ. FT.     LBS./HR. SQ. FT.         BTU/HR. SQ. FT.  F
     99.4                 .0783            360.7               4657                      6.99
```

```
RUN 11D        COARSE GLASS SPHERES          STATIC BED HEIGHT= 9 INCHES       HEATED TUBE LOC. NO. =1

PROBE LOCATION      TUBE WALL TEMPERATURE        TEMPERATURE DIFFERENCE        LOCAL HEAT TRANSFER COEFFICIENT
   INCHES           DEGREES FAHRENHEIT           DEGREES FAHRENHEIT                 BTU/HR. SQ. FT.  F
    1.0                   108.8                          8.6                              42.9
    3.0                   113.8                         14.0                              26.3
    5.0                   115.4                         15.9                              23.2
    7.0                   114.3                         15.1                              24.5
    9.0                   117.3                         18.2                              20.2
   11.0                   124.9                         25.9                              14.2
   14.0                   133.1                         34.3                              10.8
   17.0                   142.0                         43.4                               8.5
   23.0                   174.6                         76.4                               4.8
   33.0                   237.7                        140.7                               2.6
   44.0                   266.6                        170.1                               2.2
INLET TEMPERATURE      GAS DENSITY      HEAT FLUX         MASS FLOW RATE       AVG. HT. TRANS. COEFFICIENT
DEGREES FAHRENHEIT     LBS./CU. FT.   BTU/HR. SQ. FT.     LBS./HR. SQ. FT.          BTU/HR. SQ. FT.  F
    100.5                .0786           368.8                4064                       4.63

RUN 11E        COARSE GLASS SPHERES          STATIC BED HEIGHT= 9 INCHES       HEATED TUBE LOC. NO. =1

PROBE LOCATION      TUBE WALL TEMPERATURE        TEMPERATURE DIFFERENCE        LOCAL HEAT TRANSFER COEFFICIENT
   INCHES           DEGREES FAHRENHEIT           DEGREES FAHRENHEIT                 BTU/HR. SQ. FT.  F
    1.0                   120.4                         17.2                              21.0
    3.0                   124.5                         21.5                              16.7
    5.0                   123.5                         20.7                              17.4
    8.0                   124.5                         21.8                              16.6
   11.0                   130.4                         27.6                              13.1
   17.0                   138.6                         35.5                              10.2
   23.0                   146.1                         42.7                               8.4
   29.0                   154.9                         51.5                               7.0
   35.0                   164.2                         61.3                               5.9
   41.0                   171.8                         70.1                               5.1
   44.0                   179.0                         78.3                               4.6
INLET TEMPERATURE      GAS DENSITY      HEAT FLUX         MASS FLOW RATE       AVG. HT. TRANS. COEFFICIENT
DEGREES FAHRENHEIT     LBS./CU. FT.   BTU/HR. SQ. FT.     LBS./HR. SQ. FT.          BTU/HR. SQ. FT.  F
    103.4                .0776           360.5                4476                       8.53

RUN 11F        COARSE GLASS SPHERES          STATIC BED HEIGHT= 4 INCHES       HEATED TUBE LOC. NO. =1

PROBE LOCATION      TUBE WALL TEMPERATURE        TEMPERATURE DIFFERENCE        LOCAL HEAT TRANSFER COEFFICIENT
   INCHES           DEGREES FAHRENHEIT           DEGREES FAHRENHEIT                 BTU/HR. SQ. FT.  F
    1.0                   137.1                         12.3                              29.3
    3.0                   145.6                         22.8                              15.8
    5.0                   152.0                         30.6                              11.8
   11.0                   159.3                         39.8                               9.1
   17.0                   162.3                         42.9                               8.4
   23.0                   164.6                         45.1                               8.0
   29.0                   165.8                         46.7                               7.7
   35.0                   165.7                         47.4                               7.6
   41.0                   158.6                         40.5                               8.9
   43.0                   150.2                         31.8                              11.4
   44.0                   144.5                         25.7                              14.1
INLET TEMPERATURE      GAS DENSITY      HEAT FLUX         MASS FLOW RATE       AVG. HT. TRANS. COEFFICIENT
DEGREES FAHRENHEIT     LBS./CU. FT.   BTU/HR. SQ. FT.     LBS./HR. SQ. FT.          BTU/HR. SQ. FT.  F
    126.0                .0865           361.5                6213                       9.20
```

RUN 11G COARSE GLASS SPHERES STATIC BED HEIGHT= 9INCHES HEATED TUBE LOC. NO.=1

PROBE LOCATION INCHES	TUBE WALL TEMPERATURE DEGREES FAHRENHEIT	TEMPERATURE DIFFERENCE DEGREES FAHRENHEIT	LOCAL HEAT TRANSFER COEFFICIENT BTU/HR. SQ. FT. F
1.0	119.1	8.5	42.3
3.0	125.2	16.6	21.8
5.0	131.5	24.2	15.0
11.0	135.2	29.5	12.3
17.0	146.4	40.6	8.9
23.0	151.7	45.7	7.9
29.0	153.1	47.6	7.6
35.0	152.7	47.9	7.5
41.0	149.6	44.7	8.1
43.0	140.2	34.7	10.4
45.0	134.8	28.3	12.8

INLET TEMPERATURE DEGREES FAHRENHEIT	GAS DENSITY LBS./CU. FT.	HEAT FLUX BTU/HR. SQ. FT.	MASS FLOW RATE LBS./HR. SQ. FT.	AVG. HT. TRANS. COEFFICIENT BTU/HR. SQ. FT. F
111.8	.0867	361.5	6300	9.76

RUN 11 H COARSE GLASS SPHERES STATIC BED HEIGHT= 9 INCHES HEATED TUBE LOC. NO.=1

PROBE LOCATION INCHES	TUBE WALL TEMPERATURE DEGREES FAHRENHEIT	TEMPERATURE DIFFERENCE DEGREES FAHRENHEIT	LOCAL HEAT TRANSFER COEFFICIENT BTU/HR. SQ. FT. F
1.0	125.9	15.3	23.3
3.0	129.6	19.8	18.1
5.0	133.2	23.8	15.0
11.0	137.1	27.9	12.8
17.0	143.7	34.1	10.5
23.0	147.6	38.0	9.4
29.0	148.3	39.2	9.1
35.0	147.3	38.8	9.2
41.0	143.7	35.1	10.2
43.0	137.3	28.4	12.6
45.0	131.8	22.1	16.2

INLET TEMPERATURE DEGREES FAHRENHEIT	GAS DENSITY LBS./CU. FT.	HEAT FLUX BTU/HR. SQ. FT.	MASS FLOW RATE LBS./HR. SQ. FT.	AVG. HT. TRANS. COEFFICIENT BTU/HR. SQ. FT. F
111.0	.0820	357.7	5460	11.35

APPENDIX G

TABLE V. CALCULATED AVERAGE PARTICLE FRACTIONS AND NUSSELT NUMBERS FOR BATCH FLUIDIZATION

Table V. Calculated Average Particle Fractions and Nusselt Numbers for Batch Fluidization

Run Number	Tube Location	Average Section Location, inches	$1 - \epsilon$	Nu_p
Fine Glass Spheres				
1B	4	10.5	0.184	0.64
		21.5	0.011	0.10
1C		10.5	0.120	0.73
		21.5	0.050	0.50
1G		10.5	0.048	0.46
		21.5	0.070	0.36
1H		10.5	0.035	0.67
		21.5	0.025	0.24
5A	3	10.5	0.160	0.83
		21.5	0.020	0.43
5B		10.5	0.035	0.62
		21.5	0.042	0.45
		32.5	0.035	0.39
5E		10.5	0.018	0.64
		21.5	0.004	0.11
5F		10.5	0.013	0.47
		21.5	0.025	0.41
9A	2	10.5	0.180	1.18
		21.5	0.021	0.53
9B		10.5	0.085	1.00
		21.5	0.055	0.74
9D		10.5	0.375	0.74
		21.5	0.002	0.15
10B	1	10.5	0.015	0.45
		21.5	0.013	0.21

Table V. Continued

Run Number	Tube Location	Average Section Location, inches	$1 - \epsilon$	Nu_p
10C		10. 5	0. 010	0. 36
		21. 5	0. 004	0. 10
10D		10. 5	0. 106	0. 69
		21. 5	0. 075	0. 37
		32. 5	0. 025	0. 31
10E		10. 5	0. 070	0. 78
		21. 5	0. 035	0. 48
		32. 5	0. 030	0. 41
10F		10. 5	0. 080	0. 75
		21. 5	0. 060	0. 24
		32. 5	0. 030	0. 14
Coarse Glass Spheres				
3A	4	10. 5	0. 060	0. 82
		21. 5	0. 030	0. 60
3D		10. 5	0. 095	1. 27
		21. 5	0. 015	0. 51
3E		10. 5	0. 265	2. 22
		21. 5	0. 008	0. 57
3F		10. 5	0. 140	1. 40
		21. 5	0. 057	0. 88
4A	3	10. 5	0. 128	1. 46
		21. 5	0. 063	0. 86
4D		10. 5	0. 300	2. 16
		21. 5	0. 120	1. 43
		32. 5	0. 008	0. 40
4E		10. 5	0. 100	1. 31
		21. 5	0. 059	0. 93

Table V. Continued

Run Number	Tube Location	Average Section Location, inches	$1 - \epsilon$	Nu_p
4F		10.5	0.083	1.16
		21.5	0.033	0.65
8A	2	10.5	0.243	1.92
		21.5	0.053	0.88
8D		10.5	0.120	1.43
		21.5	0.063	0.99
		32.5	0.036	0.76
8G		10.5	0.105	1.35
		21.5	0.031	0.64
8H		10.5	0.060	0.94
		21.5	0.038	0.71
		32.5	0.030	0.63
11A	1	10.5	0.022	0.69
		21.5	0.020	0.60
11B		10.5	0.013	1.03
		21.5	0.005	0.43
11C		10.5	0.035	0.82
		21.5	0.024	0.57
		32.5	0.012	0.46
11D		10.5	0.065	1.39
		21.5	0.010	0.54
		32.5	0.003	0.21
11E		10.5	0.035	1.11
		21.5	0.033	0.70
		32.5	0.035	0.49
Aluminum Particles				
6A	3	10.5	0.188	3.56
		21.5	0.024	1.24
		32.5	0.003	0.52

Table V. Continued

Run Number	Tube Location	Average Section Location, inches	1 - ϵ	Nu_p
6B		10.5	0.158	3.46
		21.5	0.049	1.79
6C		10.5	0.057	1.97
		21.5	0.011	0.96
6D		10.5	0.068	2.14
		21.5	0.022	1.19
		32.5	0.010	0.80
7A	2	10.5	0.250	3.82
		21.5	0.051	1.84
7B		10.5	0.088	2.50
		21.5	0.013	1.01
		32.5	0.014	1.01
7G		10.5	0.089	2.53
		21.5	0.005	0.75
7H		10.5	0.050	1.82
		21.5	0.027	1.31
		32.5	0.010	0.89